

Copyright
By
Christopher Neil Satrom
2011

**The thesis committee for Christopher Neil Satrom
certifies that this is the approved version of the following thesis:**

**Shear Strengthening of Reinforced Concrete Beams with
Carbon Fiber Reinforced Polymer (CFRP) Under Fatigue and
Sustained Loading Applications**

**APPROVED BY
SUPERVISING COMMITTEE:**

James O. Jirsa, Supervisor

Wassim Ghannoum, Co-Supervisor

**Shear Strengthening of Reinforced Concrete Beams with
Carbon Fiber Reinforced Polymer (CFRP) Under Fatigue and
Sustained Loading Applications**

by

Christopher Neil Satrom, B.S.Arch.E.

Thesis

Presented to the Faculty of the Graduate School of
The University of Texas at Austin
in Partial Fulfillment
of the Requirements
for the Degree of

Master of Science in Engineering

The University of Texas at Austin

August 2011

Dedication

To my Lord and Savior who gave me all I have
and to my loving wife who supported me every step of the way.

Acknowledgements

I would first like to thank God the Father and the Lord Jesus Christ for providing for me every step of the way. He has given me more than I could have ever asked or imagined.

I would like to thank my beautiful wife, Crystal, for encouraging me throughout this whole process. You have been my source of refuge and encouragement during my time in graduate school. I still don't deserve you.

To my family, for giving me confidence to pursue my dreams. Thank you for teaching me the value of education and for supporting me from the start.

To Dr. Jirsa and Dr. Ghannoum, my supervising professors, I am so thankful to of have had the chance to work with you. You have taught me more than you will ever know. Thank you for all the time and energy you poured into me the last few years.

I would also like to acknowledge all of the great people I had the chance to work alongside at the Ferguson Structural Engineering Laboratory (FSEL). I want to thank Yungon Kim for his friendship and guidance as I completed my research. I would also like to thank Jose Garcia for his willingness to help me as I worked to complete my degree. I am also incredibly grateful to Kevin Quinn, David Garber, Zach Webb, Kerry Kreitman, Matt Leborgne, Nancy Larson, Brian Petruzzi, Alejandro Avendaño, Guillermo Huaco, and Catherine Hovell for their help. Lastly, the assistance of the technical support and administrative staff at FSEL including Andrew Valentine, Blake Stassney, Dennis Phillip, Mike Wason, Eric Schell, Barbara Howard, and Jessica Hanten is truly appreciated.

Lastly and certainly not least, I would like to thank the Texas Department of Transportation (TxDOT) for the financial support aiding in the completion of this project.

June 2, 2011

Abstract

Shear Strengthening of Reinforced Concrete Beams with Carbon Fiber Reinforced Polymer (CFRP) Under Fatigue and Sustained Loading Applications

Christopher Neil Satrom, M.S.E

The University of Texas at Austin, 2011

Supervisor: James O. Jirsa

Co-Supervisor: Wassim Ghannoum

Four specimens were tested to evaluate the shear performance of beams with carbon fiber reinforced polymer (CFRP) laminates and CFRP anchors under fatigue and sustained loading applications. The specimens consisted of 24-in. deep T-beams that were constructed and tested at Phil M. Ferguson Structural Engineering Laboratory at the University of Texas at Austin.

The specimens were strengthened in shear with CFRP laminates anchored with CFRP anchors. One end of each specimen was strengthened using bonded CFRP laminates while the other end was strengthened using unbonded CFRP laminates. Two specimens were used for fatigue testing and two were used for

sustained load testing. For each set of tests, one specimen was strengthened using CFRP laminates prior to cracking and one specimen was strengthened using CFRP laminates following the initial cracking of the specimen.

The CFRP laminates showed no signs of deteriorations in strength during fatigue testing, with only small increases in strain occurring in the CFRP laminates during testing. After fatigue loading was completed, the specimens were monotonically loaded to failure. The failure loads were 5 to 15% lower than beams that were not subjected to fatigue loading.

Sustained load tests were subjected to a constant midpoint load based on service load requirements for a period of 217 days. CFRP laminates performed well during sustained loading. CFRP strains increased slightly throughout testing, but no signs of deterioration were observed.

For both types of tests, specimens strengthened using bonded CFRP laminates demonstrated an increased stiffness resulting in smaller crack widths and lower strains in the internal steel. These benefits were not as great in specimens strengthened after the initial cracking of the specimen.

Table of Contents

| | |
|---|-----------|
| CHAPTER 1 INTRODUCTION..... | 1 |
| 1.1 Research significance | 1 |
| 1.2 Research objectives and scope | 2 |
| CHAPTER 2 BACKGROUND..... | 3 |
| 2.1 Relationship between transverse steel and CFRP | 3 |
| 2.1.1 Impact of transverse reinforcement on CFRP load contribution..... | 4 |
| 2.1.2 Strain effects due to internal transverse reinforcement and FRP | 5 |
| 2.1.3 Effect of transverse steel on crack angle | 6 |
| 2.2 Fatigue behavior of CFRP strengthened specimens..... | 6 |
| 2.2.1 Interaction between internal steel and CFRP | 7 |
| 2.2.2 Degradation of bond..... | 8 |
| 2.3 Failure modes of fatigue specimens strengthened with CFRP..... | 10 |
| 2.3.1 CFRP de-bonding..... | 11 |
| 2.3.2 Steel reinforcement rupture | 11 |
| 2.4 Behavior of CFRP under sustained loading | 12 |
| 2.4.1 Changes in strain over time | 12 |
| 2.4.2 Epoxy creep between the concrete-FRP interface..... | 14 |
| 2.4.3 Deflection characteristics of strengthened specimens..... | 16 |
| CHAPTER 3 TEST CONFIGURATION | 18 |
| 3.1 Introduction | 18 |
| 3.1.1 Fatigue test series | 18 |
| 3.1.2 Sustained load test series..... | 20 |

| | | |
|---|---|-----------|
| 3.2 | Test specimen construction | 22 |
| 3.2.1 | Test specimen design | 23 |
| 3.2.2 | Formwork | 25 |
| 3.2.3 | Reinforcement Cages | 29 |
| 3.2.4 | Concrete | 32 |
| 3.2.5 | CFRP Installation | 35 |
| 3.3 | Experimental test setup | 39 |
| 3.3.1 | Fatigue load tests | 39 |
| 3.3.2 | Sustained load tests | 43 |
| 3.4 | Instrumentation | 49 |
| 3.4.1 | Steel strain | 49 |
| 3.4.2 | CFRP strain | 52 |
| 3.4.3 | Deformations | 55 |
| CHAPTER 4 FATIGUE EXPERIMENTAL RESULTS | | 59 |
| 4.1 | Introduction | 59 |
| 4.2 | Fatigue test series | 60 |
| 4.2.1 | 24-3-Fatigue-1 & 2(Uncracked specimen)..... | 60 |
| 4.2.2 | 24-3-Fatigue-3 & 4 (Cracked specimen)..... | 65 |
| 4.2.2 | General observations | 71 |
| 4.3 | Fatigue failure load test series | 73 |
| 4.3.1 | 24-3-Fatigue-Fail-1 & 2 (Uncracked specimen) | 74 |
| 4.3.2 | 24-3-Fatigue-Fail-3 & 4 (Cracked specimen) | 85 |
| 4.3.2 | Discussion of results of loading to failure after completion of fatigue loading..... | 97 |

| | |
|---|------------|
| CHAPTER 5 LONG-TERM EXPERIMENTAL RESULTS..... | 100 |
| 5.1 Introduction | 100 |
| 5.2 Sustained load test series..... | 101 |
| 5.2.1 24-3-Sust-1 (Uncracked specimen, bonded CFRP) | 102 |
| 5.2.2 24-3-Sust-2 (Uncracked specimen, unbonded CFRP) | 103 |
| 5.2.3 24-3-Sust-3 (Cracked specimen, bonded CFRP) | 105 |
| 5.2.4 24-3-Sust-4 (Cracked specimen, unbonded CFRP) | 107 |
| 5.2.5 Displacements | 109 |
| 5.2 Discussion of results..... | 110 |
| CHAPTER 6 SUMMARY AND CONCLUSIONS..... | 113 |
| 7.1 Summary | 113 |
| 7.2 Conclusions | 114 |
| 7.3 Further Considerations | 114 |
| REFERENCES | 116 |
| VITA..... | 119 |

List of Tables

| | |
|---|-----|
| Table 3-1 Shear and moment capacities of test specimen..... | 25 |
| Table 4-1 Fatigue Loading Test Matrix | 60 |
| Table 4-2 Summary of highest strains recorded during fatigue loading..... | 72 |
| Table 4-3 Summary of crack widths recorded during fatigue loading..... | 73 |
| Table 4-4 Fatigue failure load test matrix | 74 |
| Table 4-5 Summary of tests to failure..... | 97 |
| Table 5-1 Sustained loading test matrix | 101 |
| Table 5-2 Summary of sustained load results | 111 |

List of Figures

| | |
|---|----|
| Figure 2-1 Influence of steel transverse reinforcement on shear force in reinforced concrete beams: (a) at de-bonding; and (b) at fracture of CFRP strips (Bousselham & Chaallal, 2004) | 4 |
| Figure 2-2 Double-lap shear test set-up (Ferrier, Bigaud, Clement, & Hamelin, 2011)..... | 9 |
| Figure 2-3 $\Delta\tau/\Delta\tau_u$ as a function of the number of cycles to failure (Ferrier, Bigaud, Clement, & Hamelin, 2011)..... | 10 |
| Figure 2-4 CFRP Strap Shear Strengthening System (Hoult & Lees, 2005) | 13 |
| Figure 2-5 Long-term CFRP strap strain vs. time under applied load (Hoult & Lees, 2005) | 14 |
| Figure 2-6 Long-term displacement of test specimens obtained from test and FE analysis (Choi, Meshgin, & Taha, 2007)..... | 16 |
| Figure 2-7 Long-term midspan deflection vs. time (Hoult & Lees, 2005) | 17 |
| Figure 3-1 Test Nomenclature..... | 19 |
| Figure 3-2 Fatigue load test setup | 20 |
| Figure 3-3 Test Nomenclature..... | 21 |
| Figure 3-4 Long-term load test setup | 22 |
| Figure 3-5 Cross section of test specimens | 24 |
| Figure 3-6 Cross section of wood and steel formwork | 25 |
| Figure 3-7 Steel side form bracing..... | 26 |
| Figure 3-8 Side view of wooden panel inserts | 27 |
| Figure 3-9 Internal form divider..... | 27 |
| Figure 3-10 Steel cross ties | 28 |
| Figure 3-11 Assembled formwork for two specimens | 29 |
| Figure 3-12 Reinforcement steel layout | 30 |
| Figure 3-13 Steel reinforcement cage with stirrups spaced at 10-in. | 30 |

| | |
|---|----|
| Figure 3-14 Placing of the steel reinforcement cage..... | 31 |
| Figure 3-15 Final placement of reinforcement cage inside formwork..... | 31 |
| Figure 3-16 Average concrete compressive strength for each cast..... | 33 |
| Figure 3-17 Placing of the concrete using 1 cubic yard concrete bucket..... | 33 |
| Figure 3-18 Vibrating the concrete | 34 |
| Figure 3-19 Screeding the top surface of the specimen | 34 |
| Figure 3-20 Hand screeding of specimen..... | 35 |
| Figure 3-21 A CFRP anchor detail (Quinn, 2009)..... | 36 |
| Figure 3-22 Completed CFRP anchor installation (Quinn, 2009) | 36 |
| Figure 3-23 Placement of CFRP patch prior to insertion of anchor..... | 37 |
| Figure 3-24 CFRP anchor with 60-degree fan angle..... | 37 |
| Figure 3-25 Completed CFRP anchor installation | 38 |
| Figure 3-26 Clear plastic liner used to prevent bond between CFRP laminates and surface of the concrete specimen | 39 |
| Figure 3-27 Completed installation of unbonded CFRP..... | 39 |
| Figure 3-28 As-built fatigue load test setup | 40 |
| Figure 3-29 Elevation view of fatigue load test setup..... | 41 |
| Figure 3-30 Load application System | 42 |
| Figure 3-31 Reaction support..... | 42 |
| Figure 3-32 Prestressed external clamps..... | 43 |
| Figure 3-33 Elevation view of sustained load test setup..... | 44 |
| Figure 3-34 Sustained load test setup..... | 45 |
| Figure 3-35 Grouted loading point..... | 45 |
| Figure 3-36 Dywidag anchorage system..... | 46 |
| Figure 3-37 Reaction support..... | 46 |
| Figure 3-38 Initial loading test setup..... | 47 |
| Figure 3-39 Hydraulic loading system for initial loading..... | 47 |
| Figure 3-40 Hydraulic loading system for final loading..... | 48 |

| | |
|--|----|
| Figure 3-41 Final loading test setup | 49 |
| Figure 3-42 Reinforcement cages after installation of steel strain gauges..... | 50 |
| Figure 3-43 Steel strain gauge grid for all test specimens | 51 |
| Figure 3-44 Steel strain gauge nomenclature | 51 |
| Figure 3-45 CFRP strain gauge (Pham, 2009) | 52 |
| Figure 3-46 Rubber pad used to protect CFRP gauge..... | 52 |
| Figure 3-47 Long-term load gauge protection covering | 53 |
| Figure 3-48 CFRP strain gauge grid for all test specimens..... | 54 |
| Figure 3-49 CFRP strain gauge nomenclature | 54 |
| Figure 3-50 LVDT used to monitor displacements during fatigue testing..... | 55 |
| Figure 3-51 DEMEC measuring device | 56 |
| Figure 3-52 DEMEC point grid | 57 |
| Figure 3-53 As-built DEMEC point grid | 57 |
| Figure 3-54 DEMEC points used to track changes in end displacements | 58 |
| Figure 4-1 24-3-Fatigue-1&2 unbonded (left) and bonded (right) CFRP test specimen | 61 |
| Figure 4-2 Load displacement response, test 24-3-Fatigue-1&2 | 62 |
| Figure 4-3 Steel strains, Tests 24-3-Fatigue-1&2 | 64 |
| Figure 4-4 CFRP strains, Tests 24-3-Fatigue-1&2 | 64 |
| Figure 4-5 24-3-Fatigue-3&4 unbonded (left) and bonded (right) CFRP test specimen | 66 |
| Figure 4-6 Load displacement response, test 24-3-Fatigue-3&4 | 67 |
| Figure 4-7 Steel strains, Tests 24-3-Fatigue-3&4 | 70 |
| Figure 4-8 CFRP strains, Tests 24-3-Fatigue-3&4 | 70 |
| Figure 4-9 Load displacement response, test 24-3-Fatigue-Fail-1&2..... | 75 |
| Figure 4-10 24-3-Fatigue-Fail-1 before (left) and after (right) loading | 76 |
| Figure 4-11 Rupture of a CFRP anchor observed during 24-3-Fatigue-Fail-1 | 76 |
| Figure 4-12 Rupture of a CFRP strip observed during 24-3-Fatigue-Fail-1 | 77 |

| | |
|--|----|
| Figure 4-13 24-3-Fatigue-Fail-1 at 0-kips applied load (0-kips applied shear) | 78 |
| Figure 4-14 24-3-Fatigue-Fail-1 at 100-kips applied load (50-kips applied shear) | 79 |
| Figure 4-15 24-3-Fatigue-Fail-1 at 200-kips applied load (100-kips applied shear) | 79 |
| Figure 4-16 24-3-Fatigue-Fail-1 at 214-kips applied load (107-kips applied shear) | 80 |
| Figure 4-17 24-3-Fatigue-Fail-2 before (left) and after (right) loading | 81 |
| Figure 4-18 CFRP anchor failure observed during 24-3-Fatigue-Fail-2..... | 81 |
| Figure 4-19 Rupture of CFRP strip observed during 24-3-Fatigue-Fail-2..... | 82 |
| Figure 4-20 24-3-Fatigue-Fail-2 at 0-kips applied load (0-kips applied shear) | 83 |
| Figure 4-21 24-3-Fatigue-Fail-2 at 100-kips applied load (50-kips applied shear) | 84 |
| Figure 4-22 24-3-Fatigue-Fail-2 at 200-kips applied load (100-kips applied shear) | 84 |
| Figure 4-23 24-3-Fatigue-Fail-2 at 270-kips applied load (135-kips applied shear) | 85 |
| Figure 4-24 Load displacement response, test 24-3-Fatigue-Fail-3&4..... | 86 |
| Figure 4-25 24-3-Fatigue-Fail-3 before (left) and after (right) loading | 87 |
| Figure 4-26 First CFRP anchor failure observed during 24-3-Fatigue-Fail-3 | 87 |
| Figure 4-27 Second CFRP anchor failure observed during 24-3-Fatigue-Fail-3.. | 88 |
| Figure 4-28 24-3-Fatigue-Fail-3 at 0-kips applied load (0-kips applied shear) | 89 |
| Figure 4-29 24-3-Fatigue-Fail-3 at 100-kips applied load (50-kips applied shear) | 90 |
| Figure 4-30 24-3-Fatigue-Fail-3 at 200-kips applied load (100-kips applied shear) | 90 |
| Figure 4-31 24-3-Fatigue-Fail-3 at 256-kips applied load (128-kips applied shear) | 91 |

| | |
|--|-----|
| Figure 4-32 24-3-Fatigue-Fail-4 before (left) and after (right) loading | 92 |
| Figure 4-33 CFRP sheet rupture observed during 24-3-Fatigue-Fail-4 | 92 |
| Figure 4-34 CFRP anchor failure observed during 24-3-Fatigue-Fail-4..... | 93 |
| Figure 4-35 24-3-Fatigue-Fail-4 at 0-kips applied load (0-kips applied shear) | 94 |
| Figure 4-36 24-3-Fatigue-Fail-4 at 100-kips applied load (50-kips applied shear) | 95 |
| Figure 4-37 24-3-Fatigue-Fail-4 at 200-kips applied load (100-kips applied shear) | 95 |
| Figure 4-38 24-3-Fatigue-Fail-4 at 283-kips applied load (142-kips applied shear) | 96 |
| Figure 5-2 Front and back of test 24-3-Sust-1 | 102 |
| Figure 5-3 Strains, test 24-3-Sust-1..... | 103 |
| Figure 5-4 Front and back of test 24-3-Sust-2 | 104 |
| Figure 5-5 Strains, test 24-3-Sust-2..... | 105 |
| Figure 5-6 Front and back of test 24-3-Sust-3 | 106 |
| Figure 5-7 Strains, test 24-3-Sust-3..... | 107 |
| Figure 5-8 Front and back of test 24-3-Sust-4 | 108 |
| Figure 5-9 Strains, test 24-3-Sust-4..... | 109 |
| Figure 5-10 End displacement DEMEC points..... | 110 |
| Figure 5-11 Average total displacement | 110 |

CHAPTER 1

Introduction

1.1 RESEARCH SIGNIFICANCE

Carbon Fiber Reinforced Polymer (CFRP) materials provide an excellent option for the repair of reinforced concrete structures due to their light weight, non-corrosive properties. CFRP laminates consist of a fabric material made of woven carbon fiber strands impregnated with a high strength structural epoxy. These laminates exhibit a high tensile strength capacity and are an excellent alternative to steel in applications where reinforced concrete structures are deficient in flexure and shear.

In cases where CFRP laminates cannot be wrapped completely around a specimen, debonding failures have been observed at tensile loads 40 to 50% lower than their ultimate capacity. As a result, several anchorage systems have been developed to help the CFRP laminates reach their ultimate tensile capacity. Most anchorage systems consist of some mechanical anchorage devices that are used to pin the ends of the CFRP laminates to the concrete surface. This research focuses on the use of anchors fabricated using CFRP materials.

Previous research by Quinn (2009) demonstrated the effectiveness of CFRP anchors in developing the full tensile capacity of the CFRP laminates. His tests focused on the ability of CFRP anchors to fully develop the full tensile capacity of the CFRP laminates under monotonic loading to failure. Limited data is available on the performance of CFRP strengthened specimens under fatigue and sustained loads. To better understand the behavior of anchored CFRP laminates in typical field applications, research on full scale reinforced concrete specimens strengthened using anchored CFRP laminates subjected to fatigue and sustained loads is needed.

1.2 RESEARCH OBJECTIVES AND SCOPE

The research presented in this report focuses on the performance of reinforced concrete specimens strengthened using CFRP laminates anchored with CFRP anchors under fatigue and sustained loading. Tests were conducted on four 24-in. deep full-scale reinforced concrete T-beams. Two specimens were subjected to fatigue loads in excess of 3.5-million cycles and two specimens were loaded for a period of 217-days at a level that resulted in strains just below yielding of the internal transverse steel reinforcement. An experimental program was developed to achieve the following objectives:

- Determine the behavior of CFRP shear reinforcement on full scale concrete elements subjected to fatigue and sustained loading.
- Determine the effect of strengthening a specimen with CFRP laminates after the initial cracking of a specimen compared with strengthened a specimen prior to initial cracking.
- Determine the effect bond between the concrete surface and CFRP laminates has on the performance of reinforced concrete specimens tested under fatigue and sustained loading.

CHAPTER 2

Background

Many bridges constructed in the United States during the late 1940's and 50's are reaching the end of their intended design life. An increase in heavy truck volume over these bridges has resulted in many of them to be posted with load limits because of shear deficiencies (Deniaud & Cheng 2001). In response to this, an increasing amount of research has gone into the field of structural rehabilitation. It is necessary to find ways to strengthen these structures in a cost effective manner. Initially, bonded steel plates and stirrups were used to repair these bridges, but these repairs resulted in new problems due to corrosion. Carbon Fiber Reinforced Polymers (CFRP) are an attractive solution for correcting these shear deficiencies due to their "low weight-to-strength ratios, non-corrosiveness, high fatigue strength, and ease of application" (Deniaud & Cheng 2003).

Since CFRP is a relatively new material, an increasing amount of research is going into studying its uses and behavior. One key element that has been under investigation in recent years has been the long term performance of CFRP in terms of fatigue or sustained load behavior. The following is a summary of background information compiled from past research on the fatigue and sustained load behavior of reinforced concrete beams strengthened using CFRP laminates. For a more in depth review of the behavior of CFRP and its uses in shear strengthening applications, please refer to Quinn (2009).

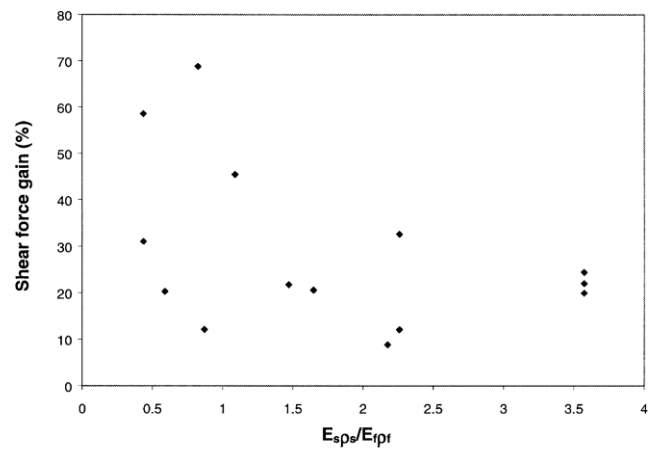
2.1 RELATIONSHIP BETWEEN TRANSVERSE STEEL AND CFRP

Many factors affect the performance of CFRP in the shear strengthening of reinforced concrete beams. One of the issues affecting the design and performance of CFRP strengthened specimens is CFRP interaction with the internal steel in a reinforced concrete beam. Because of this, it is important to note the impact transverse steel and

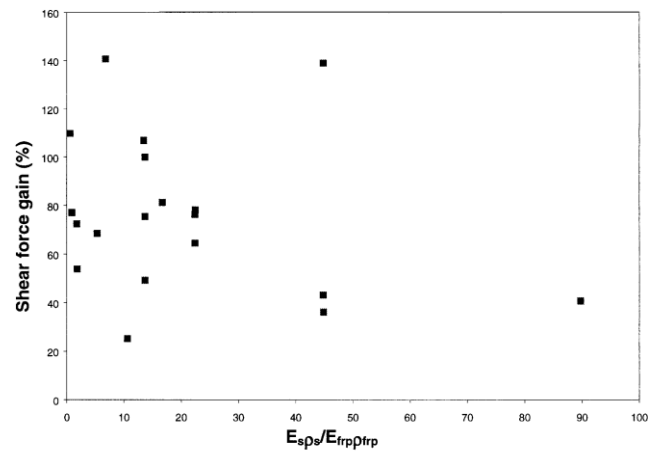
CFRP have on one another during the course of loading and to examine the behavior of each material during testing.

2.1.1 Impact of transverse reinforcement on CFRP load contribution

Bousselham and Chaallal (2004) attempted to gather all the available research of Fiber Reinforced Polymers (FRP). Their intent was to find conditions that affect the behavior of FRP. During the course of their study they were able to find evidence that the amount of shear reinforcement directly impacts the effectiveness of FRP.



(a)



(b)

Figure 2-1 Influence of steel transverse reinforcement on shear force in reinforced concrete beams: (a) at de-bonding; and (b) at fracture of CFRP strips (Bousselham & Chaallal, 2004)

Figure 2-1 represents the shear strength increase due to FRP vs. $E_s\rho_s/E_f\rho_f$, where E_s and E_f are the steel and FRP modulus respectively and ρ_s and ρ_f are the steel and FRP ratios respectively. As the $E_s\rho_s/E_f\rho_f$ ratio increases, the effectiveness of FRP as a source of additional shear strength decreases.

Deniaud and Cheng (2003) performed 8 tests on reinforced concrete beams to study the effects of transverse steel on FRP. During their tests they found that the FRP provided an increase in strength of 38% for a reinforced concrete beam with no transverse steel reinforcement, an increase in strength of 42% for a reinforced concrete beam with 400-mm (15.75-in) stirrup spacing, and an increase in strength of 21% for a reinforced concrete beam with 200-mm (7.87-in) stirrup spacing. The reinforced concrete beams with minimal or no transverse steel reinforcement performed similarly, but reinforced concrete beams that were more heavily reinforced only gained about half of the FRP capacity seen in other lighter reinforced members.

2.1.2 Strain effects due to internal transverse reinforcement and FRP

The strains experienced in the FRP and transverse steel are different at the same location; as a result, the corresponding forces are also different. The force contributions produced in these types of reinforcement do not change at the same rate. Differences in strains reflect the manner in which the materials perform during loading. Transverse steel tends to elongate over a length that depends on bond between the steel and concrete, while elongation of the FRP sheets is localized at the shear crack location (Uji 1992).

When CFRP is present, the shear force carried by the stirrups is reduced. This is a result of the CFRP sharing the load with the transverse steel (Uji 1992). The transverse steel also experiences lower strain values at corresponding loads and delayed yielding due to the presence of CFRP. The CFRP delays cracking and therefore delays the shear contribution of the transverse steel (Bousselham & Chaallal 2006). This delayed strain increase in the transverse steel can result in some non-characteristic behavior of reinforced concrete beams when CFRP is used in shear applications. In one test performed by Deniaud and Cheng (2001) of a more heavily reinforced member, this

delayed yielding and caused the beam strengthened using CFRP to fail before a reinforced concrete beam with no CFRP. Before the steel stirrups fully yielded, one of the CFRP sheets failed resulting in a sudden increase in the force in the steel stirrup causing the reinforced concrete beam to fail prematurely.

2.1.3 Effect of transverse steel on crack angle

The total shear contribution due to CFRP is based on the total area of CFRP crossing a shear crack, A_{fv} . This value increases or decreases depending on the angle of the shear crack with respect to the axis of the beam. As the shear crack angle increases the amount of CFRP material crossing the crack decreases and as the shear crack angle decreases the amount of CFRP material going over the crack increases. As the amount of transverse steel decreases, the shear crack angle decreases. This results in a larger amount of CFRP material crossing the shear crack and therefore increases the shear strength contribution of the CFRP (Deniaud & Cheng 2001).

2.2 FATIGUE BEHAVIOR OF CFRP STRENGTHENED SPECIMENS

Most of the research on the performance of Carbon Fiber Reinforced Polymers (CFRP) has been conducted on specimens loaded monotonically. Recently, some attention has been given to the behavior of CFRP under fatigue loading. Performance in fatigue is important due to the fact that many structures strengthened with CFRP will be implemented in applications where there is a fluctuation in live loads due to traffic flow or building occupancy. Harries, Reeve, and Zorn (2007) observed that beams loaded more than 2,000,000 cycles failed at lower loads compared to similar beams loaded monotonically.

In terms of fatigue loading, two major areas affect the performance of specimens strengthened using CFRP, 1) interaction between internal steel and CFRP and 2) the degradation of bond between CFRP and the concrete surface.

2.2.1 Interaction between internal steel and CFRP

In structures strengthened using CFRP, a composite section is created with the CFRP carrying some of the load being applied to the structure. This results in lower strains in the internal transverse reinforcement. When considering the fatigue performance of reinforced concrete beams strengthened with CFRP, proper attention needs to be given to the fatigue capacity of the reinforced concrete beams component parts. “The fatigue capacity of a composite beam is limited by the fatigue capacity of its component parts” (Hoult & Lees, 2005). They suggest that the unstrengthened specimen needs to be evaluated to ensure that the internal steel has not already reached its fatigue life. CFRP is a very resilient material under fatigue loading. In all cases where failure occurred prior to the loss of bond between the concrete surface and the CFRP laminate, fatigue failure was observed to be controlled by the fracture of steel stirrups (Harries, Reeve, & Zorn, 2007).

Reinforced concrete beams strengthened with FRP in flexure have demonstrated an increased fatigue life due to the FRP “relieving the stress demand on the existing steel” (Aidoo, Harries, & Petrou, 2004). Ferrier, Bigaud, Clement, & Hamelin (2011) observed a 40% increase in service load in beams strengthened using FRP composites, where service load is defined by the load producing allowable service deflections and deformations in the reinforced concrete beams. They also observed that the strain reduction seen in the internal steel in beams strengthened after the initial cracking of a specimen was not as great as the strain reduction in the steel of specimens strengthened prior to cracking. Therefore, in cases where FRP composites are used to repair beams where cracks have already formed, increases in service load capacity will not be as great.

Gussenhoven & Brena (2005) studied thirteen “small-scale” beams strengthened with CFRP in flexure and tested under repeated loading. They found that specimens cycled under a load range of less than 70% of yield of the longitudinal steel failed due to the fracture of the steel reinforcement. Whereas, specimens cycled at a load range in excess of 70% of yield of the longitudinal reinforcement failed due to delamination of the

CFRP strips. Their tests showed that as long as bond between the CFRP and concrete surface was maintained, the fatigue life of the strengthened specimen was controlled by the internal steel. Papakonstantinou, Petrou, & Harries (2001) tested strengthened and un-strengthened specimen's where stresses in the internal steel were kept within a constant range. In both cases, no discernable difference was seen in the fatigue life of specimens where the same stress levels were observed. These tests confirmed the earlier assertion that the fatigue life of a strengthened specimen is dependent on the fatigue life of the internal steel reinforcement.

2.2.2 Degradation of bond

One area of concern in the use of FRP laminates in strengthening applications is the materials propensity to delaminate from the concrete surface when the material reaches higher strains. This is particularly an issue in cases where FRP laminates cannot be wrapped completely around a beam and therefore the strength of the composite member is based on the strength of the bond between the FRP and concrete surface. De-bonding failure is exacerbated in cases of fatigue, where de-bonding occurs at lower strains than specimens loaded monotonically (Harries, Reeve, & Zorn, 2007).

Brena, Benouaich, Kreger, & Wood (2005) conducted eight tests on reinforced concrete beams strengthened with CFRP laminates. Specimens cycled at load ranges typical of service-load levels in a bridge, between 30 and 60% of yielding, performed very well and did not “exhibit significant accumulation of damage with increased number of load repetitions.” However, in cases where strengthened specimens were loaded at higher levels, de-bonding failure was observed. These de-bonding failures occurred between 15-25% of the ultimate CFRP capacity. This agrees with the results of Gussenhoven & Brena (2005) who observed failure due to de-bonding in cases where fatigue loads surpassed 70% of yield.

Ferrier, Bigaud, Clement, & Hamelin (2011) performed twelve double-lap shear tests as depicted in Figure 2-2. Of these tests, static loads were applied to three of the tests and fatigue loads were applied to the remaining nine specimens. The three statically

loaded specimens failed at an average shear stress of 1.5 MPa (0.22 ksi). These specimens all failed due to the delamination of the composite plate. The nine fatigue loaded specimens were cycled between a load range of 0.10 MPa (0.015 ksi) and 45%, 60%, and 80% of the shear stress at fracture under monotonic loading (0.67 MPa (0.10 ksi), 0.90 MPa (0.13 ksi), and 1.20 MPa (0.17 ksi)).

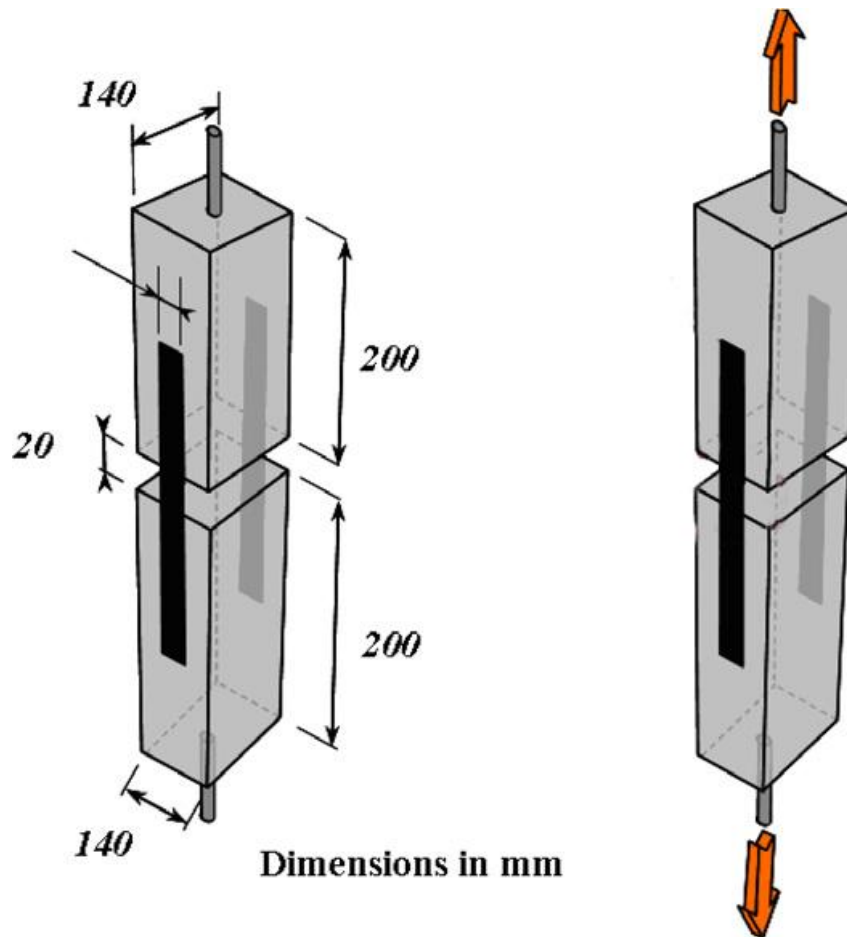


Figure 2-2 Double-lap shear test set-up (Ferrier, Bigaud, Clement, & Hamelin, 2011)

Figure 2-3 summarizes the results of twelve tests. The figure shows that as the applied range of shear stress increases in the concrete to composite interface, the fatigue life of the specimen decreases. When the number of cycles is plotted on a logarithmic scale, a linear relationship between average shear stress and number of cycles to fatigue failure results and is expressed in Equation 2-1.

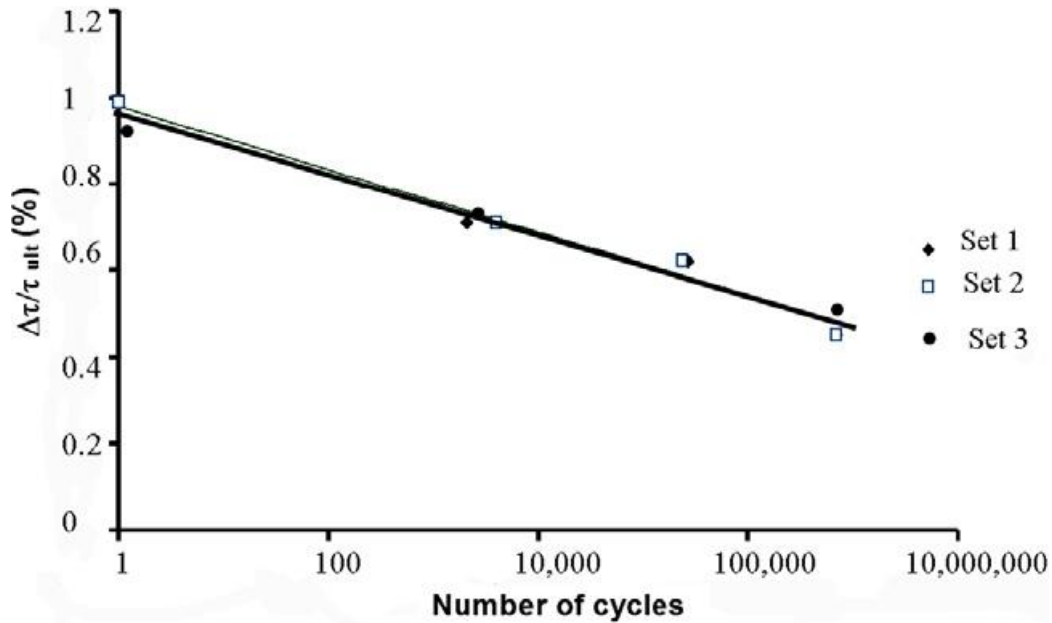


Figure 2-3 $\Delta\tau/\tau_{ult}$ as a function of the number of cycles to failure (Ferrier, Bigaud, Clement, & Hamelin, 2011)

$$\Delta\tau_{adh} = m \cdot \log(N) + b \quad \text{Equation 2-1}$$

with $m = -0.07$ and $b = 0.98$

These results effectively demonstrate how the bond between composite materials, such as CFRP, and the concrete surface degrade as applied shear stress and number of cycles applied increases.

2.3 FAILURE MODES OF FATIGUE SPECIMENS STRENGTHENED WITH CFRP

Two primary modes of failure have been observed during the fatigue testing of reinforced concrete beams strengthened with CFRP. The first is CFRP de-bonding. In this case, the CFRP material delaminates from the concrete surface prior to reaching rupture strain. Therefore, the CFRP is unable to utilize its full tensile capacity. The second failure mode is rupture of the internal steel. This failure mode is experienced when the internal steel reinforcement reaches its fatigue life and ruptures prior to the failure of the externally bonded CFRP.

2.3.1 CFRP de-bonding

The de-bonding of CFRP is a major concern in the fatigue testing of reinforced concrete beams. Many recent studies have noted the relation between fatigue loading of reinforced concrete beams and the degradation of bond between the surface of the concrete and FRP laminates (Brena et al. (2005), Aidoo et al. (2004), Gussenhaven et al. (2005), Harries et al. (2007)). Once the bond was lost between the concrete surface and the FRP laminate, the reinforced concrete beam performed as an un-retrofitted specimen (Aidoo, Harries, & Petrou, 2004). In these cases failure can often be instantaneous due to the sudden increase in load applied to the internal steel when the FRP de-bonds. Therefore, the fatigue life of a specimen is limited by the quality of bond between the FRP and concrete surface. In cases where the bond between the FRP laminates and concrete surface does not degrade, fatigue life is based on the internal steel reinforcement (Harries, Reeve, & Zorn, 2007).

2.3.2 Steel reinforcement rupture

The second, more preferred mode of failure in fatigue tested specimens is the rupture of internal steel reinforcement. As mentioned previously, one of the greatest benefits of externally bonded FRP is its ability to increase the fatigue life of a reinforced concrete beam by decreasing the demand on the internal steel (Aidoo, Reeve, & Zorn, 2004). The FRP delays cracking of reinforced concrete beams and therefore increases the service load levels of structures, while decreasing the demand on the internal steel. In cases where specimens are cracked prior to strengthening, the strain reduction in the internal steel is not as pronounced (Ferrier, Bigaud, Clement, & Hamelin, 2011).

A failure due to the rupture of internal steel is preferred because it infers that the CFRP has functioned satisfactorily by increasing the service cracking load of the beam as much as possible. Increasing fatigue life may be a primary goal for strengthening some beams with FRP laminates.

2.4 BEHAVIOR OF CFRP UNDER SUSTAINED LOADING

In addition to the study of fatigue loaded specimens strengthened using FRP; attention must be given to sustained load behavior of strengthened specimens. FRP laminates are an excellent source of strengthening for specimens loaded over long durations due to their non-corrosive nature and the low additional weight they add to structures (Hoult & Lees, 2005). The lighter weight of the FRP material means that the dead load of the strengthened specimen will be unchanged.

Several factors need to be considered when determining the performance of FRP strengthened structures loaded over long durations. These factors include, but are not limited to:

- Changes in strain over time
- Epoxy creep between the concrete-FRP interface
- Deflection characteristics of strengthened specimens

2.4.1 Changes in strain over time

It is important to note the strain behavior of FRP materials over time. Hoult & Lees (2005), along with many others, have examined the long-term behavior of CFRP strengthening systems. They tested a CFRP strap shear strengthening system shown in Figure 2-4. This system consisted of drilling four holes through the bottom and side of the top flange of a reinforced concrete T-beam. Once the holes were drilled “a strip of 3-mm (0.12-in) thick and 15-mm (0.59-in) wide polytetrafluoroethylene (PTFE) was placed in the holes to create the void that the CFRP straps would later pass through.” The holes were then filled with a high early strength concrete repair product and vibrated to minimize the voids in the grout. The CFRP straps were then inserted through the opening in the grout. A prestressing jack was placed on the bottom side of the test specimen and used to apply a prestressing force to the CFRP strap equivalent to 25% of the straps ultimate capacity. One set of beams was then left unloaded while the other set of beams was loaded for 220 days under shear loading.

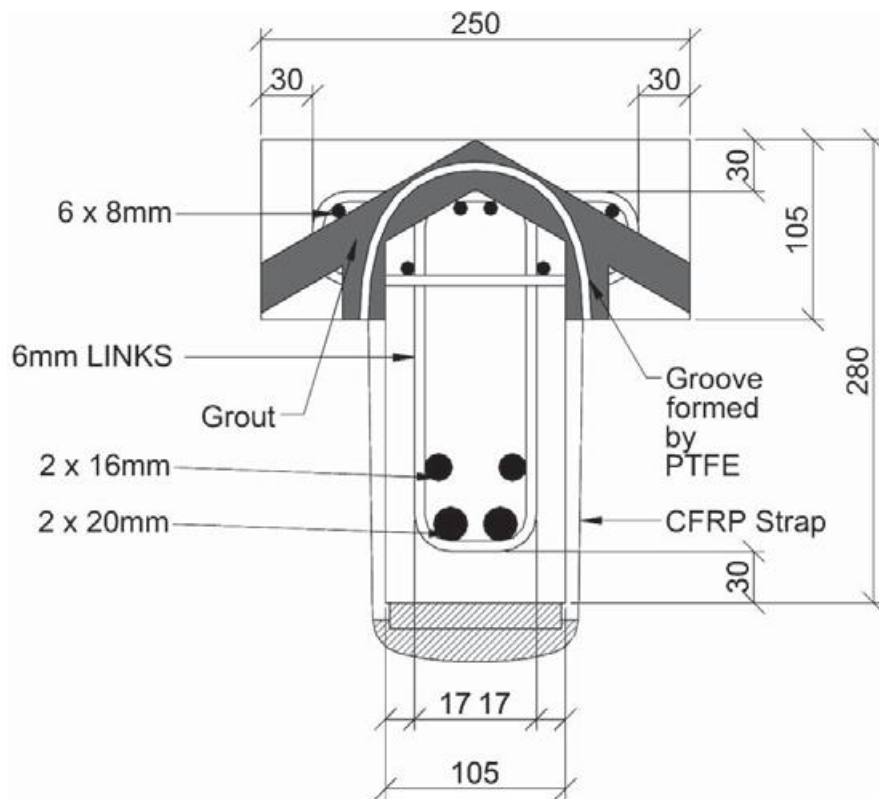


Figure 2-4 CFRP Strap Shear Strengthening System (Hoult & Lees, 2005)

The unloaded specimens demonstrated a 5% decrease in CFRP strains over the first 77 days of loading. The decreases in strain over the initial period were believed to be due to the creep in the concrete caused by the prestressing force. Additional losses in strain may have been due to relaxation of the CFRP straps. Hoult & Lees (2005) referenced work by Saadatmanesh & Tannous (1999) on CFRP prestressing rods noting that relaxation losses can range from 5-10% of the initial prestressing force over a 50 year period. The maximum strap strains increased by approximately 0.001 in/in, or 23%, in the beams loaded for 220 days. A graph of the strap strain with time results can be seen in Figure 2-5. Strain increases reached a plateau, with the most significant strain increases occurring early in the loading period. Based on these results, the straps appeared to have the satisfactory sustained load capacity.

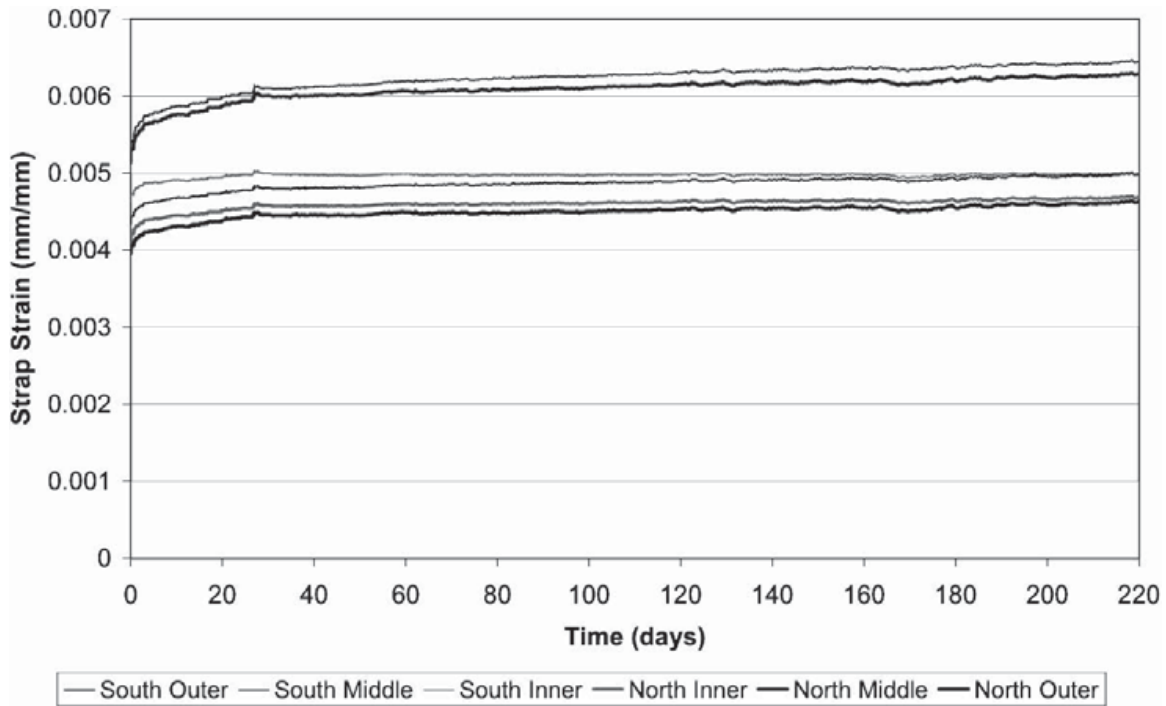


Figure 2-5 Long-term CFRP strap strain vs. time under applied load (Hoult & Lees, 2005)

Hoult & Lees (2005) observed that the long-term behavior of CFRP is more critical than the cyclic behavior of CFRP. This agrees with guidelines presented by NCHRP Report 655 that recommends placing strain limits on FRP strengthened specimens under fatigue loading to avoid creep-rupture of the reinforcement materials. NCHRP Report 655 also notes that since design is often governed by service limit state, FRP strains will remain sufficiently low and “creep rupture of the FRP is typically not of concern.”

2.4.2 Epoxy creep between the concrete-FRP interface

Another important factor affecting the long-term performance of FRP laminates is the bond characteristics of the epoxy used to bond the FRP to the concrete surface. Nishizaki, Labossiere, & Sarsaniuc (2007) studied the durability of CFRP sheets through exposure tests. They found that after 5 years, the CFRP sheets maintained good tensile

strength, but they observed the loss of some strength due to the reduction in bonding properties between the carbon fibers and epoxy resin. This reduction in strength is not believed to be due to a decrease in the strength of the epoxy itself, but instead is attributed to a reduction of bonding properties between the carbon fibers and the resin.

Choi, Meshgin, & Taha (2007) noted that the key factor affecting the performance of FRP laminates is bond between the FRP and concrete surface. They tested the bond between the FRP and concrete surface by conducting several double-lap shear tests similar to those found in Figure 2-2. The variables examined were the shear stress level and the thickness of the epoxy layer. The specimens were then loaded for 6 months. Specimen (a) was loaded at 15% of the ultimate shear stress with an epoxy thickness of 0.242-mm (0.0095-in), specimen (b) was loaded at 31% of the ultimate shear stress with an epoxy thickness of 0.176-mm (0.0069-in), and specimen (c) was loaded at 31% of the ultimate shear stress with an epoxy thickness of 1.50-mm (0.059-in). The results of the three tests can be seen in Figure 2-6. These results show that the creep between the FRP and concrete surface occurs within a relatively short amount of time (15-30 days), compared with the typical retardation time of concrete which ranges between 300 and 900 days. The finite element results presented in Figure 2-6 display a displacement plot that plateaus after the initial loading period, while experimental results demonstrate gradual increases in displacements throughout the testing process.

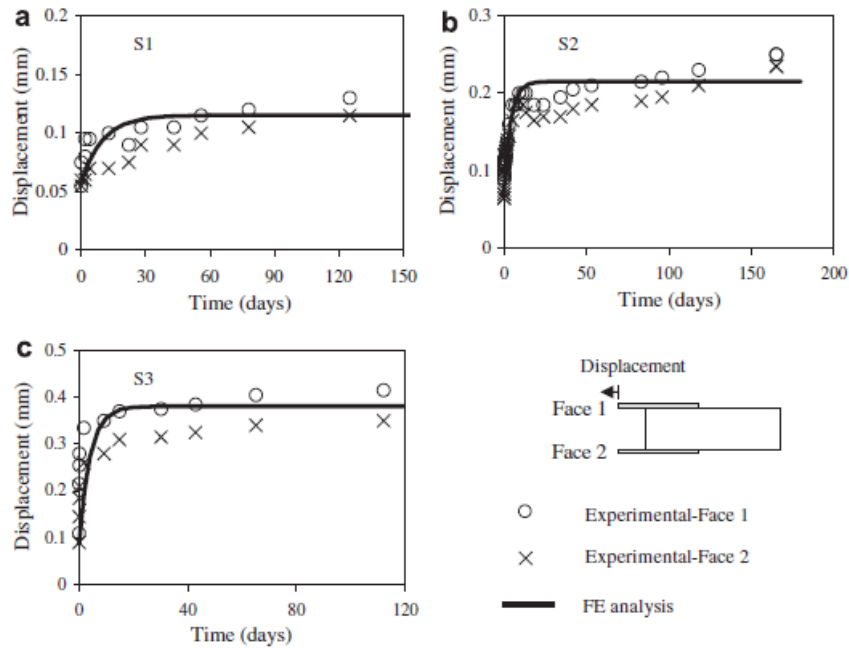


Figure 2-6 Long-term displacement of test specimens obtained from test and FE analysis (Choi, Meshgin, & Taha, 2007)

One area of concern is the redistribution of stresses in the concrete due to the creep of the epoxy. The creep in the epoxy can cause stress relief in some areas or stress increases in other areas resulting in additional tensile cracking. The magnitude of this stress redistribution is dependent on several parameters including level of shear stress, epoxy layer thickness, and concrete stiffness and creep criteria (Choi, Meshgin, & Taha, 2007).

2.4.3 Deflection characteristics of strengthened specimens

In addition to monitoring changes in strain over time of sustained load tests of CFRP strap systems, Hoult & Lees (2005) also observed significant changes in deflections over time of specimens strengthened using CFRP strap reinforcement systems. In the case of specimens loaded for a period of 220 days, they found that deflections increase by a total of 8.7-mm (0.34-in) over that time from 15.4-mm (0.61-in) to 24.1-mm (0.95-in). The greatest increase in deflections occurred over the first 25 days,

but then the deflections continued to slowly increase for the remainder of the 220 days. The deflections appeared to be leveling out toward the end of the 220 day period. The results of the long-term load deflections can be seen in Figure 2-7.

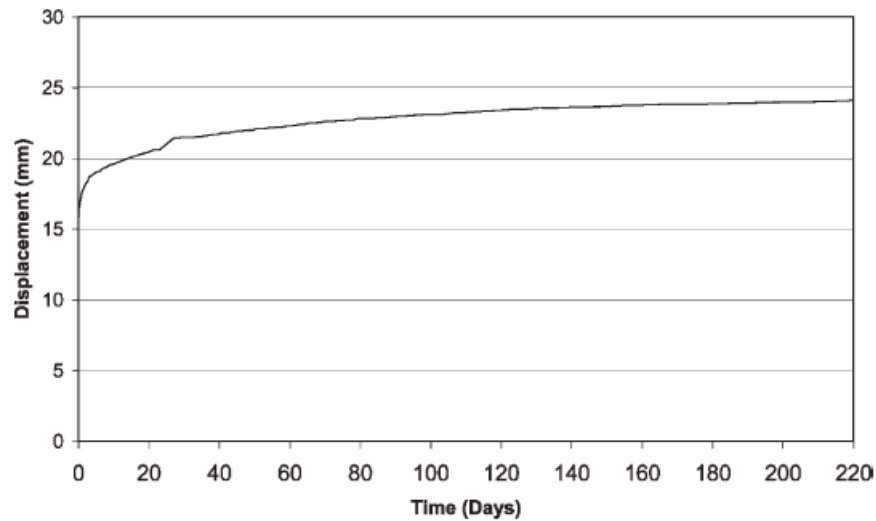


Figure 2-7 Long-term midspan deflection vs. time (Hoult & Lees, 2005)

The changes in deflection over time are based on a combination of flexural deflections and shear deflections due to creep. While design codes base long-term deflection calculations on flexural effects, increases over time in the strains in the CFRP straps and internal steel suggest that a shear component is present in the total deflection (Hoult & Lees, 2005). CFRP strap strains increased by 23% and the internal steel strains increased by 31%. These findings show that it is necessary to account for the increases in deflection due to shear effects and not strictly those attributed to flexural behavior.

Although adequate attention should be given to creep effects in structures strengthened using FRP systems, it should be noted that most structures using FRP reinforcement systems will already have been loaded for a considerable length of time and most of the concrete creep will have already taken place and therefore increases in deflection will not be as great in field repair applications as they were in laboratory specimens (Hoult & Lees, 2005).

CHAPTER 3

Test Configuration

3.1 INTRODUCTION

Four full scale reinforced concrete T-beams were constructed. CFRP was applied to the surface of the reinforced concrete beams in various layouts in accordance with the research objectives. The CFRP strips were anchored using anchors made of CFRP. The specimens were then tested to determine the effectiveness of differing CFRP layouts in fatigue and sustained loading shear applications.

3.1.1 Fatigue Test Series

Two test specimens were subjected to fatigue loading. The following sections describe the test nomenclature system and testing procedures used throughout fatigue testing.

3.1.1.1 Test nomenclature

A nomenclature system was developed to designate each test. Each test label consisted of four parts separated by hyphens. The first number indicated the overall depth of the test specimen in inches. The second number indicated the shear span-to-depth ratio. The third part indicated the type of test being conducted. Tests represented with the word “Fatigue” describe test specimens that were subjected to cycled loading and tests represented with the words “Fatigue-Fail” describe previously fatigue loaded specimens that were then monotonically loaded to ultimate failure. Finally, the fourth number represents the specific test number within the test series. For specimens tested under fatigue loading, a letter “B” follows the test number to represent the testing end of the specimen strengthened using bonded CFRP and the letter “U” represents the testing

end strengthened using unbonded CFRP. A graphical representation of this nomenclature system is presented in Figure 3-1.

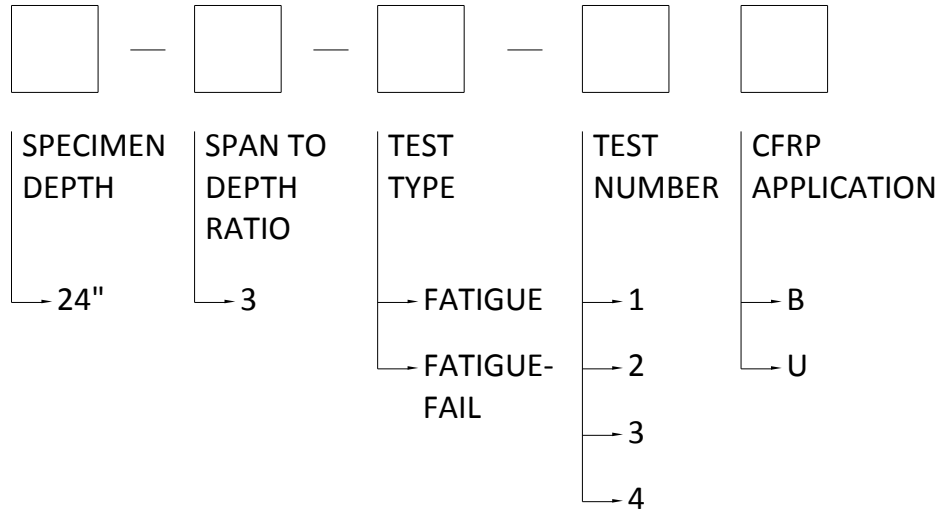


Figure 3-1 Test Nomenclature

3.1.1.2 Testing Procedure

Each test specimen was placed in the test setup displayed in Figure 3-2. The first specimen was strengthened using CFRP laminates prior to the initial cracking of the specimen. This specimen was initially loaded after strengthening using an open loop pump to a level great enough to produce shear crack widths equal to 0.013-in. on each end of the specimen, the maximum allowable crack width of in-service reinforced concrete beams in the region where testing was conducted. Once the test specimen was cracked, then the load was removed and the hydraulic ram was attached to a closed loop pump that would control fatigue loading. The second specimen was loaded using the same open loop pump to a level producing crack widths equal to 0.013-in. on each end of the specimen prior to the application of CFRP laminates. The specimen was then strengthened using CFRP laminates before cyclic loads were applied. Each test specimen was then tested between a range of 70-kips and 90-kips for approximately 1 million

cycles. After this, the test specimen was unloaded and then reloaded and cycled between a load of 110-kips and 130-kips for approximately 2.5 million additional cycles.



Figure 3-2 Fatigue load test setup

Once the test specimen reached approximately 3.5 million cycles, the load was removed and the open loop pump was reattached to the hydraulic ram so the specimen could be loaded to failure. Each specimen was then monotonically loaded until one side of the test specimen failed. The previously failed side of the test specimen was then clamped using the prestressed clamping system described in 3.2.1 and the opposite side of the test specimen was then taken to ultimate failure.

3.1.2 Sustained load test series

The two remaining test specimens were subjected to sustained load tests. The following sections describe the test nomenclature system and testing procedures used throughout the sustained load tests.

3.1.2.1 Test nomenclature

Once again, a nomenclature system similar to the system presented in 3.1.1.1 was developed to designate each test. Each test label consisted of four parts separated by hyphens. The first number indicated the overall depth of the test specimen. The second number indicated the shear span-to-depth ratio. The third part indicated the type of test being conducted. Test specimens were labeled with the letters “Sust”, an abbreviation for sustained load testing. Finally, the fourth number represents the specific test number within the test series. A graphical representation of this nomenclature system is presented in Figure 3-3.

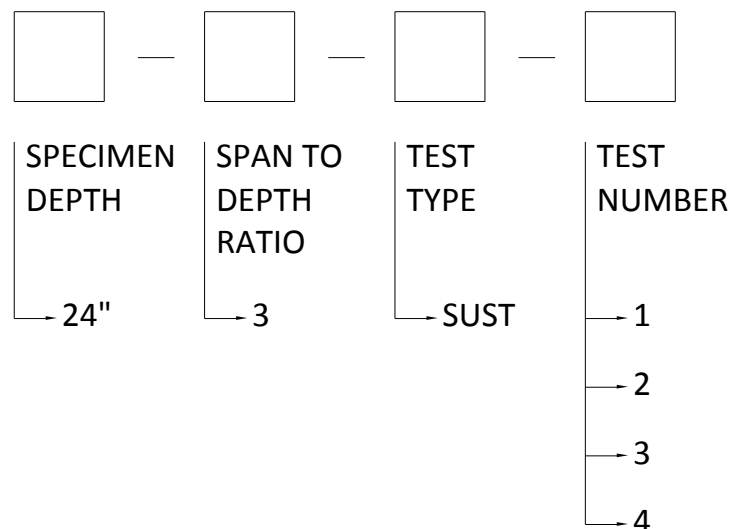


Figure 3-3 Test Nomenclature

3.1.2.2 Testing Procedure

Two test specimens were placed in the test setup displayed in Figure 3-4. The test specimens were loaded at their reaction points using hydraulic rams to a force of 80-kips. Once the 80-kip reaction force was reached, Dywidag anchor nuts were tightened down to hold the resulting force. The two 80-kip reaction forces produced an applied load of 160-kips at the midpoint of each test specimen. Therefore, each shear span experienced

an applied shear of 80-kips throughout testing. The test specimens were then moved and the load remained on the specimens for a total of 217 days.



Figure 3-4 Long-term load test setup

After a period of 107 days, hydraulic rams were placed back onto the test setup and the original load was reapplied to the test specimens. This was done to assure that the proper loading level was maintained throughout testing. The reapplication of load resulted in a slight increase in steel and CFRP strains at the 107 day point of loading.

3.2 TEST SPECIMEN CONSTRUCTION

Test specimens were constructed and cast at the Ferguson Structural Engineering Laboratory (FSEL). The following sections will describe different elements of the design and construction process including:

- Test specimen design
- Formwork
- Steel reinforcement cages
- Concrete and concrete casting
- CFRP Installation

3.2.1 Test specimen design

The test specimens were designed using AASHTO (American Association of State Highway and Transportation Officials) and ACI 318-08(American Concrete Institute) guidelines related to minimum details for shear. Since the research emphasis is on the performance of CFRP laminates in shear, test specimens were designed so that the flexural capacity of the reinforced concrete beams greatly exceeded the estimated shear capacity to ensure a shear failure in the specimen.

Spacing of the transverse reinforcement was selected based on the maximum allowable spacing of shear reinforcement. This spacing was selected to emulate RC beams used in the field that may be in need of strengthening due to deficiencies in shear. As shear reinforcement spacing is increased, the shear contribution of the transverse reinforcement decreases. Therefore, as shear reinforcement spacing increases, the likelihood of shear deficiencies increases as well.

It has been found that the tensile strength of concrete is closely related to a multiple of the square root of the 28-day compressive strength ($\sqrt{f'_c}$). Therefore, the tensile strength of the concrete increases as the concrete compressive strength increases. This results in an increase in the shear contribution of the concrete as concrete compressive strength increases. Because of this, a concrete compressive strength of 4,000-psi was used to reduce the shear contribution of the concrete. The intent was to maximize the shear contribution of the externally applied CFRP.

The last component of the shear calculation was the shear contribution of the CFRP laminates. The shear contribution of the CFRP laminates was determined using guidelines presented in ACI 440.2R-08. These design equations assume that failure will occur due to the debonding of the CFRP laminates. Therefore, tensile strains in the CFRP are limited to 40% of their ultimate capacity. Since the CFRP laminates were to be anchored using CFRP anchors, the 40% strain limit was not considered and strains were assumed to be able to reach the fracture strain of the CFRP.

The total shear capacity of the specimen was calculated using standard ACI 318-08 shear design equations for the contribution of the steel and concrete. The CFRP shear contribution was calculated using the modified ACI 440.2R-08 equations and added to the steel and concrete contributions to determine the total shear capacity of the strengthened specimen.

The T-beam geometry was chosen to compare results to beams used in monolithic floor systems or beams used in conjunction with a composite bridge deck system. It also helped to increase the area of the concrete compression block, thus providing increased flexural capacity. A cross section of the reinforced concrete test specimen can be seen in Figure 3-5. Previous monotonic tests were conducted by Quinn et al. (2009) on specimens with a top flange that was 28" wide. The size of the top flange was decreased to 21" to use steel forms readily available in the lab. The use of steel forms greatly decreased the construction time of the test specimens.

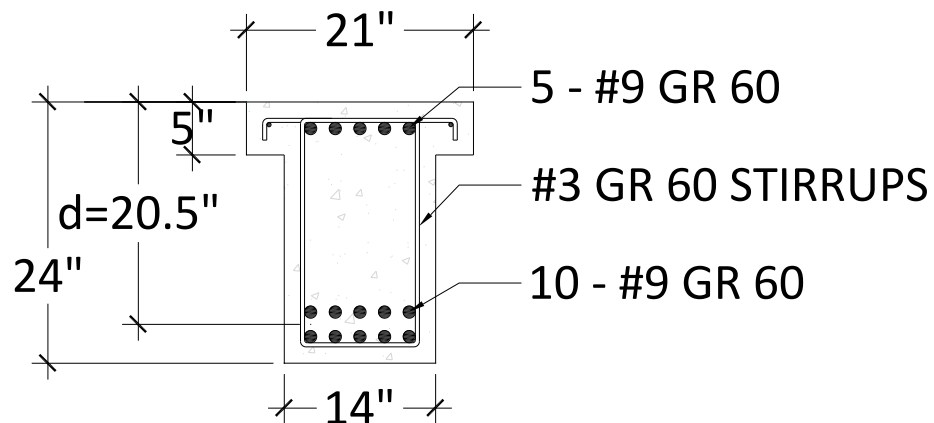


Figure 3-5 Cross section of test specimens

Following the calculation of the shear capacity, the moment capacity was calculated based on the load necessary to produce a shear failure. The moment capacity was then increased to obtain a margin above shear failure. Table 3-1 displays the shear and moment capacities of the test specimen and the corresponding moment at expected shear failure loads. A margin of 2.0 was desired to help ensure a shear failure in the test

specimen. This was made possible by providing large amounts of flexural reinforcement and by increasing the width of the top flange to increase the size of the compression block. Four test specimens, 13-ft. 8-in. long, were then constructed based on the cross section described previously.

Table 3-1 Shear and moment capacities of test specimen

| Shear Span-to-Depth Ratio (a/d) | Design Shear Capacity (kips) | | Design Moment Capacity ² (k-ft) | Applied Moment (k-ft) at Corresponding Shear Failure | | Margin ³ |
|---------------------------------|------------------------------|-----------|--|--|-----------|---------------------|
| | Without CFRP | With CFRP | | Without CFRP | With CFRP | |
| 3 | 63 ¹ | 90 | 903 | 315 | 450 | 2.0 |

¹ - As Calculated from ACI 318-08 Chapter 11 and ACI 440.2R-08 Chapter 11

² - As Calculated from ACI 318-08 Chapter 10

³ - Design Moment Capacity/Applied Moment at Corresponding Shear Failure (With CFRP)

3.2.2 Formwork

To increase the durability of the formwork to account for the casting of multiple specimens, steel side forms were used in conjunction with wooden panel inserts. The panels were made of B/C plywood to reuse for two castings. These wooden inserts created the desired T-beam shape as shown in Figure 3-6.

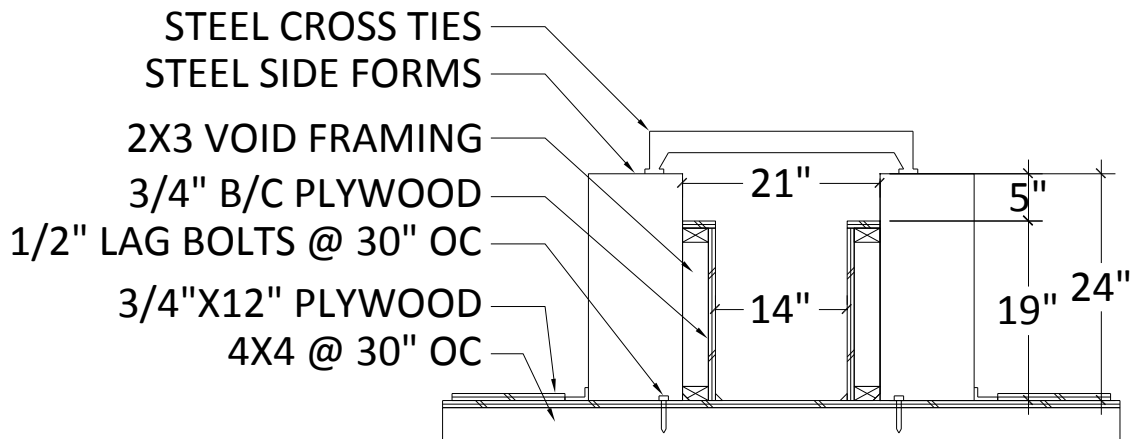


Figure 3-6 Cross section of wood and steel formwork

The base of the formwork consisted of 4-ft. sections of 4x4 lumber spaced at 30-in. on center with 4-ft. wide sections of $\frac{3}{4}$ -in. plywood placed on top. After the base was constructed, two 27-ft. 8-in. steel side forms were placed 21-in. apart to provide the proper width of the top flange. These steel side forms were then attached to the base with $\frac{1}{2}$ -in. diameter lag screws into the 4x4's beneath spaced at 30-in. centers. Once the steel side forms were in place, 12-in. strips of $\frac{3}{4}$ -in. plywood were attached to the plywood base along the bottom edge of the steel formwork to act as additional restraint for the lateral hydrostatic pressure from the concrete during casting. These plywood braces can be seen in Figure 3-7.



Figure 3-7 Steel side form bracing

In order to create the desired T-beam shape while using steel side forms, wooden panels were inserted to provide the appropriate void dimensions. The 3 $\frac{1}{2}$ -in. by 19-in. block-outs were constructed using 2x3-in. lumber with $\frac{3}{4}$ -in. plywood covering used to create a smooth surface. The 2x3-in. pieces of lumber were made by sawing 2x6-in. members in half. Modular construction consisting of four 8-ft. panel sections and four 5-ft. 8-in. panel sections were used to create the desired specimen lengths. A 4-in. wide internal form divider made of 2x3-in. lumber and $\frac{3}{4}$ -in. plywood was used so that two

specimens could be cast using the same formwork. The wooden inserts can be seen in Figure 3-8 and the internal form divider is shown in Figure 3-9.



Figure 3-8 Side view of wooden panel inserts



Figure 3-9 Internal form divider

Due to high stresses that develop in CFRP at locations where the CFRP crosses corners of a section, it is necessary to round any sharp edges prior to the application of CFRP. In order to decrease beam preparation time, chamfer strips created out of decorative molding purchased at a local hardware store were used along the bottom edge

of the formwork to help create a desired bend radius of 0.5-in (ACI 440.2R-08, 2008). The molding was stripped to the desired width using a table saw and then attached to the surface of the formwork using a combination of high strength glue and staples.

Once the panel inserts were placed inside the steel forms, end forms made of 2x4 framing and $\frac{3}{4}$ -in. plywood were bolted to the ends of the formwork. Caulking was used to seal gaps between the steel side forms and panel inserts, as well as any imperfections in the wooden formwork. Steel cross ties were placed on the steel forms to help resist the lateral hydrostatic pressure resulting from placement of fresh concrete (Figure 3-10). The completed formwork can be seen in Figure 3-11, the steel cross ties were removed prior to the photo so that the forms could be seen more clearly.



Figure 3-10 Steel cross ties



Figure 3-11 Assembled formwork for two specimens

3.2.3 Reinforcement Cages

The four test specimens were constructed using identical reinforcement layouts. The longitudinal reinforcement in each specimen consisted of ten #9, grade 60 bars placed in two rows of five bars each row. Each bar was hooked in accordance with ACI 318-08 guidelines to provide adequate anchorage so that the full tensile capacity of each bar could be developed. In addition to the ten longitudinal bars in the tensile region of the beam, five #9, grade 60 bars were placed in the compression region of the beam to increase the compressive strength of the member and to help prevent a concrete crushing failure due to flexure.

The transverse steel reinforcement consisted of #3, grade 60 stirrups. ACI 318-08 states that in cases where the a/d ratio is greater than two, the spacing of the transverse steel reinforcement must be less than half the effective depth of the beam ($d/2$). Therefore, for the case of the specimens tested ($a/d = 3$), a stirrup spacing of 10-in. was selected for the shear span. Additional transverse steel was placed in the end regions to provide confinement for the hooked bars and also under the loading point to ensure a

shear failure in the shear span. Slab steel reinforcement consisting of #3 bars was placed in the top flange of the T-beam specimen with spacing equal to that of the transverse reinforcement. Figure 3-12 depicts the reinforcing steel layout.

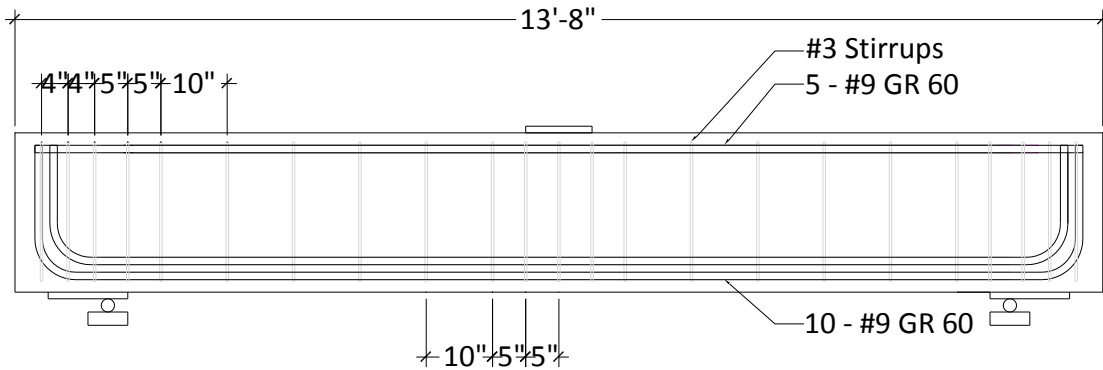


Figure 3-12 Reinforcement steel layout

Two reinforcement cages were constructed simultaneously on steel stands and then instrumented with the appropriate strain gauges. The completed reinforcement cages can be seen in Figure 3-13.



Figure 3-13 Steel reinforcement cage with stirrups spaced at 10-in.

The completed reinforcement cages were then placed inside the formwork using an overhead crane (Figure 3-14). Reinforcing chairs were used to help maintain the minimum concrete cover of 1.5-in. between the steel reinforcement and the forms. The

final placement of the reinforcement cage inside the formwork can be seen in Figure 3-15.



Figure 3-14 Placing of the steel reinforcement cage

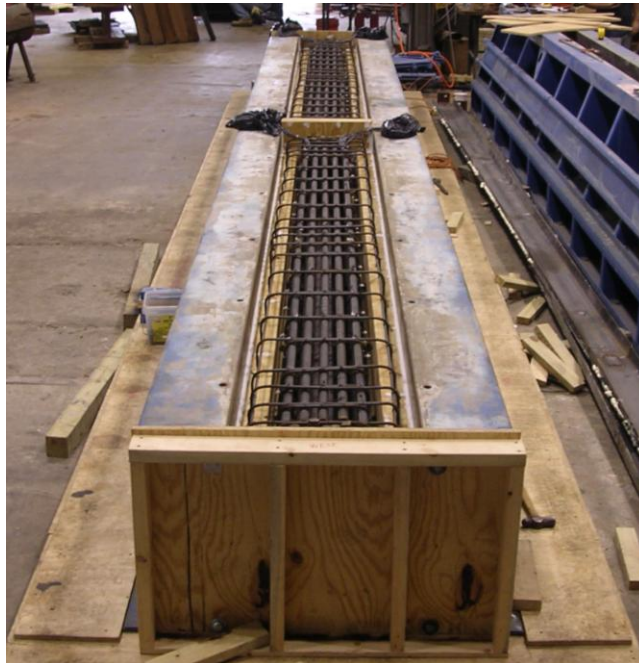


Figure 3-15 Final placement of reinforcement cage inside formwork

3.2.4 Concrete

As discussed previously in section 3.1.1, it was important to maintain a relatively low concrete compressive strength. Therefore, a 28-day concrete compressive strength of less than 4,000-psi was desired for all casts. A concrete compressive strength of 3,000-psi was specified to help minimize the shear contribution of the concrete and therefore maximize the shear contribution from the externally applied CFRP.

The mix design of the concrete specified is as follows:

- 4-1/4 Sacks of Cement
- 25% Fly Ash
- 3/4-in. Maximum Aggregate Size
- 6 to 8-in. Slump

The mix design was chosen in accordance with previous specimens cast in association with the research project. Previous specimens were loaded monotonically and procedures can be found in Quinn (2009). A super plasticizer was included to help increase the workability of the concrete and to help control the curing time due to the high temperatures experienced in the laboratory during the summer months. No other admixtures were used.

The four beams were fabricated in two castings about a month apart. The first cast consisted of the two beams used for the sustained loading portion of the project. The second cast was for the two beams used for the fatigue loading portion of the project. Several 4-in. by 8-in. concrete cylinders were cast with each set of beams and were kept in a curing environment similar to the beams cast. The results of the compression tests of the cylinders can be found in Figure 3-16. The 28-day compressive strengths for each specimen were relatively close to one another and well below 4,000-psi.

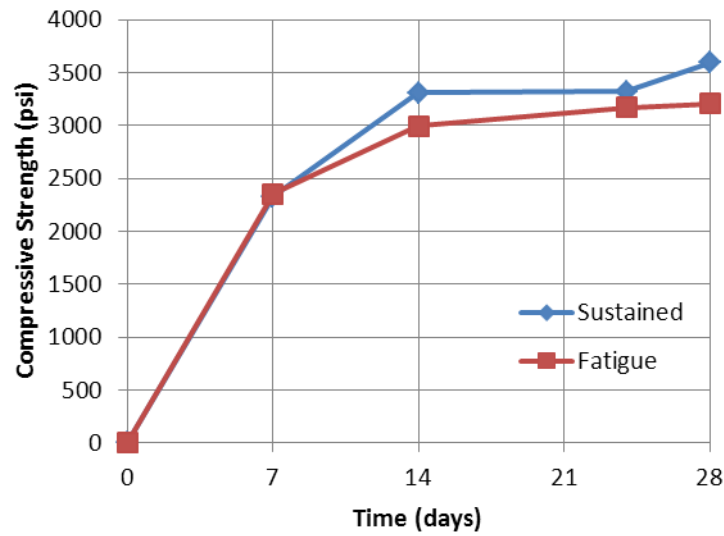


Figure 3-16 Average concrete compressive strength for each cast

The concrete was placed using an overhead crane and a 1 cubic yard concrete bucket that moved the concrete from the delivery truck to the forms (Figure 3-17). The



Figure 3-17 Placing of the concrete using 1 cubic yard concrete bucket

concrete was placed in three layers. The first layer covered the bottom layer of longitudinal steel. The second layer filled the web of the T-beam and covered the transverse steel reinforcement. The third layer covered the slab reinforcement and the

remainder of the beam. Each layer of concrete was vibrated to ensure that no voids remained in the specimen (Figure 3-18).



Figure 3-18 Vibrating the concrete

Once the concrete was sufficiently vibrated, the surface of the concrete was screeded using a large, smooth 2x4 to remove all excess concrete and then hand screeded to smooth out any remaining imperfections (Figure 3-19 & Figure 3-20).



Figure 3-19 Screeding the top surface of the specimen



Figure 3-20 Hand screeding of specimen

After screeding, the specimens were covered in a plastic tarp for a minimum of three days and left to cure. Once the plastic covering was removed, the beams were left to cure until testing.

3.2.5 CFRP Installation

A detailed, step-by-step description of the installation process used to apply the CFRP was identical to that described by Quinn (2009) except for two slight modifications:

- On the anchor detail and
- bonded vs. unbonded CFRP strips

3.2.5.1 Anchor detail modification

The previously researched anchor detail consisted of an anchor made of CFRP material inserted 6-in. into the concrete surface then fanned out to a fan angle of 60 degrees over the CFRP laminate on the surface of the beam. Once the anchor was inserted into the specimen, two 5-in. by 5-in. CFRP patches were placed over the top of the CFRP anchor. The first patch was oriented with the fibers perpendicular to the direction of the CFRP sheet and the second patch was then placed directly over the top of

the first patch with the fibers running perpendicular to the fibers of the patch underneath. The two 5-in. by 5-in. patches helped to distribute CFRP anchor stresses more evenly across the surface of the CFRP laminate. This detail can be seen in Figure 3-21, with a picture of the finished installation in Figure 3-22.

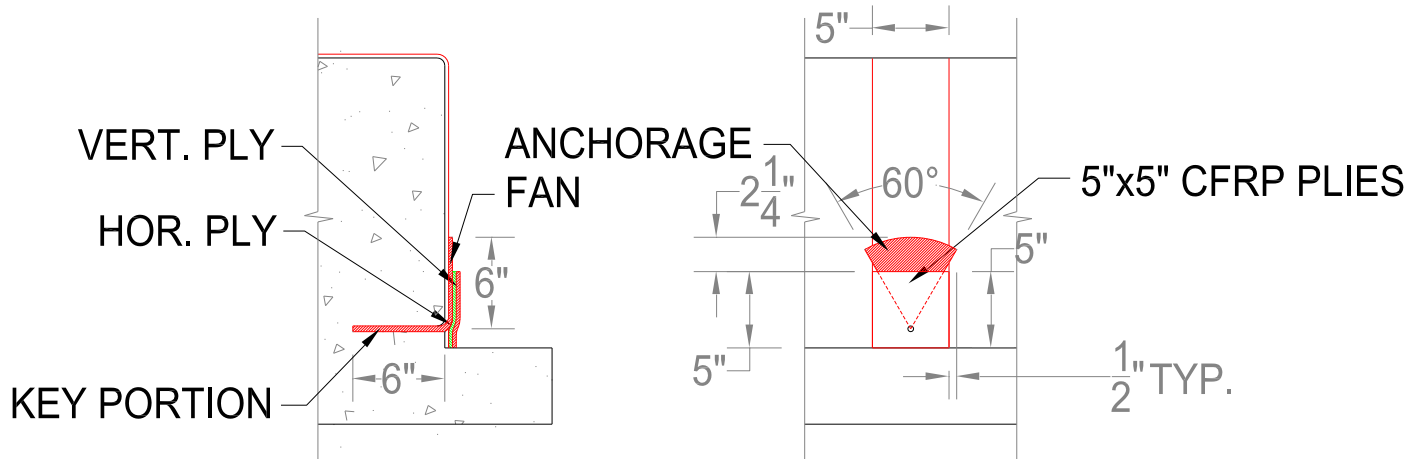


Figure 3-21 A CFRP anchor detail (Quinn, 2009)

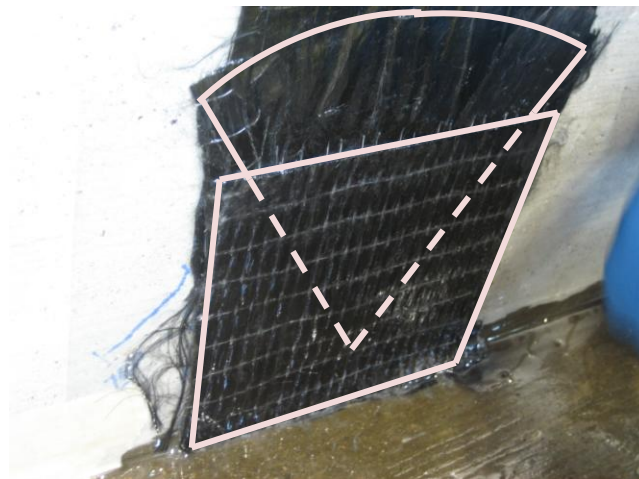


Figure 3-22 Completed CFRP anchor installation (Quinn, 2009)

After further examination, the previous anchor detail was modified to help transfer the stresses from the CFRP anchor to the CFRP laminate in a more efficient manner. The following procedure was then used to install the CFRP anchor. The modified anchor detail involves placing a 5-in. by 5-in. CFRP patch on top of the CFRP

sheet with the CFRP fibers in the patch running perpendicular to the CFRP fibers in the CFRP sheet. This patch is placed prior to the installation of the CFRP anchor as seen in Figure 3-23.



Figure 3-23 Placement of CFRP patch prior to insertion of anchor

Once the CFRP patch is placed perpendicular to the direction of the CFRP sheet, then the CFRP anchor is inserted and fanned out to a 60-degree angle (Figure 3-24).



Figure 3-24 CFRP anchor with 60-degree fan angle

After the placement of the CFRP anchor, an additional 5-in. by 5-in. CFRP patch is placed over the top of the CFRP anchor with patch fibers running in the same direction as the CFRP sheet beneath it. Therefore, the fibers of the two CFRP patches are oriented

perpendicular to each other with the CFRP anchor placed in between the two layers of CFRP patch material. The completed CFRP anchor detail can be seen in Figure 3-25.



Figure 3-25 Completed CFRP anchor installation

3.2.5.2 Bonded and unbonded CFRP application

In cases where CFRP anchors are used in conjunction with CFRP sheets, a failure due to the rupture of the CFRP sheets can be obtained without the presence of bond between the surface of the concrete and the CFRP laminates. While bond is not necessary to reach the ultimate strength of the CFRP laminates, it has been found to benefit the serviceability characteristics of reinforced concrete beams. Therefore, bonded and unbonded CFRP strips were subjected to fatigue and sustained loading situations.

Each of the four specimens tested had equal amounts of CFRP applied along each shear span. On one side of the specimen, the CFRP was bonded to the surface of the concrete as is typical in CFRP applications. On the opposite shear span, a clear plastic liner purchased at a local supermarket was placed over the surface of the concrete prior to the application of the CFRP laminates. The clear plastic liner prevented the CFRP laminates from bonding to the surface of the concrete. During testing, all forces in the CFRP laminates were transferred to the concrete through the CFRP anchor. The clear plastic liner used during the installation process can be seen in Figure 3-26.

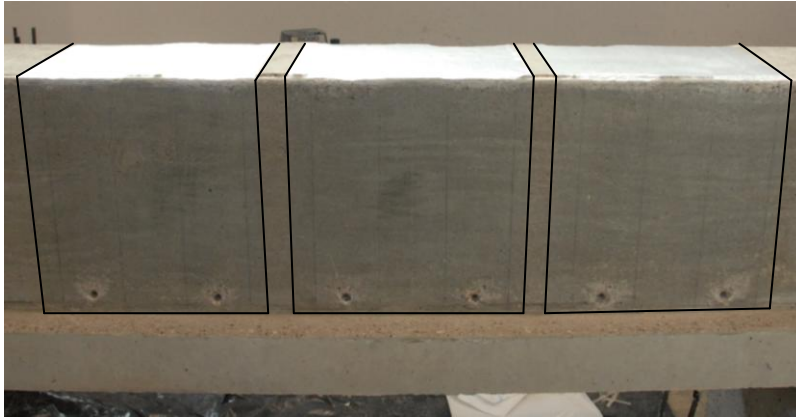


Figure 3-26 Clear plastic liner used to prevent bond between CFRP laminates and surface of the concrete specimen

Once the clear plastic liner was placed over the surface of the beam, the CFRP installation process continued with the same steps as used for the bonded case. The completed installation of the unbonded CFRP can be seen in Figure 3-27.

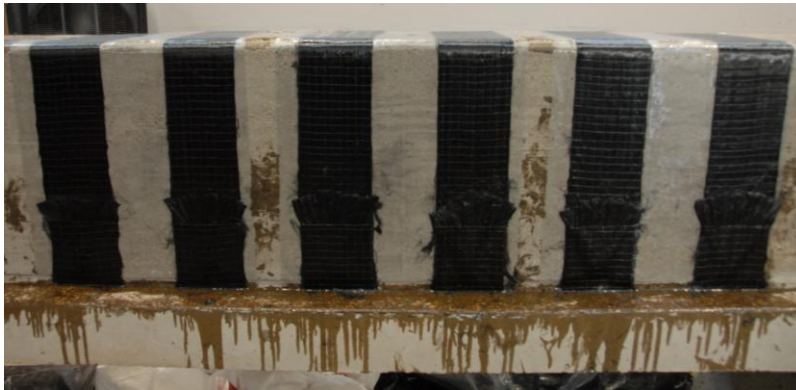


Figure 3-27 Completed installation of unbonded CFRP

3.3 EXPERIMENTAL TEST SETUP

Separate setups were developed for fatigue and sustained loading tests.

3.3.1 Fatigue load tests

The fatigue load test setup consisted of a three point loading system. Four large steel columns were erected and bolted to the strong floor below in the laboratory. Each

column was connected to a bolt group that could withstand a total force of 200-kips. Therefore, the fatigue test setup could resist a total load of 800-kips, far exceeding the needed capacity.

A large steel W-section was bolted to the bottom of two steel W-sections bolted to the erected columns. The large steel W-section supported a hydraulic ram capable of applying cyclic or monotonic loads. The hydraulic ram had a capacity of 235-kips when attached to a closed loop system capable of applying cyclic loads and a 784-kip capacity when attached to an open loop system capable of applying monotonic loads. For the case of fatigue loading, the closed loop system was then attached to a controller that allowed the user to program the desired applied load range and to monitor the number of load cycles applied. The beam was then loaded on the top flange. A photo of the fatigue test setup is shown in Figure 3-28 with an elevation view of the test setup displayed in Figure 3-29.



Figure 3-28 As-built fatigue load test setup

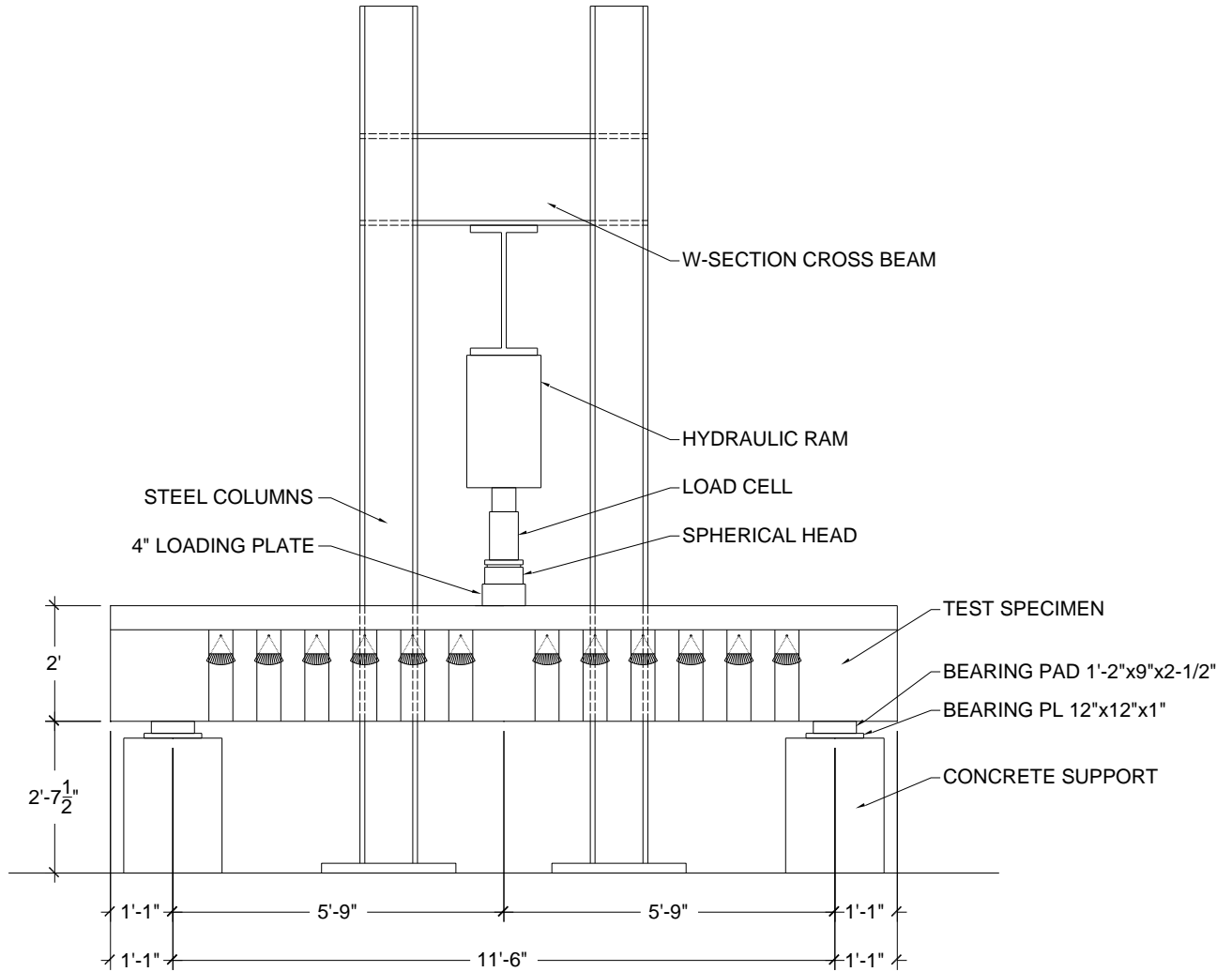


Figure 3-29 Elevation view of fatigue load test setup

3.3.1.1 Loading and reaction points

A 300-kip load cell was attached to the hydraulic ram to monitor the load applied to the beam. A large steel plate was then used as a spreader beam to help uniformly distribute the load to the test specimen. The steel plate was placed on the surface of the test specimen using hydrostone to help ensure uniform contact across the length of the steel plate. A spherical head was used to transfer load from the load cell and steel plate

to adjust for alignment imperfections between the hydraulic ram and the test specimen. A picture of the loading apparatus is shown in Figure 3-30.

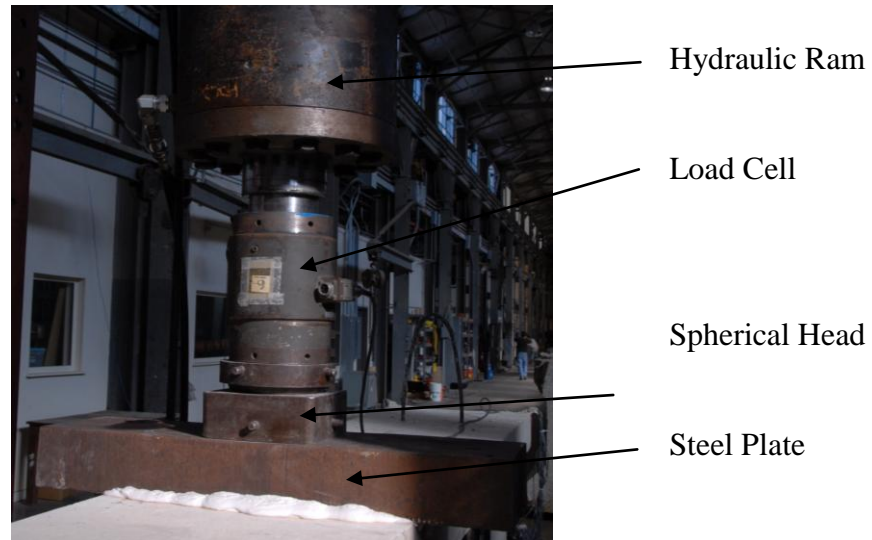


Figure 3-30 Load application System

The reaction points consisted of neoprene bearing pads (1'-2"x9"x2 1/2") centered on steel plates (12"x12"x1"). The steel plates were grouted with hydrostone to the surface of the concrete end supports and the concrete end supports were then hydrostoned to the floor below. The hydrostone was used to help provide a level loading surface for the test specimen. Figure 3-31 shows the as-built end reaction support.



Figure 3-31 Reaction support

3.3.1.2 Prestressed external clamps

Following the completion of fatigue loading, the test specimens were loaded to failure to help determine the effects of fatigue loading on ultimate load capacity. The test specimens were initially loaded until failure occurred on one side of the test specimen, either on the bonded or unbonded side. Then prestressed external clamps (Figure 3-32) were used to provide external reinforcement to the already failed side. These prestressed clamps consisted of two HSS 8x8x1/2" tubes placed on the top flange of the specimen and under the bottom side of the concrete web. They were connected using two high strength, one inch diameter threaded rods. Each threaded rod was prestressed with a force of 30-kips and therefore each external clamp provided a 60-kip clamping force to the test specimen. This clamping system was very effective in providing adequate additional strength so that a shear failure of both ends could be produced.



Figure 3-32 Prestressed external clamps

3.3.2 Sustained load tests

A test set up was developed for the long-term (sustained) load test specimens so that two specimens could be loaded simultaneously to the same level. The test setup consisted of one beam being placed in the normal loading direction and resting on two concrete end supports near each reaction point. A 1'-6"x10"x5" steel plate was then placed at the center of the top flange and grouted in place. The second test specimen was

then rotated flange down and grouted in place directly above the first test specimen. A large clamping system consisting of steel HSS tubes, high strength Dywidag rods, and springs was used to provide a reaction force of 80-kips to each end of the test specimen. This resulted in a midpoint load of 160-kips being applied to each test specimen. The tested shear spans are equivalent to those tested during the fatigue loading portion of the research project. An elevation view of the test setup is displayed in Figure 3-33 and a photo of the test setup is shown in Figure 3-34.

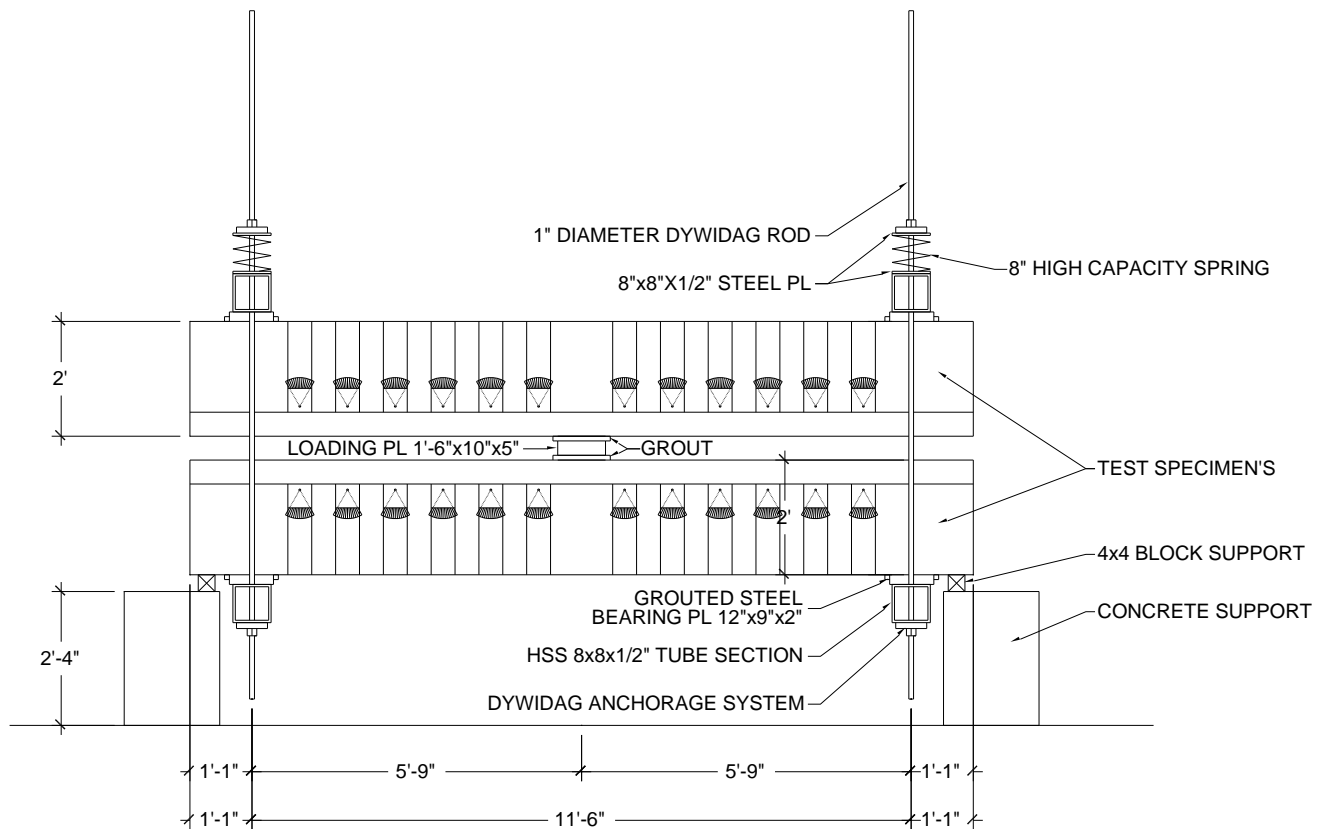


Figure 3-33 Elevation view of sustained load test setup



Figure 3-34 Sustained load test setup

3.3.2.1 Loading and reaction points

The loading point consisted of a 1'-6"x10"x5" steel plate centered between both test specimens. The steel plate was grouted in place to help prevent the beams from rotating during the loading process. It was important to center the steel plate between the two test specimens to ensure stability during loading. Figure 3-35 displays a photo of the grouted steel plate.



Figure 3-35 Grouted loading point

The load was applied to the test specimens through the reaction points. Each reaction point consisted of a 12"x9"x2" steel plate that was grouted to the bottom surface of the concrete specimen. Then a steel HSS 8x8x1/2" tube was used to transfer the force to the steel bearing plate. Holes were drilled in each end of the steel tube to allow for a 1-in. diameter, high strength Dywidag rod to pass through the steel tube. The Dywidag rods were then anchored using a 1 1/4-in. thick steel plate and a domed anchor nut (Figure 3-36). Figure 3-37 displays a photo of the end reaction support prior to stressing.



Figure 3-36 Dywidag anchorage system



Figure 3-37 Reaction support

3.3.2.2 Initial loading system

One major variable associated with the testing conducted was the performance of CFRP on specimens strengthened prior to cracking of the reinforced concrete beam compared with specimens strengthened after initial cracking. In order to accommodate this, the top test specimen was strengthened prior to cracking and before it was placed in

the test setup. The bottom specimen was placed in the test setup prior to the application of CFRP and then cracked using the current test setup. Four center hole, hydraulic rams were used on the bottom side of the specimen to provide a load of 160-kips at the midpoint of the specimen (Figure 3-38). The hydraulic rams were placed on the bottom side of the test setup to provide easy access to the hydraulic pump. One hydraulic ram was placed over each Dywidag road and anchored to the bottom side of the test setup (Figure 3-39). All four hydraulic rams were then attached to the same hydraulic pump to ensure that the load was applied evenly over all four loading points. Once the bottom beam was cracked then the load was released and the hydraulic rams were removed.



Figure 3-38 Initial loading test setup



Figure 3-39 Hydraulic loading system for initial loading

3.3.2.3 Final loading setup

After the application of CFRP on the cracked specimen, the final load was applied. Four, 8-in. springs were used to reduce any losses due to relaxation or creep and to maintain a nearly constant load over the duration of the test. Four springs were used in the test. One spring was placed over each Dywidag rod with the Dywidag rod running through the center of the spring. A steel plate, 8"x8"x1/2", was placed on either side of the spring to provide a level surface to transfer the forces from the spring to the HSS tube below. Once the springs were in place, the Dywidag anchorage system was then secured to the top of the springs. Steel loading chairs were placed on top of the Dywidag anchorage system and hydraulic rams were placed above the loading chairs and secured using the previous anchorage system (Figure 3-40). Once again, the four hydraulic rams were attached to the same hydraulic pump to provide a uniform force at each loading point. An 80-kip load was applied to each end of the test specimen resulting in a midpoint load of 160-kips. Once the appropriate load was reached, the domed anchor nuts were tightened down above the spring and the load was released. The tightened nuts then held the previously applied midpoint load of 160-kips. The test setup was loaded from the top of the setup due to a lack of space beneath the specimen because of the additional height of the springs and loading chairs. A photo of the final load application can be seen in Figure 3-41.



Figure 3-40 Hydraulic loading system for final loading



Figure 3-41 Final loading test setup

3.4 INSTRUMENTATION

3.4.1 Steel strains

The strain in the steel reinforcement was monitored using strain gauges. These gauges were placed on the steel stirrups and on the longitudinal steel. The majority of gauges were placed on the steel stirrups to monitor changes in strain in the stirrups. Some additional gauges were then placed on the longitudinal steel to monitor flexural response.

Standard electrical resistance gauges were bonded to the surface of the steel reinforcement. Prior to installation, the bar lugs located where the gauge was to be placed was ground off to provide a smooth surface for the gauge. The smooth surface was then cleaned to remove any dirt and the gauge was bonded to the surface of the steel using a high strength adhesive. A wax coating was then used to cover the gauge to help prevent water damage from the concrete during casting. Once the wax solidified, a rubber pad was wrapped around the steel, covering the surface of the gauge in the process. The rubber pad helped to prevent the gauges from being damaged by

mechanical vibrators used during casting. The yellow rubber pads can be seen in Figure 3-42.



Figure 3-42 Reinforcement cages after installation of steel strain gauges

A grid system was developed to maintain consistency in the placement of the steel strain gauges for all the test specimens. The grid developed for the steel strain gauges is displayed in Figure 3-43. For each test specimen, gauges were placed along certain intersections of the grid lines on one side of the test specimen. Several redundant gauges were also placed on the opposite side of the reinforcement cage in critical locations along the shear span. Steel strain gauges were placed in the same grid locations for all four test specimens.

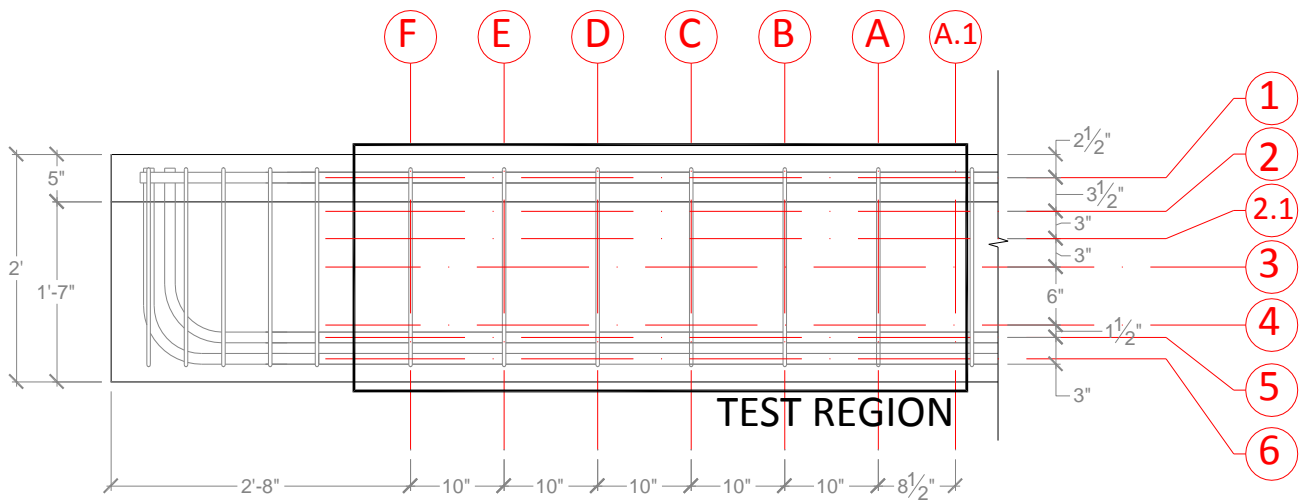


Figure 3-43 Steel strain gauge grid for all test specimens

In order to keep track of the gauges used during testing, nomenclature was developed to organize the strain information. Each gauge was designated by its grid placement. Redundant gauges were labeled with an additional R and gauges located on the side strengthened using unbonded CFRP were labeled with an additional O. Figure 3-44 presents details of the nomenclature described above.

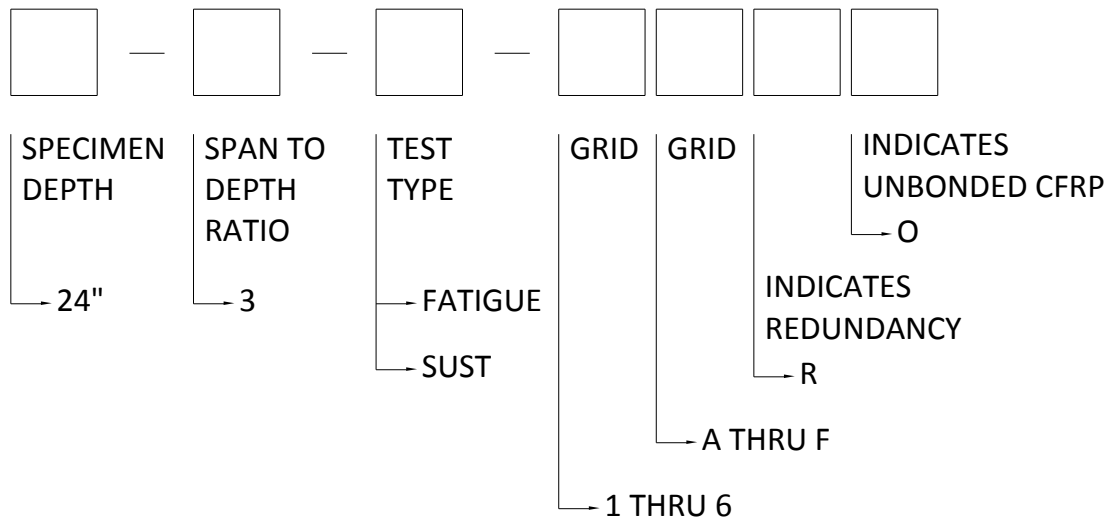


Figure 3-44 Steel strain gauge nomenclature

3.4.2 CFRP strain

CFRP strains were monitored using a system similar to that used for monitoring steel strains. The CFRP gauges consisted of a standard electrical resistor similar to the ones used in the steel gauges and displayed in Figure 3-45. A two-part composite material was placed on the surface of the CFRP in the areas where strains were to be monitored. Once cured, the composite material provided a smooth surface so that the CFRP gauge could bond cleanly to the surface of the CFRP.



Figure 3-45 CFRP strain gauge (Pham, 2009)

Since the CFRP gauges would be exposed on the surface of the CFRP strips, it was important to protect the gauges from any external damage. In the case of gauges used during fatigue testing, a black rubber pad was placed over the surface of the CFRP gauge to shield the gauge from damage prior to and during testing (Figure 3-46).

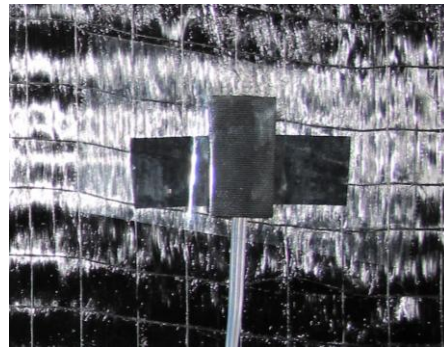


Figure 3-46 Rubber pad used to protect CFRP gauge

For gauges used to monitor CFRP strains in the sustained load tests, a different protection system was used. Since the tests were going to be conducted over a long period of time, preparations were made so that the test specimens could be moved outdoors. Because of this, the CFRP gauges needed to be protected against the elements. A small wax coating was placed over the surface of the gauge to prevent water from damaging the gauge. Then a silicone coating was used to seal the wax around the gauge and to provide an additional layer of protection against any external damage throughout the course of testing. A photo of the protection system used for the long-term CFRP gauges is shown in Figure 3-47.



Figure 3-47 Long-term load gauge protection covering

A second grid system was developed to help maintain consistency in the placement of the CFRP strain gauges for all the test specimens. The grid developed for the CFRP strain gauges is displayed in Figure 3-48. For each test specimen, gauges were placed along certain intersections of the grid lines on one side of the test specimen. Once again, several redundant gauges were also placed on the opposite side of the test specimen in critical locations along the shear span. Similar to the steel gauges, CFRP strain gauges were placed in the same grid locations for all four test specimens.

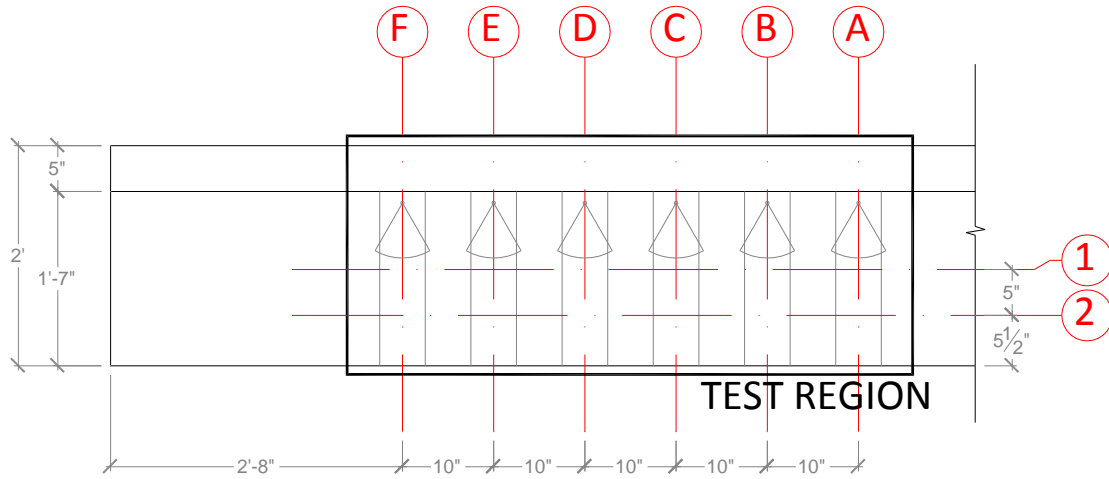


Figure 3-48 CFRP strain gauge grid for all test specimens

In order to keep track of the CFRP gauges used during testing, separate nomenclature (Figure 3-49) was developed to organize the strain information. Each gauge was once again designated by its grid placement, but each CFRP gauge was prefaced by a letter F, denoting a gauge placed directly on the fiber material. Redundant gauges were labeled with an additional R and gauges located on unbonded CFRP were labeled with an additional O.

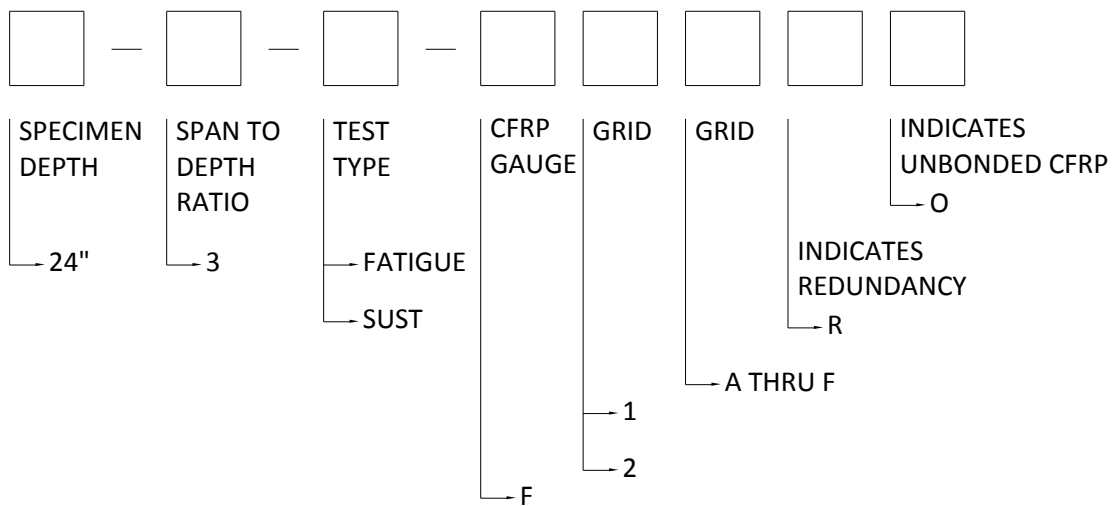


Figure 3-49 CFRP strain gauge nomenclature

3.4.3 Deformations

Several measurement devices were used to help collect information about deformations during testing. The following sections describe the instruments used to collect the deformation data including:

- Linear Variable Differential Transformers (LVDTs)
- Demountable Mechanical (DEMEC) strain gauges

3.4.3.1 Linear Variable Differential Transformers (LVDTs)

Linear Variable Differential Transformers (LVDTs) were used to monitor the displacements of the test specimen during fatigue loading. Two LVDTs were placed on either side of the test specimen at the location of the applied load at the midpoint of the specimen. The plunger of the LVDT rested on a steel plate that was attached to the bottom surface of the test specimen as shown in Figure 3-50. A high strength epoxy was used to bond the steel plate to the surface of the concrete to help maintain bond between the concrete and the plate during cyclic loading.

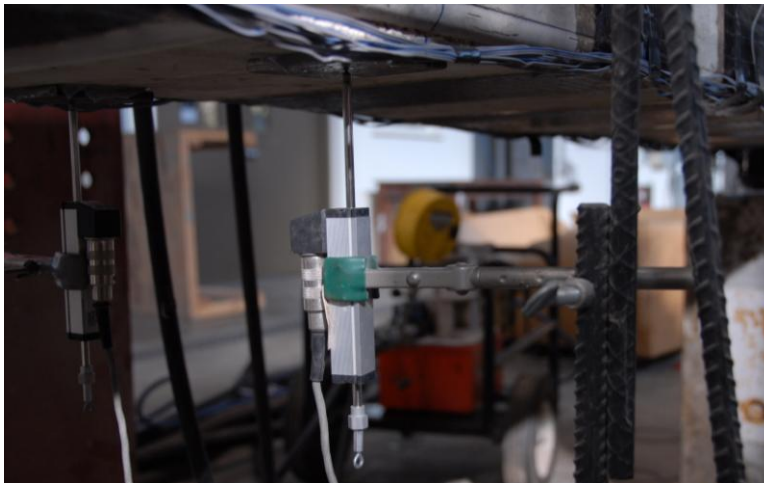


Figure 3-50 LVDT used to monitor displacements during fatigue testing

3.4.3.2 Demountable Mechanical (DEMEC) strain gauges

Demountable Mechanical (DEMEC) strain gauges were used to monitor surface strains during the long-term load tests. These measurement devices provided an

additional source of strain data in case the electrical strain gauges drifted or failed over time. This measurement system consisted of an extensometer equipped with a digital dial to provide on-the-spot readings and a 16-in. by 16-in. grid of DEMEC points attached to the surface of the test specimen. The DEMEC measurement device is shown in Figure 3-51.



Figure 3-51 DEMEC measuring device

The DEMEC measuring device was used to measure the distance between a grid of pre-drilled stainless steel discs referred to as DEMEC points. These DEMEC points were attached to the surface of the concrete specimen using a high strength, two-part epoxy to form a 16-in. by 16-in. grid with 8-in. spacing between the DEMEC points. The dimensions of the DEMEC point grid are displayed in Figure 3-52. The grid of DEMEC points was located in the center of the shear span of the test specimen as displayed in Figure 3-53. The DEMEC measuring system was used to track changes in surface strain throughout testing and also provided information about the changes in crack width over time.

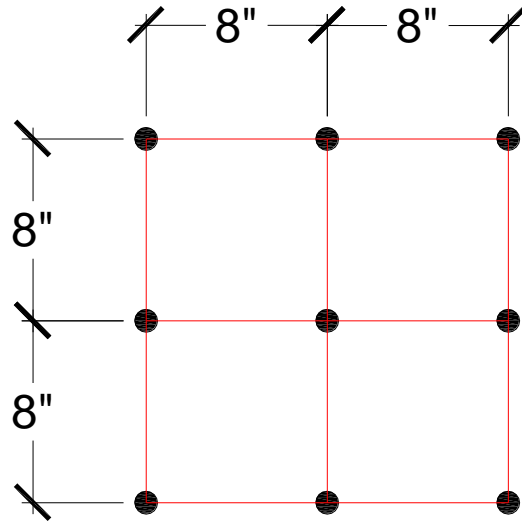


Figure 3-52 DEMEC point grid

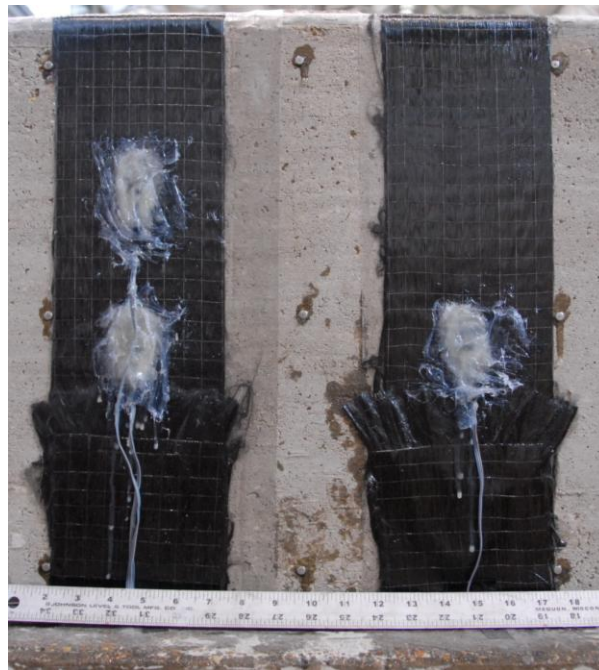


Figure 3-53 As-built DEMEC point grid

The DEMEC measuring system was also used to track the changes in end deflections between the two test specimens during testing. DEMEC points were placed

on the surface of the end regions of the top and bottom specimens at each end of the test specimen as shown in Figure 3-54.



Figure 3-54 DEMEC points used to track changes in end displacements

CHAPTER 4

Test Results Under Fatigue Loading

4.1 INTRODUCTION

The test results and data obtained under fatigue loading are presented in this section. Data is presented for two types of test: (1) specimens fatigue tested at a high number of cycles (greater than 1 million cycles) and (2) previously fatigue tested specimens monotonically loaded to failure.

The following information is presented:

- Strains in the steel stirrups and CFRP strips as number of cycles increase
- Load-displacement curves for cycled specimens
- Load-displacement curves for specimens taken to ultimate failure
- Strains in the steel stirrups and the CFRP strips at ultimate failure

4.2 FATIGUE TEST SERIES

The fatigue loading test series consisted of four tests described in Table 4-1.

Table 4-1 Fatigue Loading Test Matrix

| <i>Fatigue Loading Test Series</i> | | | | <i>a/d ratio equal to 3</i> |
|------------------------------------|----------------------|------------------|---------------------------|-----------------------------|
| Test Number | Load Range | Number of Cycles | Procedure | Bonded/Unbonded CFRP |
| 24-3-Fatigue-1B | 70-kips to 90-kips | 1,028,000 | Strengthened Uncracked | Bonded |
| 24-3-Fatigue-1U | 70-kips to 90-kips | 1,028,000 | Strengthened Uncracked | Unbonded |
| 24-3-Fatigue-2B | 110-kips to 130-kips | 2,450,000 | Strengthened Uncracked | Bonded |
| 24-3-Fatigue-3B | 70-kips to 90-kips | 1,254,000 | Strengthened Cracked | Bonded |
| 24-3-Fatigue-3U | 70-kips to 90-kips | 1,254,000 | Strengthened Cracked | Unbonded |
| 24-3-Fatigue-4B | 110-kips to 130-kips | 2,337,000 | Strengthened Cracked | Bonded |
| 24-3-Fatigue-4U | 110-kips to 130-kips | 2,337,000 | Strengthened Cracked | Unbonded |

In this matrix, the first column identifies the test as defined by Figure 3-1. The second column indicates the load range applied. The next column indicates the number of cycles applied to the test specimen at the load range noted in the previous column. The CFRP layout used in all instances consisted of 5-in. CFRP strips spaced at 10-in. on-center. Each CFRP strip was anchored to the top of the concrete web using one CFRP anchor on each side of the test specimen. So each CFRP strip was anchored using two CFRP anchors. The next column specifies whether the test specimen was strengthened with CFRP laminates prior to or after initial cracking of the specimen. The final column specifies whether the CFRP laminates used were bonded to the surface of the concrete or unbonded.

4.2.1 24-3-Fatigue-1 & 2 (Uncracked specimen)

The test specimen was strengthened before cracking using CFRP laminates. One end of the test specimen was strengthened using bonded CFRP laminates and the other end was strengthened using unbonded CFRP laminates. The test specimen was then

loaded until a crack width of 0.013-in. developed on each end of the test specimen. As a result of the increased stiffness due to the presence of bonded CFRP, an initial load of 125-kips was needed to produce the desired crack width on each end of the specimen. The test specimen was then unloaded prior to the application of the cycled load.

Each specimen was subjected to two different series of cycled loads. The first series, 24-3-Fatigue-1, was cycled between a load of 70-kips and 90-kips for approximately 1 million cycles. For the second series, 24-3-Fatigue-2, the cycled load range was increased to 110-kips and 130-kips and cycled for an additional 2.5 million cycles. Photos of the test specimen after completion of the cycled load series can be seen in Figure 4-1. Concrete cracks observed during testing are outlined in red.

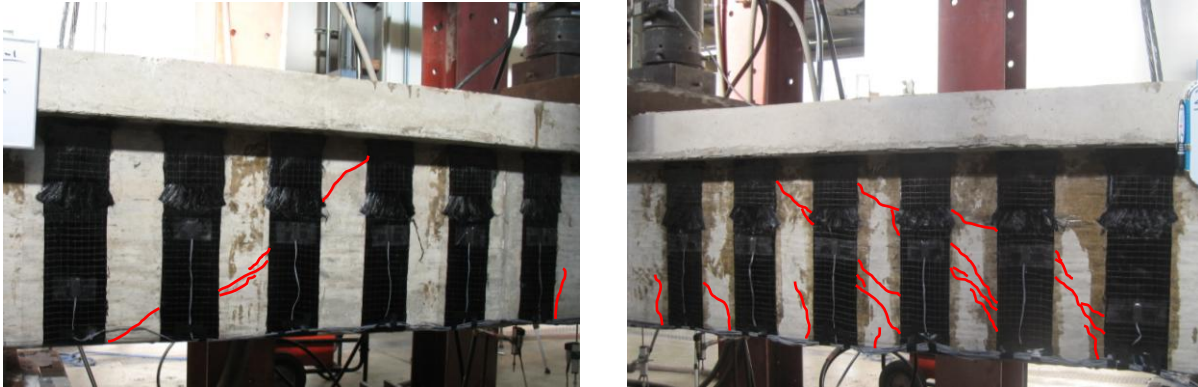


Figure 4-1 24-3-Fatigue-1&2 unbonded (left) and bonded (right) CFRP test specimen

The load-displacement response was recorded for the initial cracking of the test specimen as well as for both series of cycled load tests. The data for the unloading curve of the load displacement response was not recorded for tests 24-3-Fatigue-1 and 2. The load-displacement response of these tests is shown in Figure 4-2 and a linear unloading curve was assumed for tests 24-3-Fatigue-1 and 2. For the purpose of the load-displacement plot, the peak load and displacement values were used to plot the portion of the load-displacement curve during the cycled loading portion of the test. This resulted in a plateau forming at the peak of the load-displacement plot for tests 24-3-Fatigue-1 and 2.

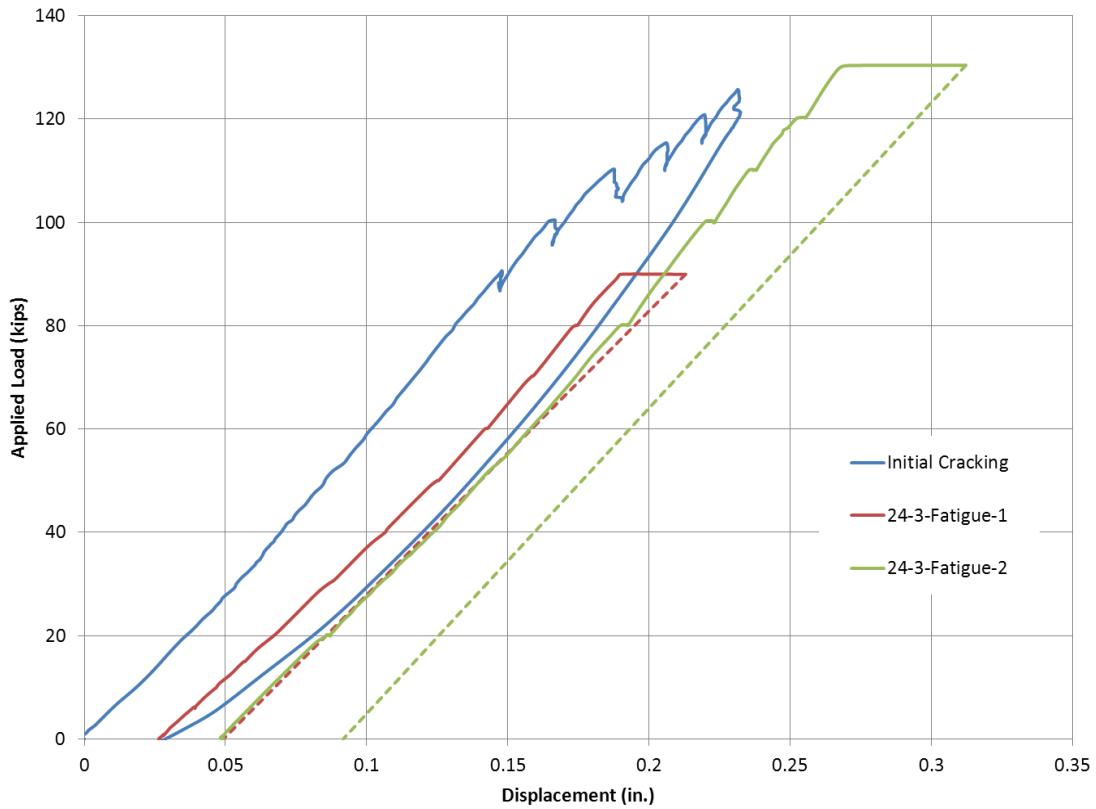


Figure 4-2 Load displacement response, test 24-3-Fatigue-1&2

4.2.1.1 Test 24-3-Fatigue-1U (Uncracked specimen , unbonded CFRP)

For the end strengthened using unbonded CFRP, large cracks were observed during the course of testing. One large shear crack developed in the shear span after the initial loading of the test specimen and continued to widen throughout the course of the cycled loading. Crack widths increased from 0.025-in. at the start of cyclic loading to 0.037-in. after the completion of 1,028,000 cycles. Steel strains were relatively high throughout the course of testing and remained near yielding for the duration of loading.

CFRP strains remained very low throughout testing. In cases where bond between the CFRP and the surface of the concrete was removed, large deformations were observed in the concrete without large increases in the CFRP strain. The lack of bond allowed for large strains to develop in the steel stirrups with minimal strain in the CFRP.

After the completion of test 24-3-Fatigue-1, clamps were placed on the unbonded end of the test specimen prior to the increasing of the cycled load to prevent a premature failure of the specimen on the unbonded end due to increasingly high strains in the internal stirrups.

4.2.1.2 Test 24-3-Fatigue-1B & 2B (Uncracked specimen , bonded CFRP)

For the end strengthened using bonded CFRP, relatively small cracks were observed during the course of testing. Several small shear cracks developed throughout the shear span as opposed to the one large shear crack that developed on the unbonded end of the test specimen. Crack widths increased from 0.007-in. at the start of cyclic loading to 0.011-in. after the completion of 1,028,000 cycles at the lower load level. Once fatigue testing resumed following the clamping of the unbonded end of the test specimen, shear cracks increased from 0.017-in. to 0.024-in. after the completion of 2,450,000 cycles at the higher load level. Crack widths remained significantly smaller than those on the unbonded end of the test specimen throughout testing. After the completion of approximately 3.5 million cycles, crack widths on the bonded end of the specimen were 0.013-in. smaller than crack widths on the unbonded end of the specimen following only 1 million cycles at a lower load level.

Steel strains remained relatively low throughout testing. These strains showed very small increases during testing and were significantly less than steel strains observed on the unbonded end of the test specimen.

CFRP strains were observed to be much higher on the bonded end of the test specimen. The presence of bond allowed for the CFRP to contribute to the shear capacity of the specimen at much smaller deformations and increased the fatigue life of the internal steel by decreasing the strains in the steel at similar load levels due to the load sharing effect described in 2.2.1.

4.2.1.3 Discussion of tests 24-3-Fatigue-1 & 2

Steel and CFRP strains for tests 24-3-Fatigue-1 and 2 are presented in Figure 4-3 and Figure 4-4 respectively.

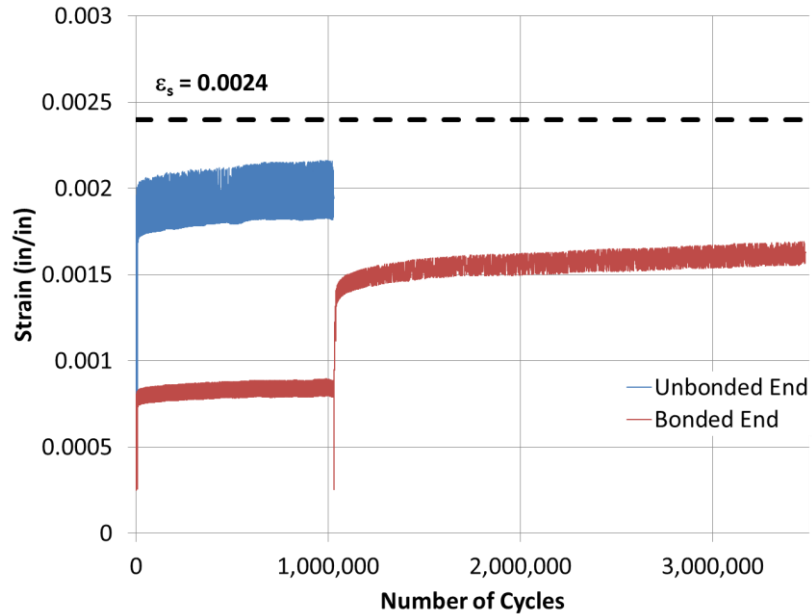


Figure 4-3 Steel strains, Tests 24-3-Fatigue-1&2

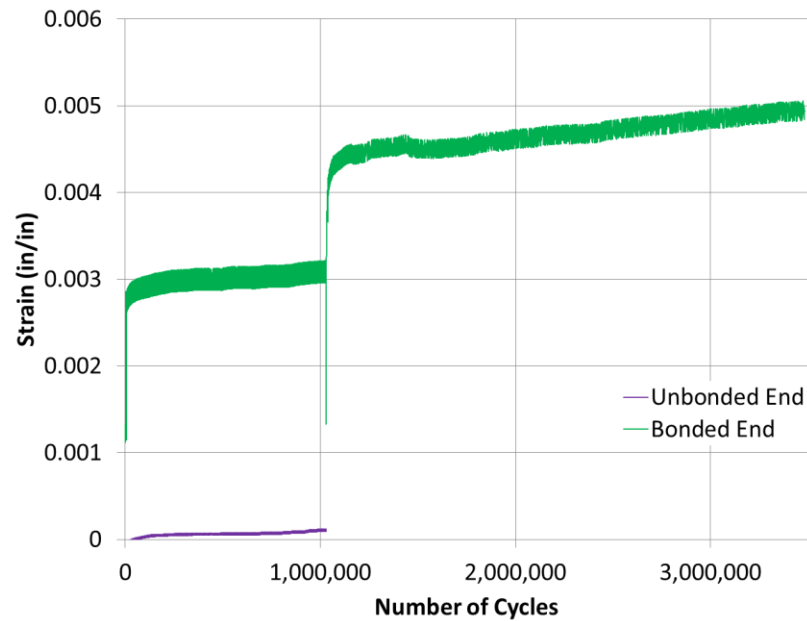


Figure 4-4 CFRP strains, Tests 24-3-Fatigue-1&2

The presence of bond between the concrete surface and CFRP laminates greatly reduced the recorded steel strains in test 24-3-Fatigue-1B compared with test 24-3-1U. The highest strains observed in the internal transverse reinforcement in test 24-3-Fatigue-2B after 3.5-million cycles were lower than the strains observed in the internal steel for test 24-3-Fatigue-1U after only 1-million cycles at a lower load range. These lower strain values indicate an increase in fatigue life in specimens strengthened using bonded CFRP laminates. This agrees with work done by Aidoo, Harries, and Zorn (2004) where they found that specimens strengthened using bonded CFRP laminates demonstrated an increased fatigue life due to the bonded laminates relieving stress demand on the steel. It is noteworthy here that the location of steel strain gauges with respect to the critical shear cracks affects the recorded strains significantly. Steel strain gauges were located very close to the critical shear crack for both bonded and unbonded tests.

The CFRP strains in the testing end strengthened with bonded CFRP laminates were considerably higher than the strains present in the CFRP on the end strengthened using unbonded CFRP. The presence of bond allowed for localized strains to form in regions near cracks, resulting in higher strain readings. This same effect was not present in the end strengthened using unbonded laminates. For the unbonded laminates, strains resulted from elongation of the CFRP strip over the entire length of the CFRP sheet. Therefore, larger steel strains and crack widths developed without larger corresponding strains in the CFRP. CFRP strains on both ends of the test specimen increased gradually throughout testing, but no deteriorations in strength were observed.

4.2.2 24-3-Fatigue-3 & 4 (Cracked specimen)

The second fatigue test specimen was strengthened using CFRP laminates following the cracking of the reinforced concrete beam. The unstrengthened specimen was initially loaded until a crack width of 0.013-in. developed on each end of the test specimen. Since neither end was strengthened prior to the initial cracking of the test specimen, the desired crack widths were produced using a much lower applied load than

the cracking load in tests 24-3-Fatigue-1 and 2. The test specimen was then unloaded and CFRP laminates were applied to the test specimen prior to the application of the cycled load. One end of the test specimen was strengthened using bonded CFRP laminates and the alternate end of the specimen was strengthened using unbonded CFRP laminates.

Similar to the previous beam tested, each specimen was subjected to two different series of cyclic loads. The first series, 24-3-Fatigue-3, was cycled between a load of 70-kips and 90-kips for approximately 1 million cycles. For the second series, 24-3-Fatigue-4, the cycled load range was increased to a load between 110-kips and 130-kips and cycled for approximately 2.5 million more cycles. Photos of the test specimen after completion of the cycled load series can be seen in Figure 4-5. Concrete cracks observed during testing are outlined in red.

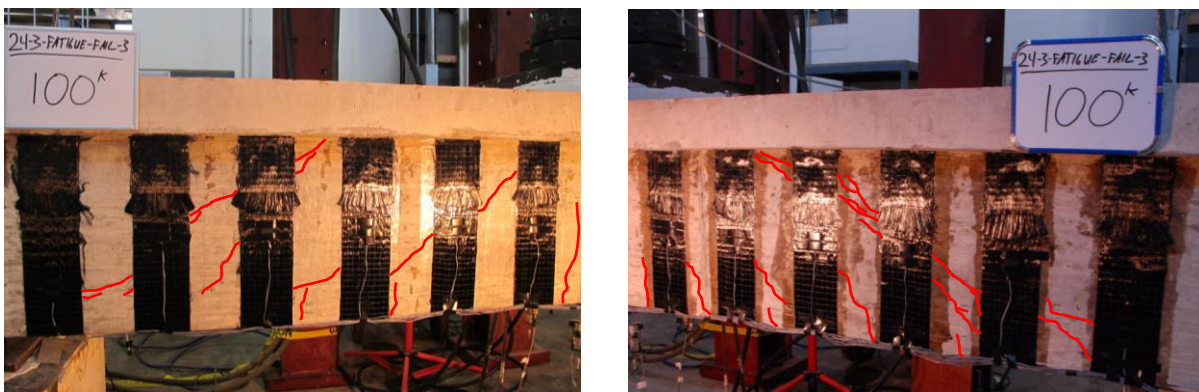


Figure 4-5 24-3-Fatigue-3&4 unbonded (left) and bonded (right) CFRP test specimen

Once again, the load-displacement response was recorded for the initial cracking of the test specimen as well as for both series of cycled load tests. The data for the unloading curve of the load displacement response was not recorded for tests 24-3-Fatigue-3 and 4. The load-displacement response of these tests is shown in Figure 4-6 and a linear unloading curve is assumed for tests 24-3-Fatigue-3 and 4. As stated previously, the peak load and displacement values were used to plot the portion of the load-displacement curve during the cycled loading portion of the test. This resulted in a plateau forming at the peak of the load-displacement plot for tests 24-3-Fatigue-3 and 4.

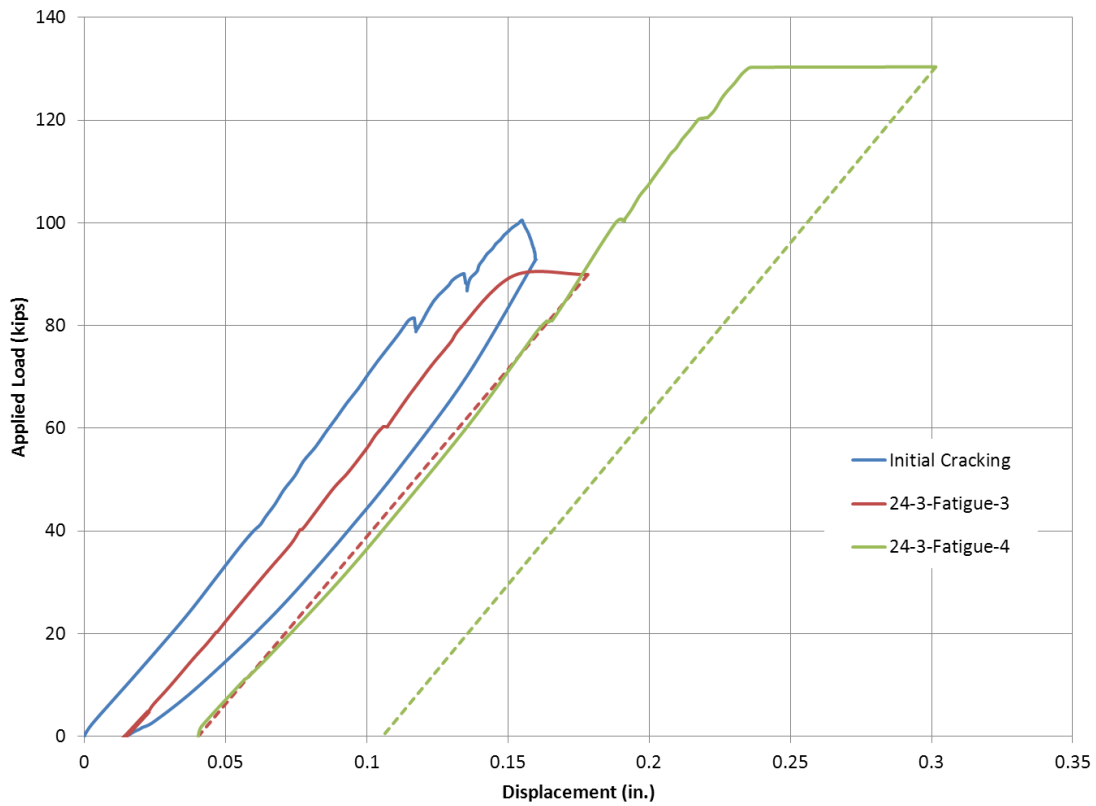


Figure 4-6 Load displacement response, test 24-3-Fatigue-3&4

4.2.2.1 Test 24-3-Fatigue-3U & 4U (Cracked specimen , unbonded CFRP)

For the end strengthened using unbonded CFRP, a shear crack opened near the support after the initial loading of the test specimen with few additional cracks forming throughout testing at the lower load level. The main shear crack continued to widen throughout testing in a similar manner to test 24-3-Fatigue-1U. Since shear crack widths were relatively equivalent on both the bonded and unbonded ends of the test specimen and strains in the internal steel on the unbonded end were lower than previously observed in test 24-3-Fatigue-1U, the unbonded end of the test specimen was left unclamped for the second series of fatigue loading, test 24-3-Fatigue-4. A second large shear crack opened near the loading point within 100,000 cycles of the increased loading test. Shear cracks increased from 0.037-in. to 0.055-in. after the completion of 2,337,000 cycles at

the higher load level. The two main shear cracks accounted for the majority of increased deformations, with few other cracks forming during testing.

Steel strains were measured at approximately sixty percent of yield during testing at the lower load level and increased to near yielding levels throughout the higher load test. These strains showed very little increases throughout testing.

CFRP strains were observed to be much higher on the unbonded end of the test specimen that was strengthened after cracking compared with the specimen that was strengthened prior to cracking. The increased load being carried by the CFRP strips resulted in lower strains in the internal steel.

4.2.2.2 Test 24-3-Fatigue-3B & 4B (Cracked specimen , bonded CFRP)

For the testing end strengthened using bonded CFRP, the main shear crack opened in the middle of the shear span and no other major cracks formed during fatigue testing. Similar to the previous bonded CFRP test, smaller cracks formed near the main shear crack during the lower range of fatigue loading as opposed to the widening of the major crack observed in the unbonded tests. Additional small shear cracks formed closer to the loading point during the higher range of loading, but no additional major shear cracks formed during fatigue testing at the higher load range. Shear cracks increased from 0.028-in. to 0.033-in. after the completion of 2,337,000 cycles at the higher load level.

Steel strains remained lower at corresponding load levels compared to the end of the specimen strengthened using unbonded CFRP sheets, but the strains were closer than for tests 24-3-Fatigue-1 and 2. These strains showed gradual increases throughout testing.

Once again, CFRP strains were observed to be higher on the bonded end of the test specimen compared to the unbonded end of the test specimen. An increased load sharing effect was seen on the bonded end of the test specimen. Higher strains were present in the bonded CFRP laminates as compared with the unbonded CFRP laminates

of tests 24-3-Fatigue-1U and 2U. Also, steel strains were much lower at the same location in tests 24-3-Fatigue-1B and 2B compared with tests 24-3-Fatigue-1U and 2U.

4.2.2.3 Discussion of tests 24-3-Fatigue-3 & 4

Steel and CFRP strains for tests 24-3-Fatigue-3 and 4 are presented in Figure 4-7 and Figure 4-8 respectively.

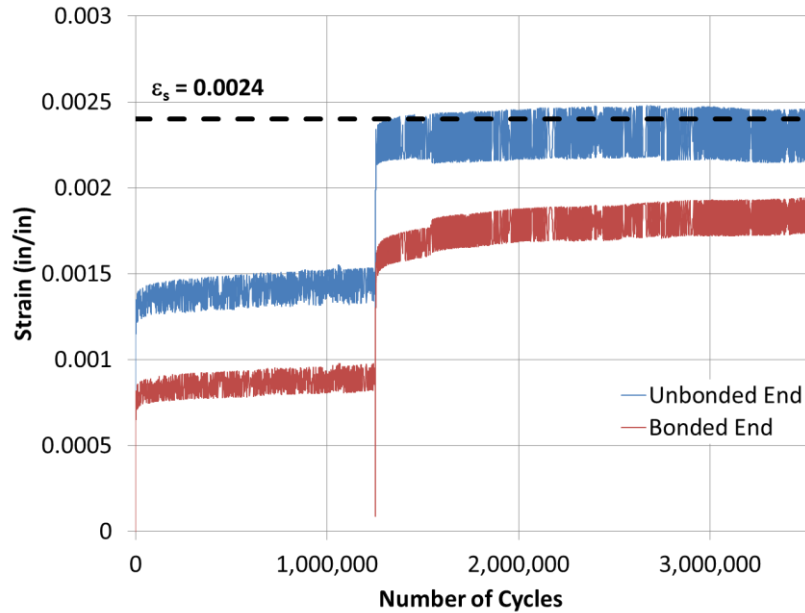


Figure 4-7 Steel strains, Tests 24-3-Fatigue-3&4

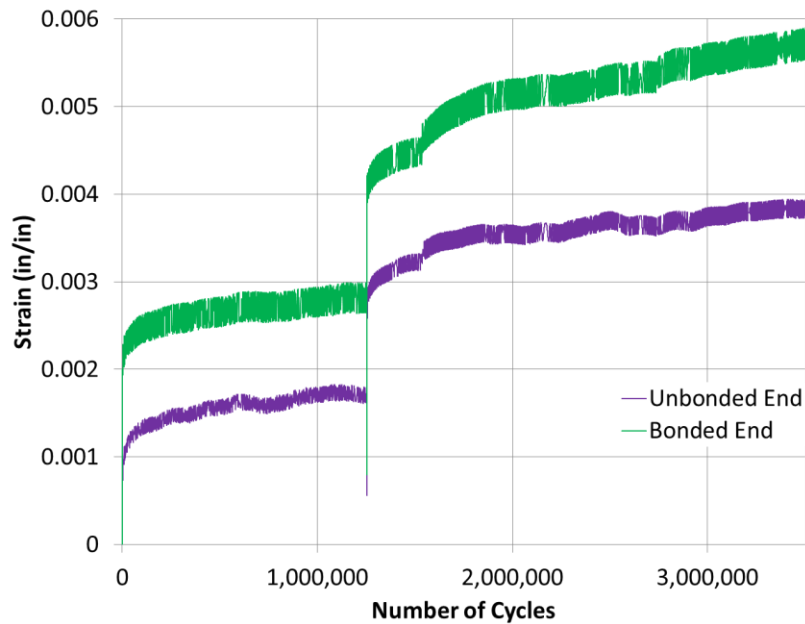


Figure 4-8 CFRP strains, Tests 24-3-Fatigue-3&4

Once again, the presence of bond helped to decrease the strains present in the internal transverse reinforcement. The steel strain reduction in the end strengthened using bonded CFRP laminates was not as great as the reduction observed in tests 24-3-Fatigue-1B and 2B. This agrees with work done by Ferrier, Bigaud, Clement, and Hamelin (2011) where they found that the strain reduction in the internal steel reinforcement was not as great in specimens cracked prior to the application of CFRP compared with those strengthened prior to the cracking of the specimen.

The initial cracking of the specimen allowed for greater strains to develop in the unbonded CFRP. This enabled the unbonded CFRP to share more of the force with the internal steel, resulting in lower strains in the transverse steel reinforcement in test 24-3-Fatigue-3U compared with test 24-3-Fatigue-1U. Once again, CFRP strains were higher in the bonded CFRP compared with the unbonded CFRP due to localized strains developing in the bonded CFRP. The greater contribution from the unbonded CFRP helped to increase the fatigue life of the specimen in a similar way as the previous tests strengthened using bonded CFRP laminates. CFRP strains on both ends of the test specimen increased gradually throughout testing, but no deteriorations in strength were observed. A small increase in strain occurred after approximately 1.5-million cycles due to the fatigue testing machine being tripped and subsequently restarted.

4.2.3 General observations

A summary of the highest strains recorded in the internal transverse reinforcement and the CFRP sheets are presented in Table 4-2.

Table 4-2 Summary of highest strains recorded during fatigue loading

| Test Number | Steel | | CFRP | | Testing Conditions | |
|------------------------|--------|----------------|--------|----------------|---------------------|-----------------------|
| | Strain | Gauge Location | Strain | Gauge Location | Bonded/ Unbonded | Cracked/ Uncracked |
| 24-3-Fatigue-1U | 0.0022 | 4DO | 0.0004 | F1DO | Unbonded | Uncracked |
| 24-3-Fatigue-1B | 0.0010 | 3C | 0.0032 | F1DR | Bonded | Uncracked |
| 24-3-Fatigue-2B | 0.0018 | 3C | 0.0068 | F1D | Bonded | Uncracked |
| 24-3-Fatigue-3U | 0.0016 | 4EO | 0.0018 | F2EO | Unbonded | Cracked |
| 24-3-Fatigue-3B | 0.0010 | 4DR | 0.0030 | F1DR | Bonded | Cracked |
| 24-3-Fatigue-4U | 0.0025 | 4EO | 0.0039 | F2EO | Unbonded | Cracked |
| 24-3-Fatigue-4B | 0.0019 | 4DR | 0.0059 | F1DR | Bonded | Cracked |

In general, steel strains in the end strengthened using bonded CFRP laminates were lower than steel strains in the end strengthened using unbonded CFRP laminates. In a similar manner, strains were higher in the bonded CFRP compared with the unbonded CFRP in all tests. For both tests strengthened with bonded CFRP laminates, CFRP strains were 50-percent higher than the code allowable strain of 0.004 required for cases where CFRP laminates cannot be completely wrapped around a specimen and no deterioration of strength was observed. This demonstrated that CFRP anchors are capable of maintaining large strains in the CFRP in cases of cyclic loading.

Higher strains developed in the bonded CFRP for the test strengthened prior to cracking due to increased localized strains in the CFRP. While strains in the unbonded CFRP for the test strengthened after initial cracking of the specimen were substantially higher than strains in the unbonded CFRP on the specimen strengthened prior to cracking. This demonstrates that for specimens strengthened after the initial cracking of the specimen, the quality of bond between the surface of the concrete and the CFRP laminates is not as vital as for cases of uncracked beams being strengthened. The initial deformations present in the beam following cracking allow for the unbonded CFRP to demonstrate a greater strength contribution during loading for specimens strengthened using unbonded CFRP laminates after initial cracking.

A summary of the maximum crack widths recorded at the beginning and completion of loading are presented in Table 4-3.

Table 4-3 Summary of crack widths recorded during fatigue loading

| Test Number | Max Crack Widths | | Testing Conditions | |
|------------------------|----------------------|--------------------|--------------------|--------------------|
| | Start of Cycled Load | End of Cycled Load | Bonded/Unbonded | Cracked/Un-cracked |
| 24-3-Fatigue-1U | 0.015-in. | 0.037-in. | Unbonded | Un-cracked |
| 24-3-Fatigue-1B | 0.003-in. | 0.011-in. | Bonded | Un-cracked |
| 24-3-Fatigue-2B | 0.017-in. | 0.024-in. | Bonded | Un-cracked |
| 24-3-Fatigue-3U | x* | x* | Unbonded | Cracked |
| 24-3-Fatigue-3B | x* | x* | Bonded | Cracked |
| 24-3-Fatigue-4U | 0.037-in. | 0.055-in. | Unbonded | Cracked |
| 24-3-Fatigue-4B | 0.028-in. | 0.033-in. | Bonded | Cracked |

* - Crack width information was unavailable for test 24-3-Fatigue-3

In general, a large crack would form on the end of the specimen strengthened with unbonded CFRP laminates and widen throughout cyclic loading. The end strengthened with bonded CFRP laminates tended to develop several smaller cracks throughout loading as opposed to having one larger crack. Crack widths increased at a greater rate initially and then plateaued as cyclic loading continued. For the specimen strengthened prior to cracking, crack widths were significantly smaller in the bonded end of the specimen compared with the unbonded specimen. But for the specimen strengthened after initial cracking, crack widths remained closer in value throughout loading and both ends demonstrated similar cracking patterns.

4.3 FATIGUE FAILURE LOAD TEST SERIES

After completion of the fatigue testing described in the previous section, each test specimen was taken to failure. The end of the test specimen that failed first was strengthened using external prestressed clamps described in 3.3.1.2. This allowed the alternate end of the test specimen to also be loaded to failure. Thus, each test specimen produced two separate failure loads.

The fatigue failure load test series consisted of four tests described in Table 4-4.

Table 4-4 Fatigue failure load test matrix

| Fatigue Failure Load Test Series | | | <i>a/d ratio equal to 3</i> |
|---|-----------------------------|----------------------------|------------------------------------|
| Test Number | Bonded/Unbonded CFRP | Procedure | Failure Load |
| 24-3-Fatigue-Fail-1 | Unbonded | Strengthening Uncracked | 214-kips |
| 24-3-Fatigue-Fail-2 | Bonded | Strengthening Uncracked | 270-kips |
| 24-3-Fatigue-Fail-3 | Bonded | Strengthening Cracked | 256-kips |
| 24-3-Fatigue-Fail-4 | Unbonded | Strengthening Cracked | 284-kips |

In this matrix, the first column identifies the test as defined by Figure 3-1. The second column indicates whether the CFRP laminates used were bonded to the surface of the concrete or unbonded. The next column specifies whether the test specimen was strengthened using CFRP laminates prior to or following the initial cracking of the specimen. The last column specifies failure load of the test. Since the load was applied to the test specimen at the midpoint of the specimen, the applied shear load for each test is equal to approximately one half of the total applied load.

4.3.1 24-3-Fatigue-Fail-1 & 2 (Uncracked specimen)

As mentioned previously, the first fatigue test specimen was strengthened using CFRP laminates prior to the cracking of the reinforced concrete beam. One end of the test specimen was strengthened using bonded CFRP laminates and the alternate end of the specimen was strengthened using unbonded CFRP laminates. The unbonded end of

the test specimen failed first at an applied load of 214-kips (applied shear equal to 107-kips). The bonded end of the test specimen failed second at an applied load of 270-kips (applied shear equal to 135-kips). The complete load-displacement response of tests 24-3-Fatigue-Fail-1 and 2 are presented in Figure 4-9.

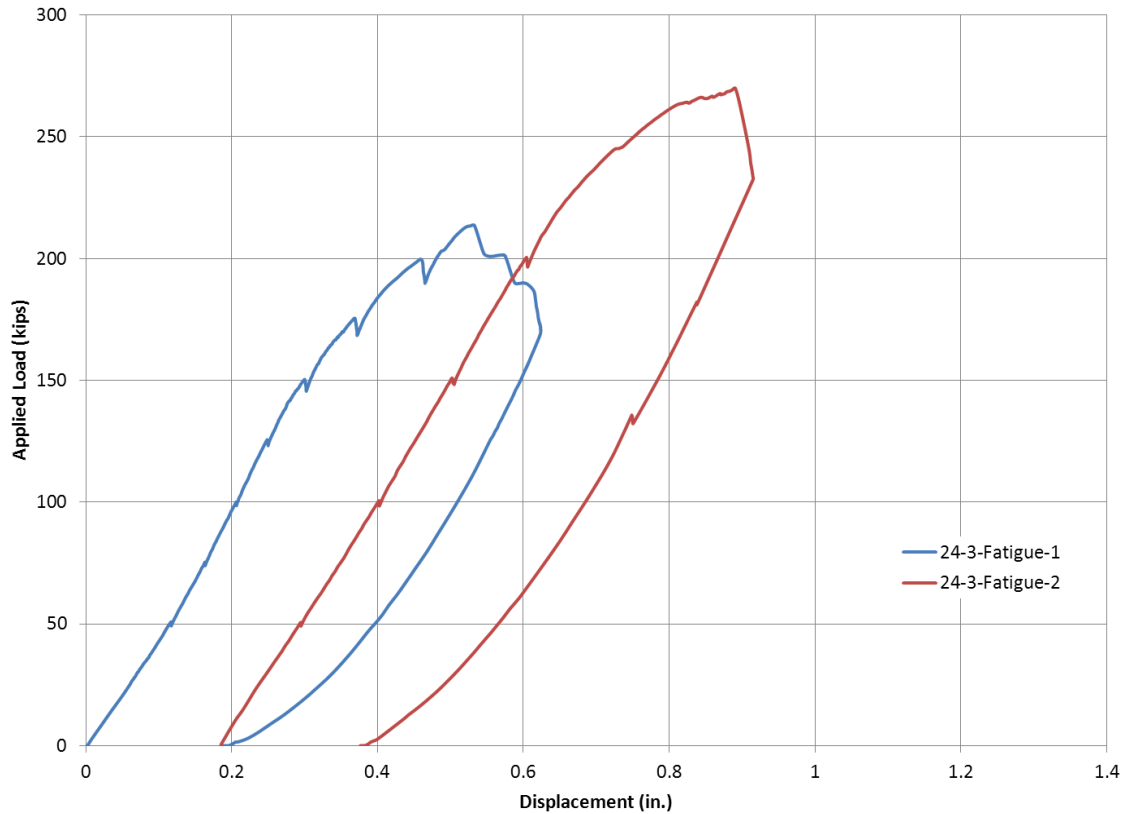


Figure 4-9 Load displacement response, test 24-3-Fatigue-Fail-1&2

4.3.1.1 24-3-Fatigue-Fail-1 (Uncracked specimen, unbonded CFRP)

Test 24-3-Fatigue-Fail-1 failed at an applied load of 214-kips (applied shear = 107-kips). Shear failure of the test specimen was initiated by rupture of a CFRP anchor. Photos of the test specimen before loading and after failure are displayed in Figure 4-10. Concrete cracks observed during testing are marked in green, cracks marked in blue and red developed during the previous fatigue testing of the specimen.

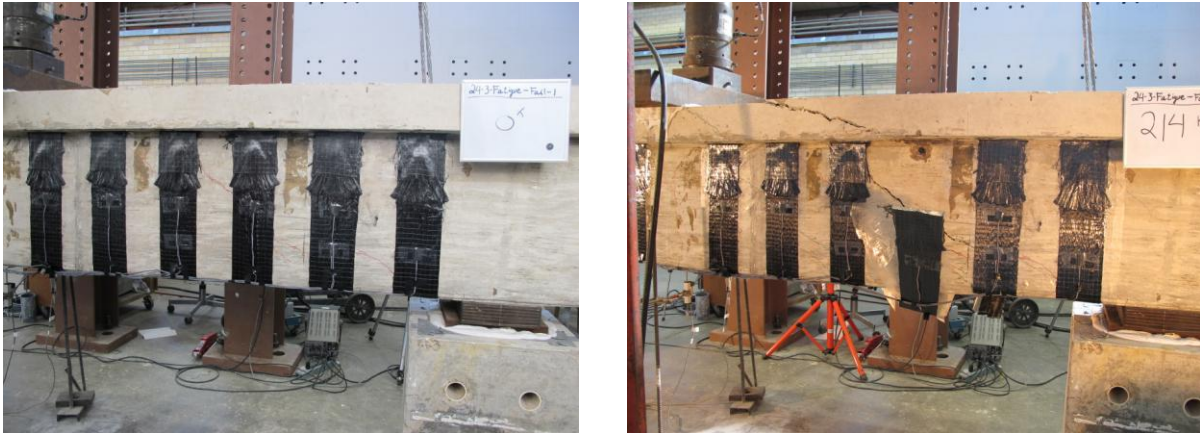


Figure 4-10 24-3-Fatigue-Fail-1 before (left) and after (right) loading

Shear failure of the test specimen followed the rupture of the CFRP anchor (Figure 4-11). After the rupture of the CFRP anchor, the CFRP sheet adjacent to the sheet where the anchor failed ruptured at the bottom corner of the CFRP sheet (Figure 4-12). Just prior to failure, a large crack opened in the top flange of the test specimen.

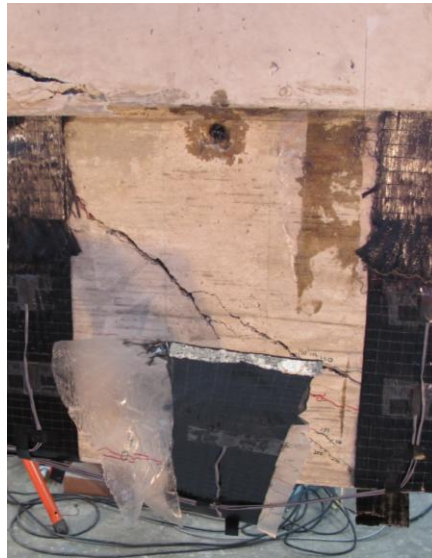


Figure 4-11 Rupture of a CFRP anchor observed during 24-3-Fatigue-Fail-1



Figure 4-12 Rupture of a CFRP strip observed during 24-3-Fatigue-Fail-1

Strains in the steel stirrups were monitored throughout testing with several strain gauges. First yielding of the transverse reinforcement occurred at an applied load of 100-kips (applied shear = 50-kips). Strains were also monitored in the CFRP sheets. The maximum recorded CFRP strain during test 24-3-Fatigue-Fail-1 was 0.0057. The high strain value was recorded at the location where the CFRP strip fractured, but was lower than the manufacturer reported ultimate tensile strain value of 0.0105.

The strain values recorded in the CFRP and steel at various stages of the loading process and corresponding photos are presented in Figures 4-15 through 4-18. Strain data and photos of the specimen prior to loading are included to display the residual stresses present in the specimen following the fatigue loading of the beam. The strain values presented are the maximum strain values recorded for each material at given distances from the location of applied load.

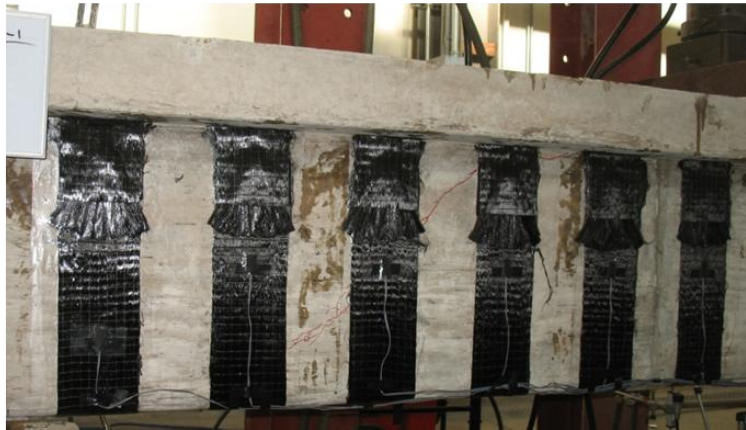
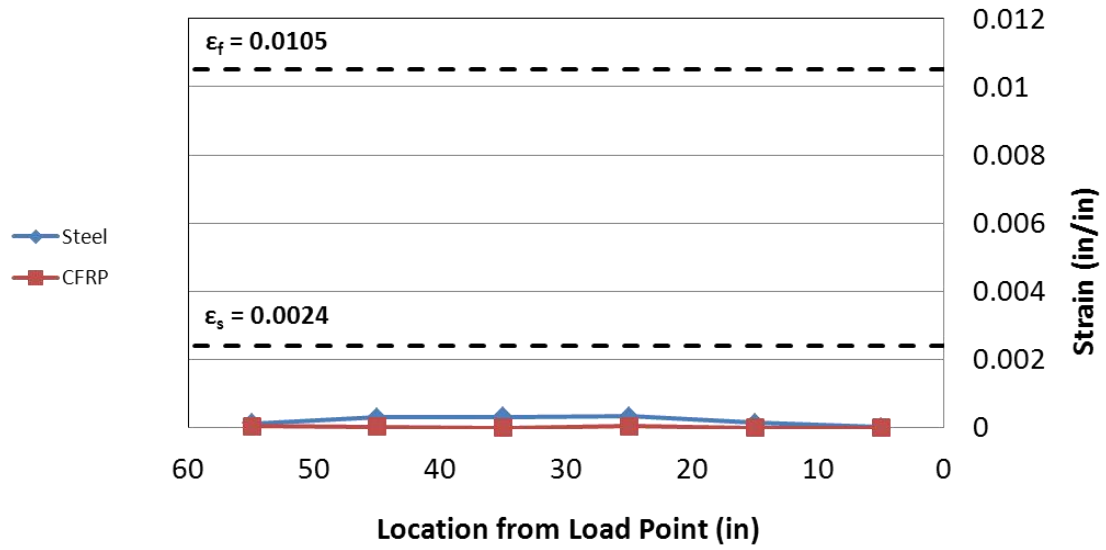


Figure 4-13 24-3-Fatigue-Fail-1 at 0-kips applied load (0-kips applied shear)

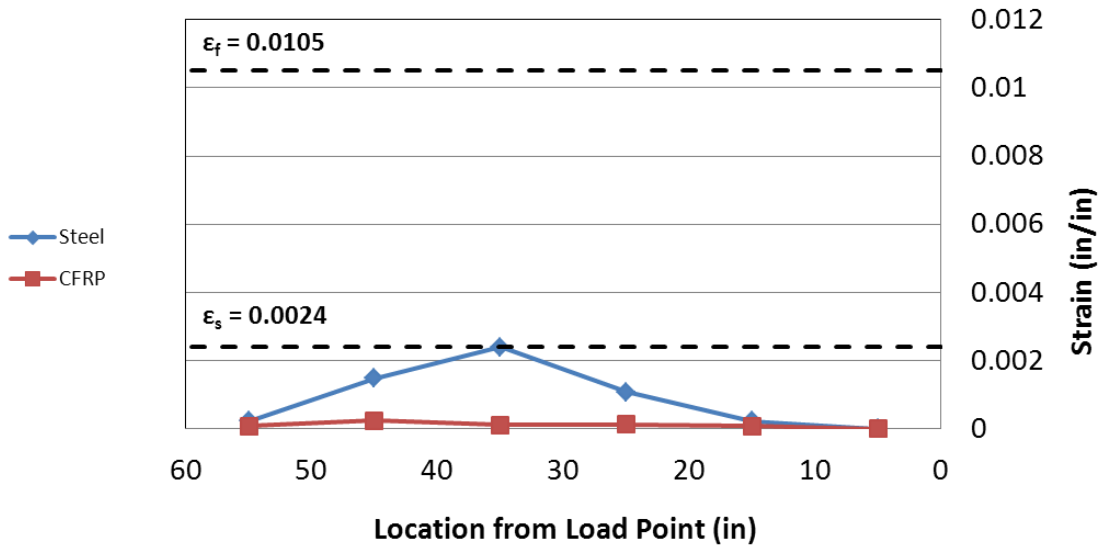


Figure 4-14 24-3-Fatigue-Fail-1 at 100-kips applied load (50-kips applied shear)

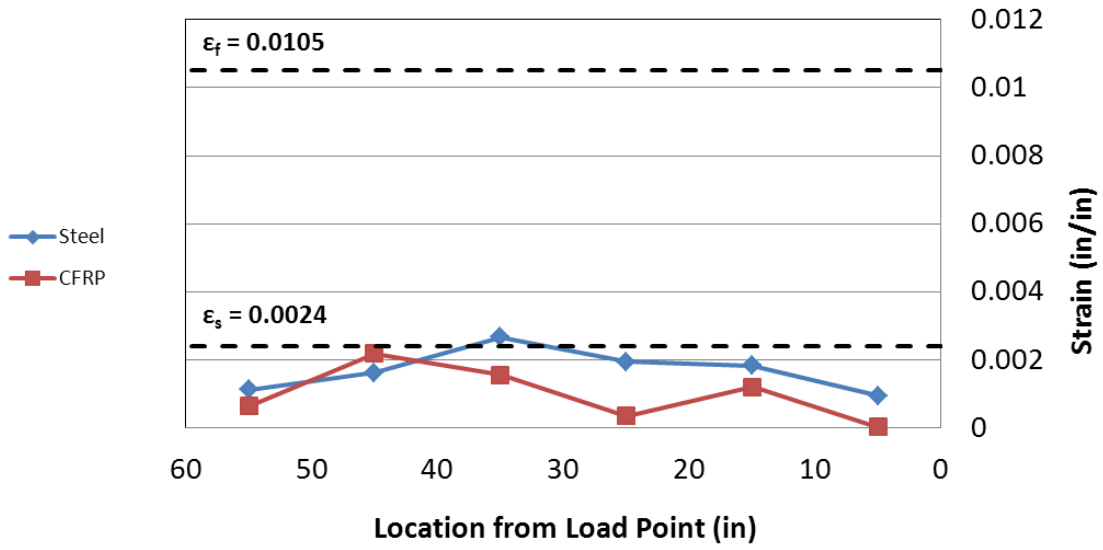


Figure 4-15 24-3-Fatigue-Fail-1 at 200-kips applied load (100-kips applied shear)

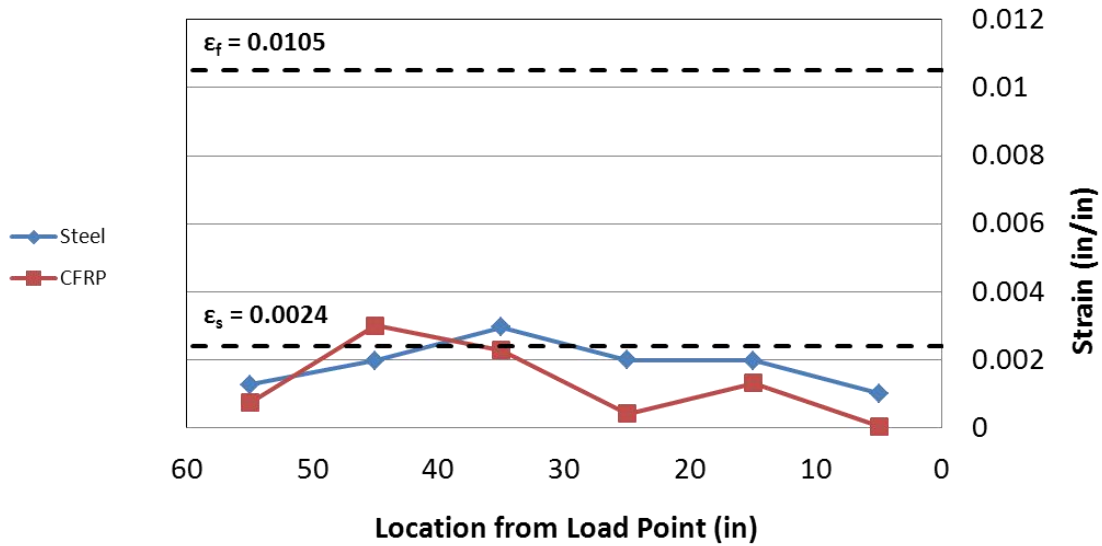


Figure 4-16 24-3-Fatigue-Fail-1 at 214-kips applied load (107-kips applied shear)

4.3.1.2 24-3-Fatigue-Fail-2 (Uncracked specimen, bonded CFRP)

Test 24-3-Fatigue-Fail-2 failed at an applied load of 270-kips (applied shear = 135-kips). Once again, shear failure of the test specimen was initiated by rupture of a CFRP anchor. Photos of the test specimen before loading and after failure are displayed in Figure 4-17. Concrete cracks observed during testing are marked in green, cracks marked in blue and red developed during the previous fatigue testing of the specimen.

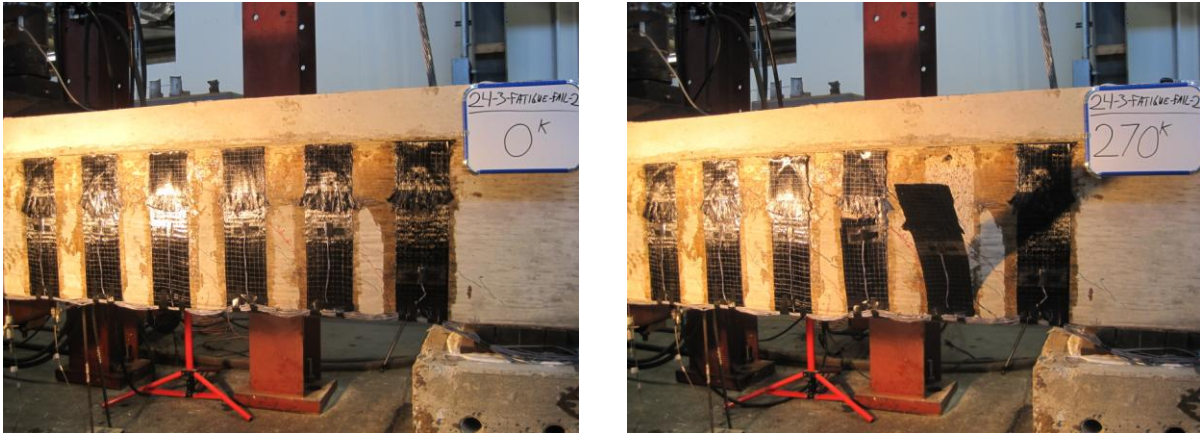


Figure 4-17 24-3-Fatigue-Fail-2 before (left) and after (right) loading

Shear failure of the test specimen was initiated by a combination of rupture of the CFRP strips and the CFRP anchors. First, the CFRP anchor ruptured on one side of the test specimen and the same sheet fractured on the opposite side of the specimen. A photo of the failed anchor can be seen in Figure 4-18. The CFRP sheet adjacent to the initially failed strip then ruptured due to increased load from the redistribution of shear force following the initial strips failure (Figure 4-19).



Figure 4-18 CFRP anchor failure observed during 24-3-Fatigue-Fail-2

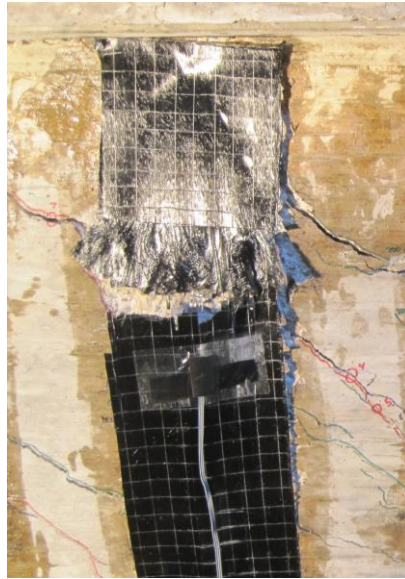


Figure 4-19 Rupture of CFRP strip observed during 24-3-Fatigue-Fail-2

Strains in the steel stirrups were monitored throughout testing with several strain gauges. First yielding of the transverse reinforcement occurred at an applied load of 173-kips (applied shear = 87-kips). Strains were also monitored in the CFRP sheets. The maximum recorded CFRP strain during test 24-3-Fatigue-Fail-2 was 0.0130. The high strain value was recorded at the location where the CFRP strip fractured on the opposite side of the anchor failure location and was higher than the manufacturer reported ultimate tensile strain value of 0.0105.

The strain values recorded in the CFRP and steel at various stages of the loading process and corresponding photos are presented in Figures 4-22 through 4-25. Strain data and photos of the specimen prior to loading are included to display the residual stresses present in the specimen following the fatigue loading of the beam. The strain values presented are the maximum strain values recorded for each material at given distances from the location of applied load.

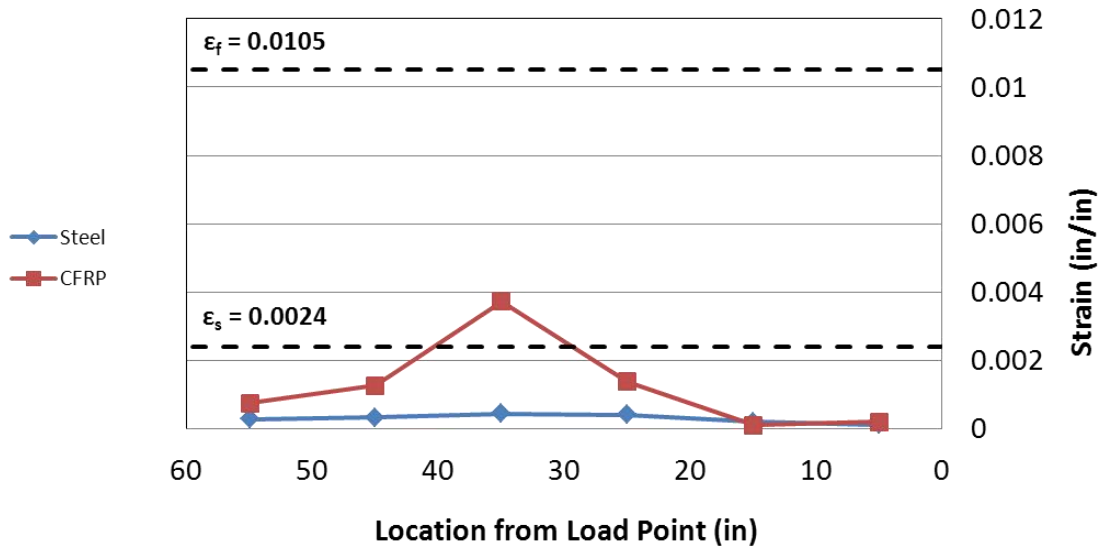


Figure 4-20 24-3-Fatigue-Fail-2 at 0-kips applied load (0-kips applied shear)

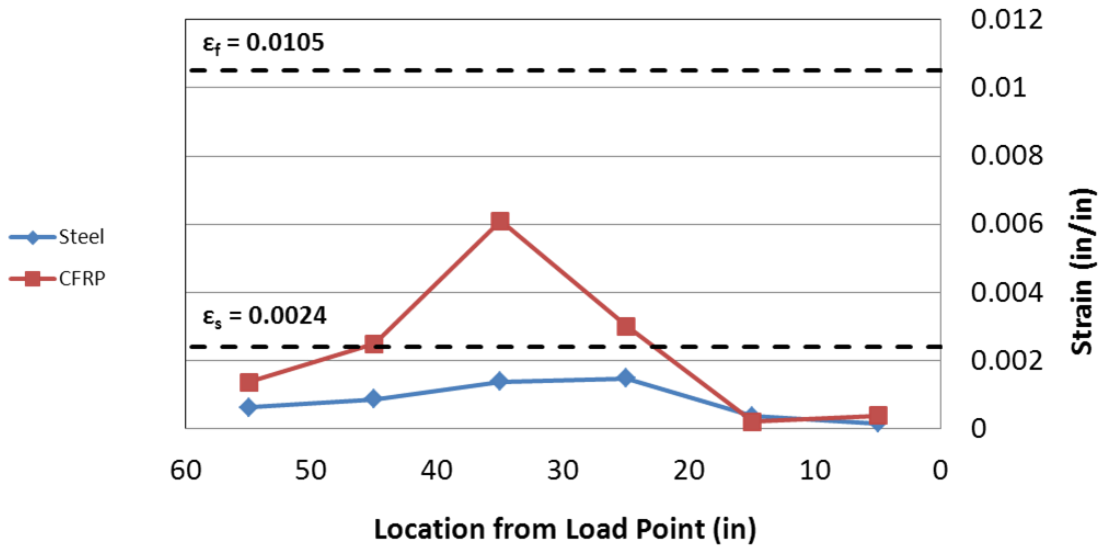


Figure 4-21 24-3-Fatigue-Fail-2 at 100-kips applied load (50-kips applied shear)

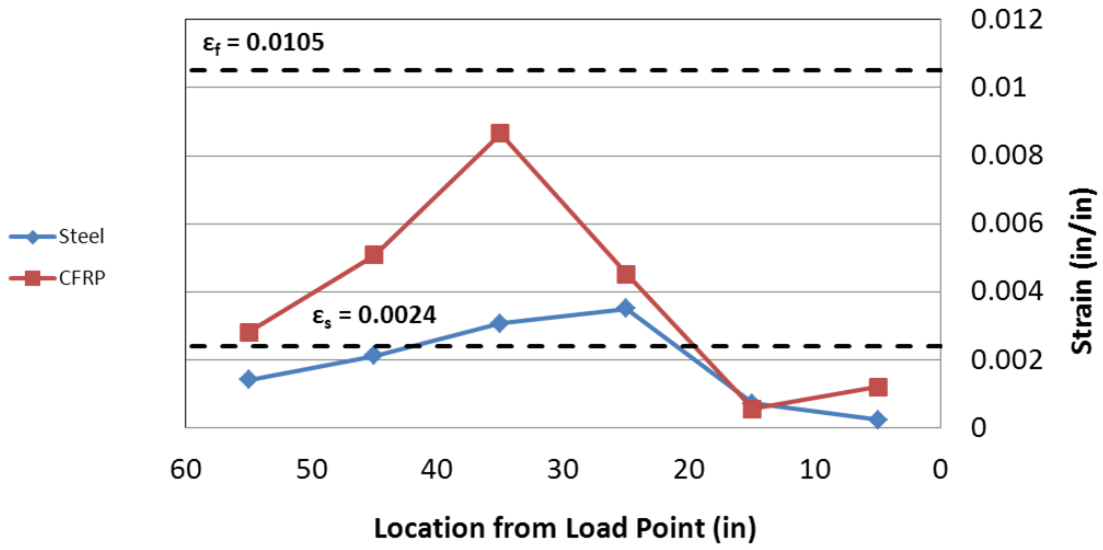


Figure 4-22 24-3-Fatigue-Fail-2 at 200-kips applied load (100-kips applied shear)

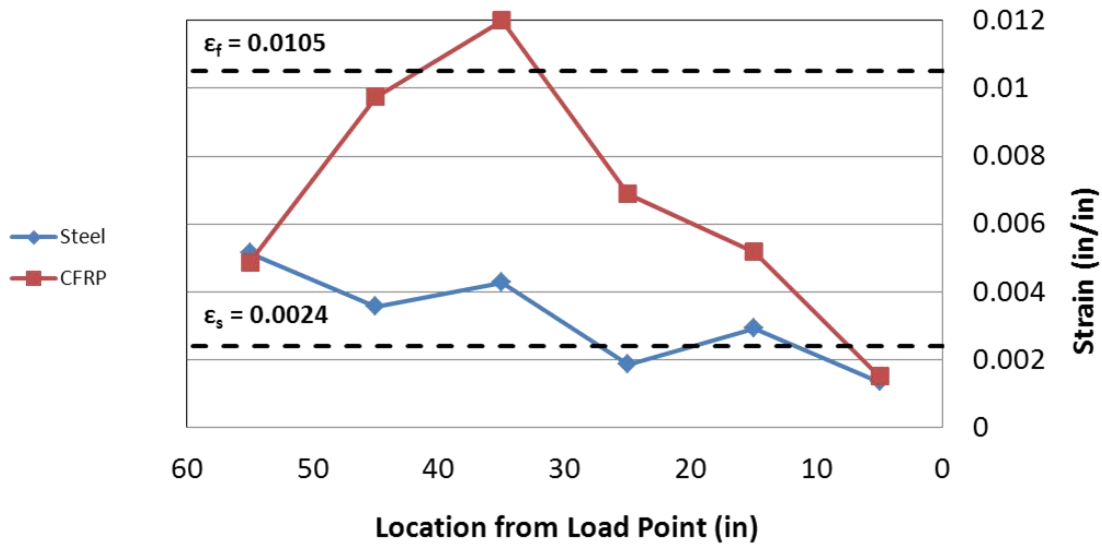


Figure 4-23 24-3-Fatigue-Fail-2 at 270-kips applied load (135-kips applied shear)

4.3.2 24-3-Fatigue-Fail-3&4 (Cracked specimen)

As described previously, the second fatigue test specimen was strengthened using CFRP laminates following the initial cracking of the reinforced concrete beam. One end of the test specimen was strengthened using bonded CFRP laminates and the alternate end of the specimen was strengthened using unbonded CFRP laminates. The bonded end of the test specimen failed first at an applied load of 256-kips (applied shear equal to 128-kips). The unbonded end of the test specimen failed second at an applied load of 283-kips (applied shear equal to 142-kips). The complete load-displacement response of tests 24-3-Fatigue-Fail-3 and 4 are presented in Figure 4-24.

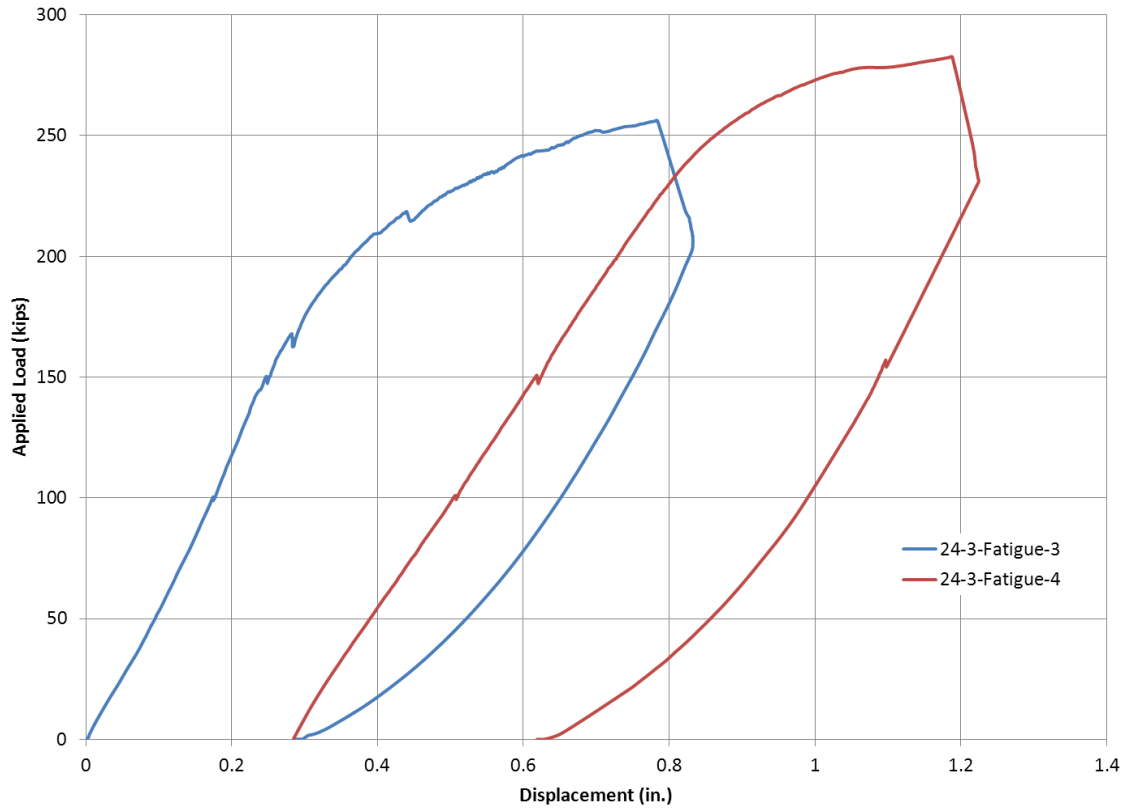


Figure 4-24 Load displacement response, test 24-3-Fatigue-Fail-3&4

4.3.2.1 24-3-Fatigue-Fail-3 (Cracked specimen, bonded CFRP)

Test 24-3-Fatigue-Fail-3 failed at an applied load of 256-kips (applied shear = 128-kips). Once again, shear failure of the test specimen was initiated by rupture of a CFRP anchor. Photos of the test specimen before loading and after failure are displayed in Figure 4-25. Concrete cracks observed during testing are marked in red. Cracks marked in blue and green developed during the previous fatigue testing of the specimen.



Figure 4-25 24-3-Fatigue-Fail-3 before (left) and after (right) loading

Shear failure of the test specimen was initiated by the rupture of a CFRP anchor. First, the CFRP anchor ruptured on one side of the test specimen and then the anchor on the same sheet on the opposite side of the specimen failed. Photos of the failed anchors can be seen in Figure 4-26 and Figure 4-27. Once again, a large crack developed in the top flange prior to failure. In addition, a second large shear crack opened above the support prior to failure.



Figure 4-26 First CFRP anchor failure observed during 24-3-Fatigue-Fail-3

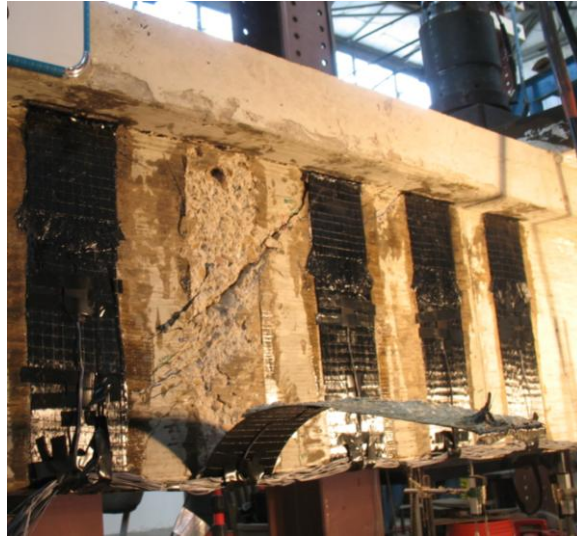


Figure 4-27 Second CFRP anchor failure observed during 24-3-Fatigue-Fail-3

Strains in the steel stirrups were monitored throughout testing with several strain gauges. First yielding of the transverse reinforcement occurred at an applied load of 163-kips (applied shear = 82-kips). Strains were also monitored in the CFRP sheets. The maximum recorded CFRP strain during test 24-3-Fatigue-Fail-3 was 0.0154. The high strain value was recorded at the location where the CFRP strip failed due to the rupture of the CFRP anchor and was higher than the manufacturer reported ultimate tensile strain value of 0.0105.

The strain values recorded in the CFRP and steel at various stages of the loading process and corresponding photos are presented in Figures 4-30 through 4-33. Strain data and photos of the specimen prior to loading are included to display the residual stresses present in the specimen following the fatigue loading of the beam. The strain values presented are the maximum strain values recorded for each material at given distances from the location of applied load.

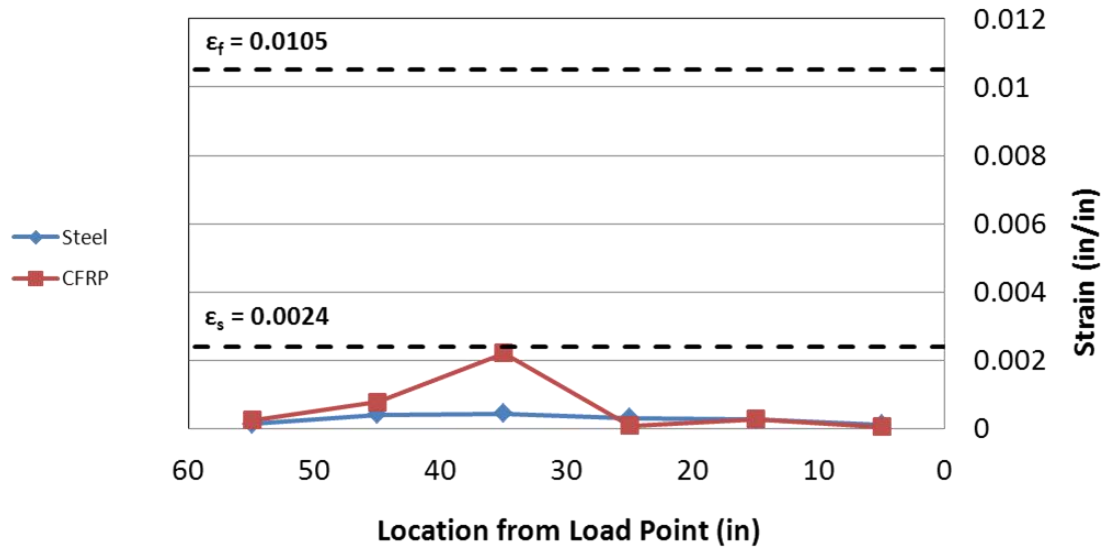


Figure 4-28 24-3-Fatigue-Fail-3 at 0-kips applied load (0-kips applied shear)

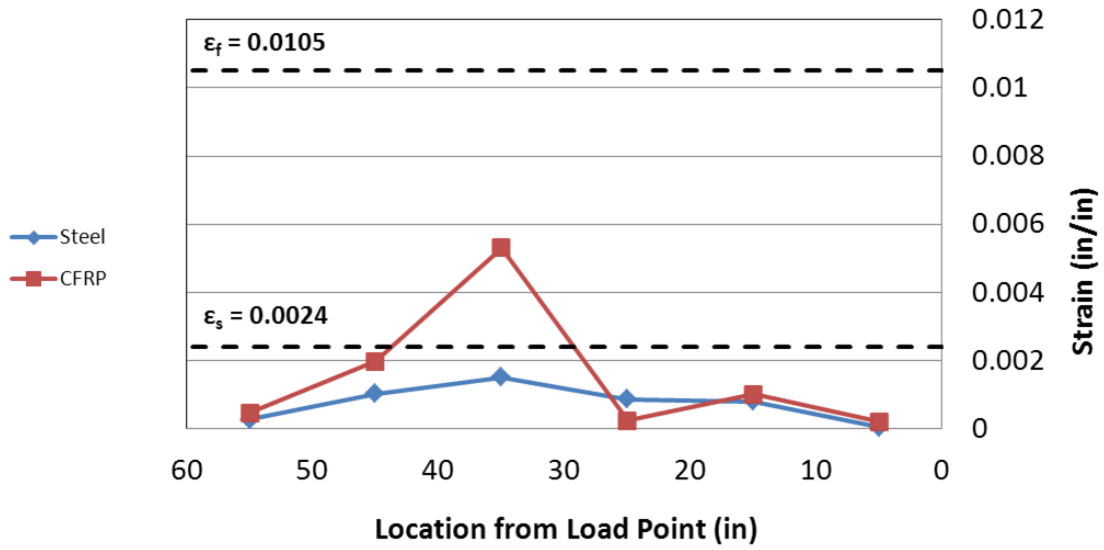


Figure 4-29 24-3-Fatigue-Fail-3 at 100-kips applied load (50-kips applied shear)

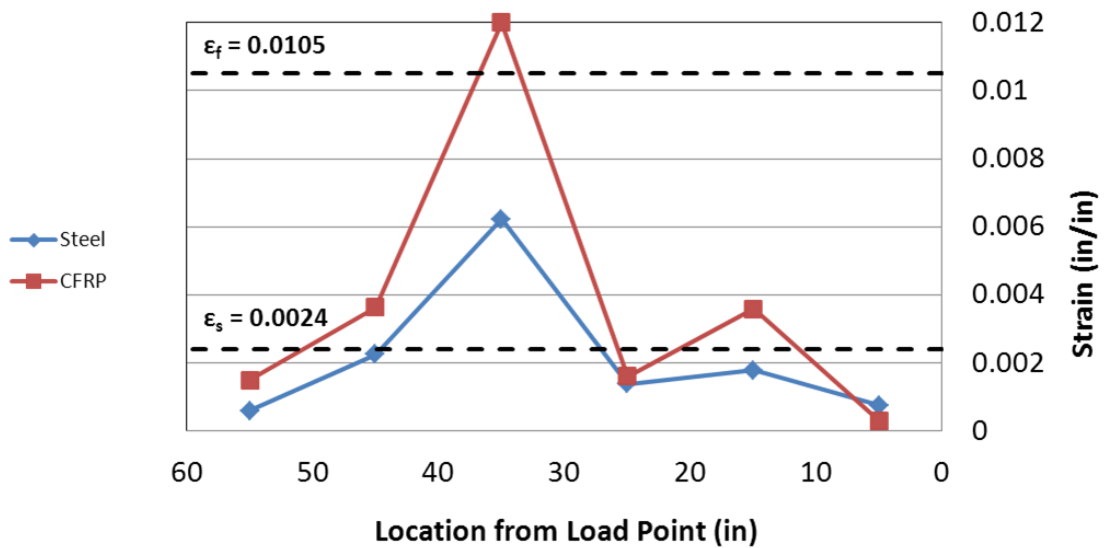


Figure 4-30 24-3-Fatigue-Fail-3 at 200-kips applied load (100-kips applied shear)

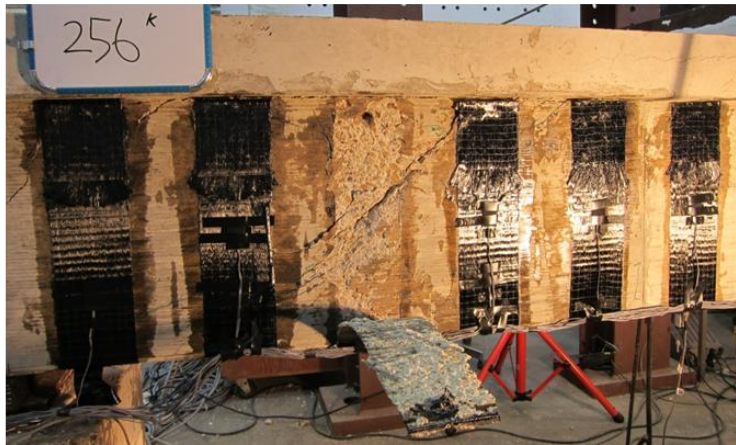
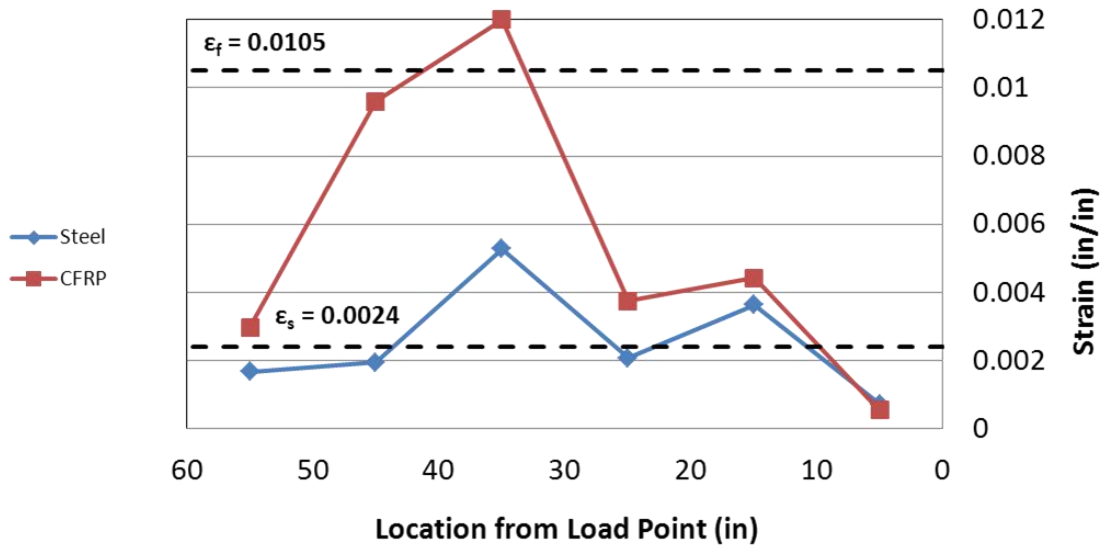


Figure 4-31 24-3-Fatigue-Fail-3 at 256-kips applied load (128-kips applied shear)

4.3.2.2 24-3-Fatigue-Fail-4 (Cracked specimen, unbonded CFRP)

Test 24-3-Fatigue-Fail-4 failed at an applied load of 283-kips (applied shear = 142-kips). Once again, shear failure of the test specimen was initiated by rupture of a CFRP anchor. Photos of the test specimen before loading and after failure are displayed in Figure 4-32. Concrete cracks observed during testing are marked in red. Cracks marked in blue and green developed during the previous fatigue testing of the specimen.



Figure 4-32 24-3-Fatigue-Fail-4 before (left) and after (right) loading

Shear failure of the test specimen was initiated by the rupture of a CFRP anchor in the second strip nearest to the support. Once the first CFRP anchor failed, then the adjacent strip failed due to the rupture of a CFRP anchor. After the second sheet failed due to the rupture of a CFRP anchor, then a third CFRP sheet failed due to the rupture of the CFRP sheet at the bottom bend of the CFRP sheet (Figure 4-33). A photo of one of the failed anchors can be seen in Figure 4-34. Two large shear cracks formed in the middle of the shear span with the ultimate failure resulting from the shear crack closest to the support.



Figure 4-33 CFRP sheet rupture observed during 24-3-Fatigue-Fail-4

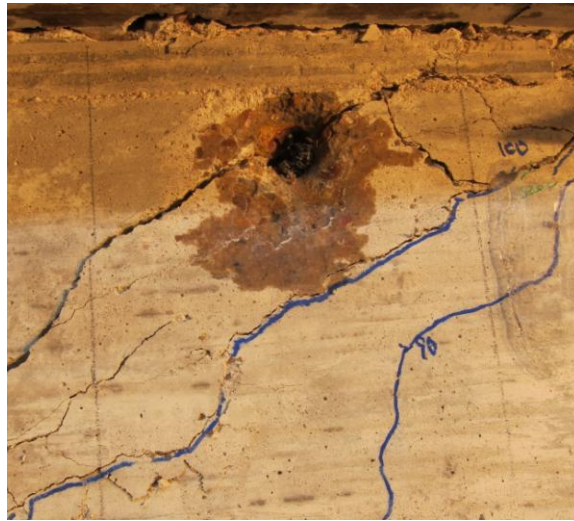


Figure 4-34 CFRP anchor failure observed during 24-3-Fatigue-Fail-4

Strains in the steel stirrups were monitored throughout testing with several strain gauges. First yielding of the transverse reinforcement occurred at an applied load of 150-kips (applied shear = 75-kips). Strains were also monitored in the CFRP sheets. The maximum recorded CFRP strain during test 24-3-Fatigue-Fail-3 was 0.0129. The high strain value was recorded at the location where the first CFRP strip failed due to the rupture of the CFRP anchor and was higher than the manufacturer reported ultimate tensile strain value of 0.0105.

The strain values recorded in the CFRP and steel at various stages of the loading process and corresponding photos are presented in Figures 4-37 through 4-40. Strain data and photos of the specimen prior to loading are included to display the residual stresses present in the specimen following the fatigue loading of the beam. The strain values presented are the maximum strain values recorded for each material at given distances from the location of applied load. Strains in the CFRP increased at a much more uniform rate due to the lack of bond between the CFRP and concrete surface. At failure, 5 strips had a strain greater than 0.006 and three strips had a strain greater than 0.009.

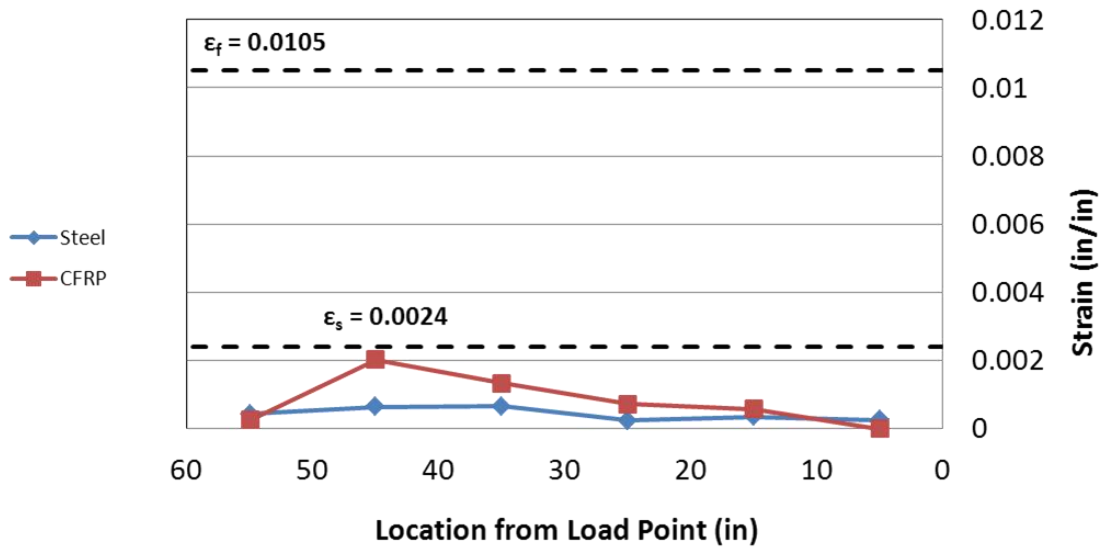


Figure 4-35 24-3-Fatigue-Fail-4 at 0-kips applied load (0-kips applied shear)

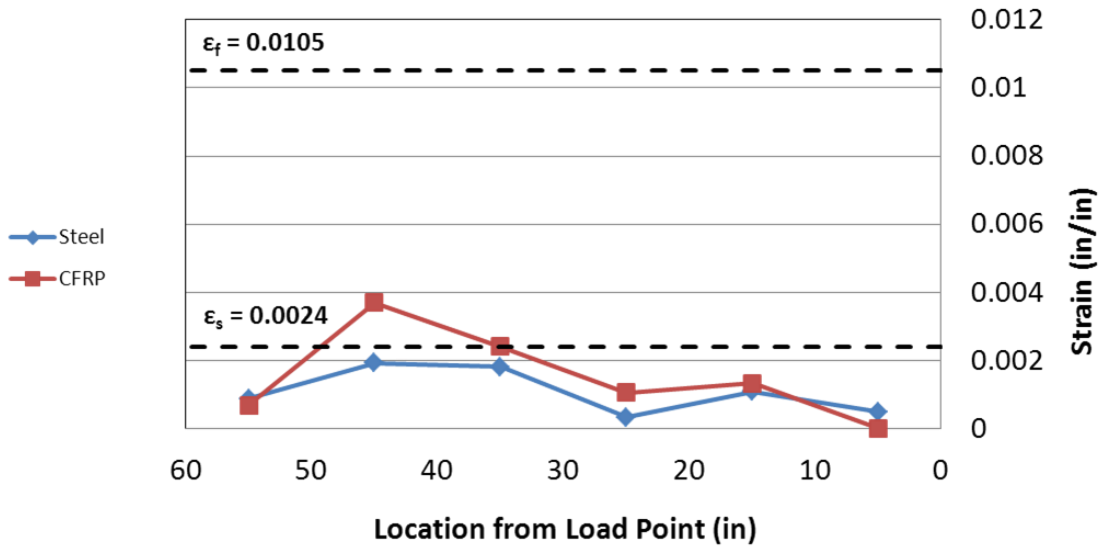


Figure 4-36 24-3-Fatigue-Fail-4 at 100-kips applied load (50-kips applied shear)

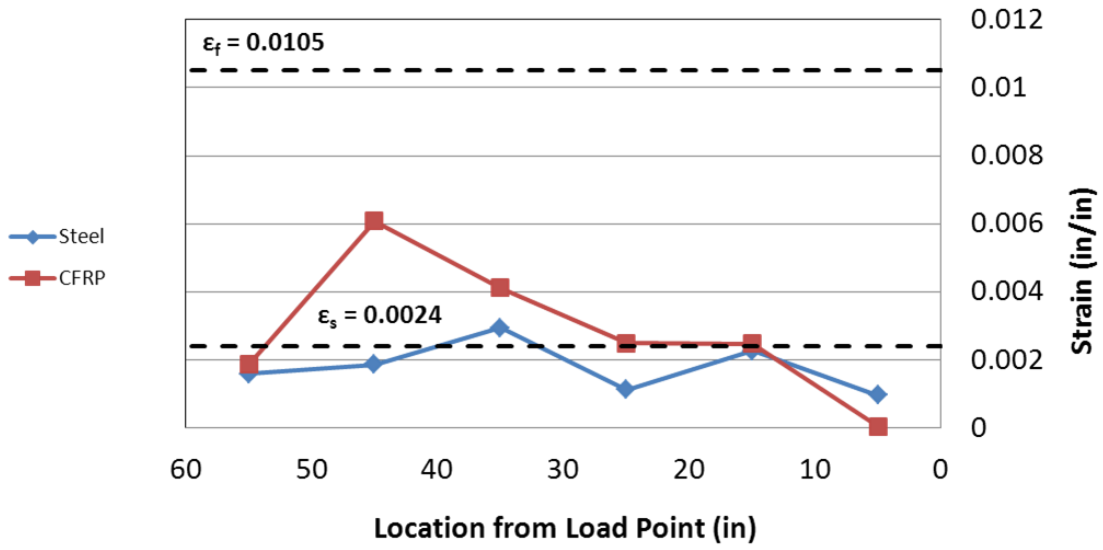


Figure 4-37 24-3-Fatigue-Fail-4 at 200-kips applied load (100-kips applied shear)

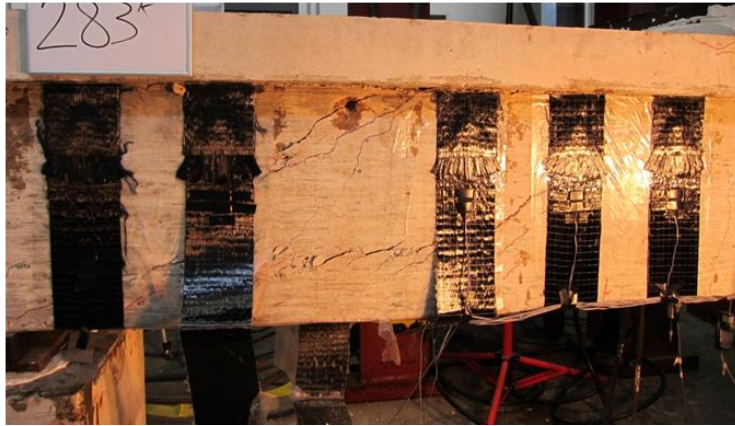
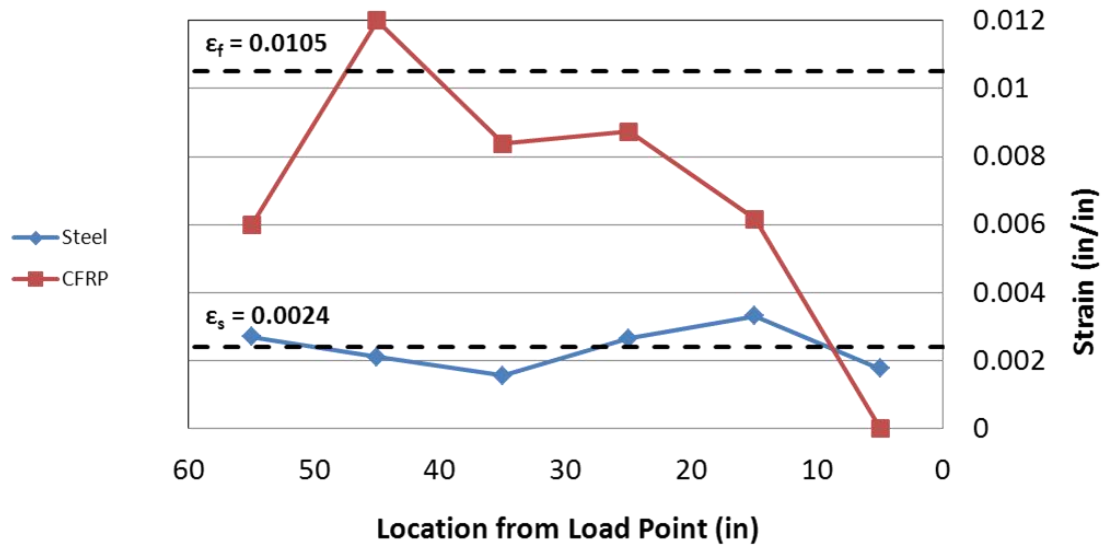


Figure 4-38 24-3-Fatigue-Fail-4 at 283-kips applied load (142-kips applied shear)

4.3.3 Discussion of results of loading to failure after completion of fatigue loading

The results of the failure load tests and previous monotonically loaded failure tests conducted by Quinn (2009) are summarized in Table 4-5.

Table 4-5 Summary of tests to failure

| Test Type | Test Number | Bonded/ Unbonded | Cracked/ Uncracked | Load Steel Yielded (Shear) | Max CFRP Strain | Failure Load (Shear) | Ratio of Measured/ Control |
|---|---------------------|---------------------|-----------------------|-------------------------------|--------------------|-------------------------|----------------------------------|
| Load to Failure of Fatigue Specimens | 24-3-Fatigue-Fail-1 | Unbonded | Uncracked | 50-kips | 0.0057 | 107-kips | 1.02 |
| | 24-3-Fatigue-Fail-2 | Bonded | Uncracked | 87-kips | 0.0130 | 135-kips | 1.29 |
| | 24-3-Fatigue-Fail-3 | Bonded | Cracked | 82-kips | 0.0154 | 128-kips | 1.22 |
| | 24-3-Fatigue-Fail-4 | Unbonded | Cracked | 75-kips | 0.0129 | 142-kips | 1.35 |
| Monotonic to Failure | Test 1 | Control | - | 73-kips | - | 105-kips | 1.0 |
| | Test 2 | Unbonded | Cracked | 103-kips | 0.0126 | 151-kips | 1.44 |
| | Test 3 | Bonded | Cracked | 73-kips* | 0.0123 | 151-kips | 1.44 |

-Fatigue specimens were cast from the same truck and differences in concrete compressive strength are assumed to be negligible.

-Fatigue beams consisted of steel and CFRP materials were from the same batches and assumed to have nominally identical properties.

** - Specimen was previously loaded to yielding of the steel stirrups prior to the application of CFRP*

The first column distinguishes between tests that had been previously fatigued prior to failure and tests conducted by Quinn (2009) where beams were loaded monotonically to failure. The second column identifies the test as defined by Figure 3-1. The third column indicates whether the CFRP laminates were installed using a bonded or unbonded application. The fourth column specifies whether the beam was cracked or uncracked prior to the installation of CFRP. The fifth column specifies the load at which the transverse steel reinforcement yielded. The sixth column displays the highest recorded strain in the CFRP laminates. The next column displays the shear at failure. The final column presents the ratio of increased strength compared with the control specimen tested by Quinn (2009). His specimens also consisted of a T-beam with a 24-in. depth and a 14-in. web.

Both tests of strengthened specimens conducted by Quinn produced shear failure loads of approximately 151-kips. He found that the absence of bond between the surface

of the concrete and the CFRP laminates did not decrease the ultimate capacity of the test specimen. Both tests were able to develop strains in the CFRP laminates that were higher than the manufacturer reported ultimate tensile strain value of 0.0105. The strengthened specimens produced an ultimate shear failure load that was 44-percent greater than the unstrengthened specimen, which failed at a shear load of 105-kips.

Test 24-3-Fatigue-Fail-1 was strengthened using unbonded CFRP prior to cracking and failed at an applied shear of 107-kips. The capacity of test 24-3-Fatigue-Fail-1 is only slightly greater than the control specimen tested by Quinn (a 2-percent increase in strength). During fatigue testing, the strains in the transverse steel reinforcement on the unbonded end reached values near yielding. The CFRP laminates had very small strains and were contributing little additional strength to the specimen. The high strain levels may have caused the internal steel to be close to its fatigue capacity prior to monotonic loading and thus contributed to a premature failure.

Hoult and Lees (2005) noted that attention needs to be given to the fatigue capacity of a beams component parts. Failure in test 24-3-Fatigue-Fail-1 may have resulted from a premature fracture of the internal steel stirrups prior to the anchor rupture due to their capacity being decreased as a result of fatigue loading. Following the initial cyclic loading series, this end of the specimen was clamped to prevent premature failure during the cyclic loading of the other end of the specimen at higher levels. It is unknown if the clamping procedure resulted in further decreases in the ultimate shear capacity of the unbonded end.

The results of the other three tests were favorable with strength gains between 20 and 35-percent. All four tests resulted in lower failure loads than monotonically loaded tests that had not been fatigue loaded. This agrees with results of tests conducted by Harries, Reeve, and Zorn (2007) where they found that beams that had been fatigue tested more than 2-million cycles failed at lower loads than non-fatigued, monotonically loaded specimens. These tests show that while the ultimate capacity of strengthened specimens decreases after substantial fatigue loading, considerable gains in strength are still possible as a result of CFRP strengthening after extreme fatigue loading.

CFRP failure occurred initially due to rupture of the CFRP anchor in each of the four tests. Even though failure occurred due to rupture of the CFRP anchor, the final three failure tests produced strains in the CFRP that were higher than the manufacturer reported ultimate tensile strain value of 0.0105. This demonstrates that the CFRP anchors are capable of developing the full capacity of the CFRP strip. Therefore, in cases where it is not possible to fully wrap CFRP laminates around a specimen, CFRP anchors should be used so that the full capacity of the CFRP laminate can be utilized. Attention must be given to the amount of damage accumulated in the internal steel due to fatigue loading when calculating the ultimate capacity of a specimen strengthened using CFRP laminates.

CHAPTER 5

Test Results Under Sustained Loading

5.1 INTRODUCTION

The test results and data obtained from the sustained loading portion of the research project are presented in this section. Data is presented for two test specimens loaded for a period of 217 days.

The following information is presented:

- Strains in the steel stirrups
- Strains in the CFRP strips
- Surface strains recorded using DEMEC measuring system
- Displacements of test specimens during testing

5.2 SUSTAINED LOAD TEST SERIES

The sustained load test series consisted of four tests described in Table 5-1.

Table 5-1 Sustained loading test matrix

| <i>Sustained Load Test Series</i> | | | <i>a/d ratio equal to 3</i> |
|-----------------------------------|--------------|----------------------|-----------------------------|
| Test Number | Applied Load | Bonded/Unbonded CFRP | Procedure |
| 24-3-Sust-1 | 160-kips | Bonded | Strengthened Uncracked |
| 24-3-Sust-2 | 160-kips | Unbonded | Strengthened Uncracked |
| 24-3-Sust-3 | 160-kips | Bonded | Strengthened Cracked |
| 24-3-Sust-4 | 160-kips | Unbonded | Strengthened Cracked |

In this matrix, the first column identifies the test as defined by Figure 3-3. The second column indicates the load applied to the midpoint of each test specimen. The next column indicates whether the CFRP material was bonded to the surface of the concrete specimen or if bond was removed by placing a layer of clear plastic shelf liner between the CFRP and the concrete surface. The CFRP layout used in all instances consisted of 5-in. CFRP strips spaced at 10-in. on-center. Each CFRP strip was anchored to the top of the concrete web using one CFRP anchor on each side of the test specimen. So each CFRP strip was anchored using two CFRP anchors. The last column specifies whether the test specimen was strengthened using CFRP laminates prior to the initial cracking of the specimen or after cracking.

5.2.1 24-3-Sust-1 (Uncracked specimen, bonded CFRP)

Test 24-3-Sust-1 consisted of a specimen that was strengthened using CFRP laminates prior to the initial cracking of the test specimen. CFRP was applied to the test specimen using a bonded application. Photos of the loaded test specimen can be seen in Figure 5-1. Concrete cracks observed during testing are outlined in red.

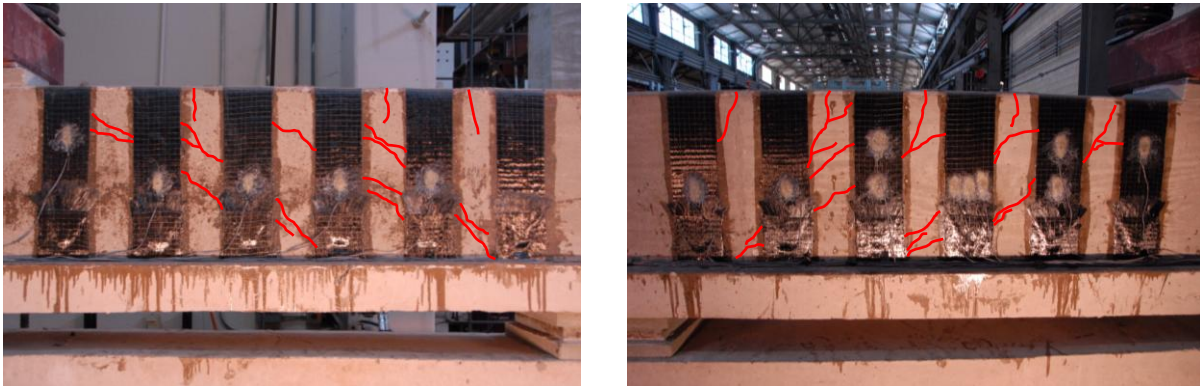


Figure 5-1 Front and back of test 24-3-Sust-1

Multiple small cracks opened in the shear span after loading with few additional cracks opening up after the final load was applied. Concrete crack widths changed slightly with crack widths increasing from 0.013-in. at the start of loading to 0.020-in. after 217 days of loading. Strains in the transverse steel reinforcement, CFRP laminates, and concrete surface were monitored during testing. A small increase in strain was observed at the 107-day point when the load was adjusted to the desired level. Steel strains remained relatively constant throughout testing. The maximum reported strain in the steel stirrups during test 24-3-Sust-1 was 0.00180. The maximum steel strain was recorded after the load was reapplied 107 days after initial loading. Steel strains then decreased slightly after this point.

CFRP strains increased moderately during test 24-3-Sust-1 with a maximum reported strain of 0.00459. CFRP strains continued increasing during testing with the maximum CFRP strain being recorded on day 217. The average CFRP strain of all strips crossing shear cracks was 0.00376. The lowest strain of any CFRP strip crossing a shear crack was 0.00276. Surface strains were monitored using the DEMEC measuring system

described in 3.4.3.2. Surface strains remained relatively constant throughout testing with minimal increases in strain. The bonded application of CFRP materials greatly reduced the size of crack widths and minimized increases in surface strains during testing. A plot of the strains recorded using steel gauges, CFRP gauges, and DEMEC device are presented in Figure 5-2. DEMEC readings measure the average strain over an 8-in. gauge length, whereas the steel and CFRP gauges measure strain at a specific point on the steel and CFRP. Because of this, DEMEC readings can be higher compared with steel and CFRP strains in locations where large cracks formed in the concrete. These differences in strain may also be related to the location of the critical crack compared with the location of the steel and CFRP gauges. The closer these gauges were to the critical crack, the more precise the measurements.

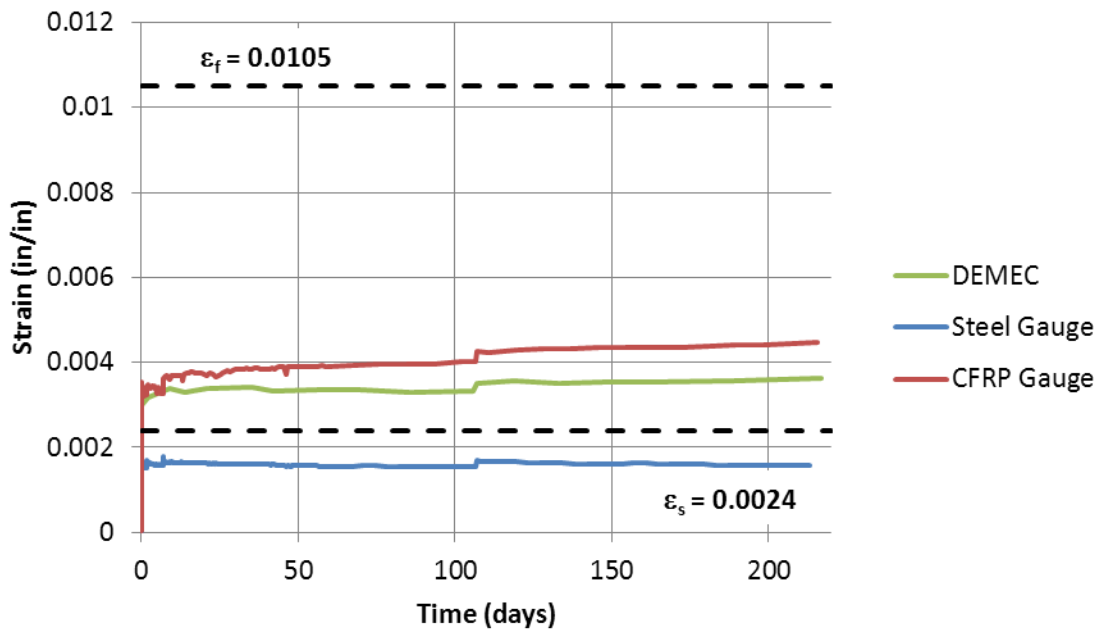


Figure 5-2 Strains, test 24-3-Sust-1

5.2.2 24-3-Sust-2 (Uncracked specimen, unbonded CFRP)

Test 24-3-Sust-2 consisted of a specimen that was strengthened using CFRP laminates prior to the initial cracking of the test specimen. CFRP was applied to the test

specimen using an unbonded application. Photos of the loaded test specimen can be seen in Figure 5-3. Concrete cracks observed during testing are outlined in red.

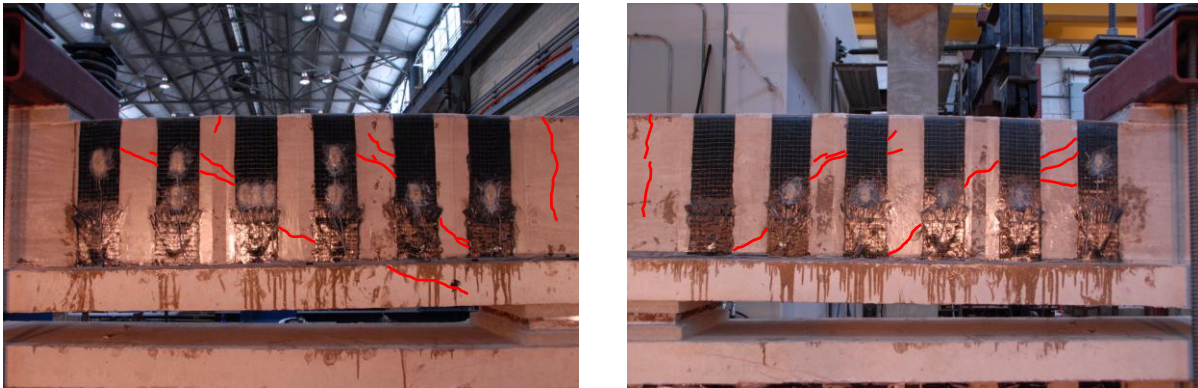


Figure 5-3 Front and back of test 24-3-Sust-2

Cracking in the unbonded specimen was limited to two large shear cracks that formed in the shear span. Few additional cracks formed after the initial loading of the test specimen. Concrete crack widths increased from 0.040-in. at the start of loading to 0.080-in. after 217 days of loading. Strains in the transverse steel reinforcement, CFRP laminates, and concrete surface were monitored during testing. A small increase in strain was observed at the 107-day point when the load was adjusted. Once again, steel strains remained little changed during testing. The maximum reported strain in the steel stirrups during test 24-3-Sust-2 was 0.00251. The maximum steel strain was recorded after the application of the initial load. Steel strains decreased after initial loading, but remained near 0.0020 throughout testing.

Similar to the previous test, CFRP strains increased moderately during test 24-3-Sust-2 with a maximum reported strain of 0.00477. CFRP strains increased rapidly at the beginning of testing, but then remained relatively constant thereafter. The maximum CFRP strain was recorded near the end of the 217 day period. In contrast to the previous test, the average CFRP strain of all strips crossing shear cracks was 0.00196. After the CFRP strip that recorded the maximum strain of 0.00477, no other strip had a strain greater than 0.0020. Once again, surface strains were monitored using the DEMEC measuring system described in 3.4.3.2. Surface strains increased steadily during testing

and coincided to similar increases seen in concrete crack widths. The lack of bond between the surface of the concrete and the CFRP laminates allowed for greater increases in deformations during testing. A plot of the strains recorded using steel gauges, CFRP gauges, and DEMEC device are presented in Figure 5-4. DEMEC readings measure the average strain over an 8-in. gauge length, whereas the steel and CFRP gauges measure strain at a specific point on the steel and CFRP. DEMEC readings were significantly higher than steel and CFRP gauge readings for test 24-3-Sust-2 due to a large crack that formed between the DEMEC points used to take measurements.

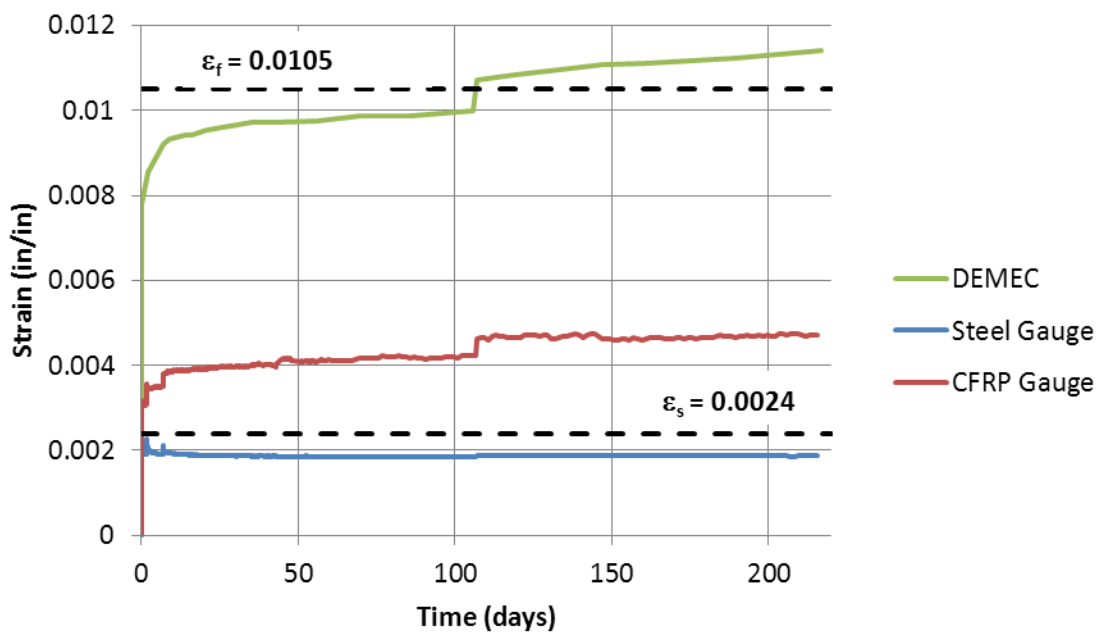


Figure 5-4 Strains, test 24-3-Sust-2

5.2.3 24-3-Sust-3 (Cracked specimen, bonded CFRP)

Test 24-3-Sust-3 was strengthened using CFRP laminates following the initial cracking of the test specimen. CFRP was applied to the test specimen using a bonded application. Photos of the loaded test specimen can be seen in Figure 5-5. Once again, concrete cracks observed during testing are outlined in red.

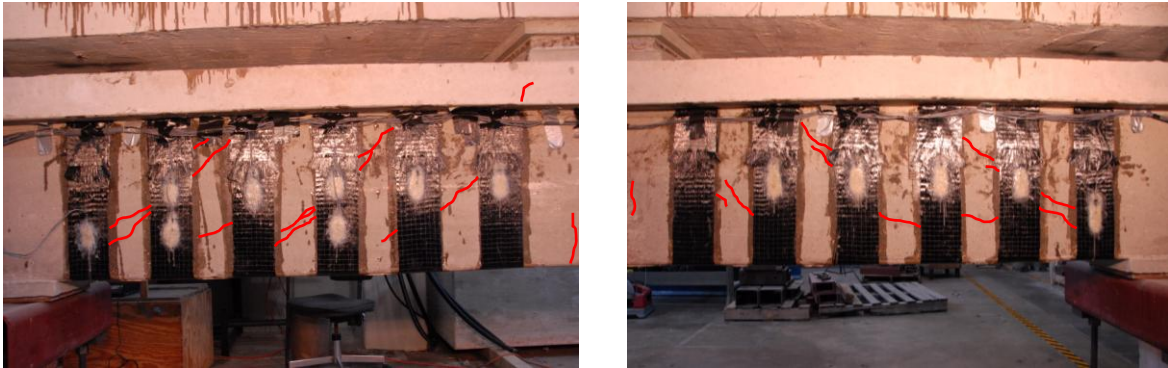


Figure 5-5 Front and back of test 24-3-Sust-3

The majority of shear cracks formed in test 24-3-Sust-3 during the initial cracking of the test specimen prior to the application of CFRP materials. Initial cracks widened after application of the sustained load, with minimal additional cracks forming. Concrete crack widths increased from 0.030-in. at the start of loading to 0.060-in. after 217 days of loading. Strains in the transverse steel reinforcement, CFRP laminates, and concrete surface were monitored during testing. Once again, a small increase in strain was observed at the 107-day point when the load was adjusted. After initial increases, strains in the transverse steel reinforcement remained constant throughout the test. Several steel stirrups reached yielding during the initial loading of the test specimen. After this, the stirrups remained near yielding for the duration of the test with a maximum recorded strain of 0.00233 in the steel stirrups after 217 days of loading.

Similar to the other tests, CFRP strains increased moderately during test 24-3-Sust-3 with a maximum reported strain of 0.00637. CFRP strains increased throughout testing and the maximum reported CFRP strain was recorded on day 217. The average strain in all CFRP strips crossing shear cracks was 0.00296. The CFRP strain gauges on this specimen were placed at the known locations of the cracks that formed prior to the application of CFRP. The higher recorded CFRP strains compared to those recorded in 24-3-Sust-1 could be the product of CFRP gauges being placed closer to the critical cracks. Once again, surface strains were monitored using the DEMEC measuring system described in 3.4.3.2. Surface strains remained relatively constant throughout testing.

Similar to the initial bonded test, 24-3-Sust-1, the presence of bond between the surface of the concrete and the CFRP laminates appears to have limited increases in surface strains during testing. A plot of the strains recorded using steel gauges, CFRP gauges, and DEMEC device are presented in Figure 5-6. DEMEC readings measure the average strain over an 8-in. gauge length, whereas the steel and CFRP gauges measure strain at a specific point on the steel and CFRP. Once again, DEMEC readings were slightly higher than steel and CFRP gauge readings for test 24-3-Sust-3 due to a large crack that formed between the DEMEC points used to take measurements.

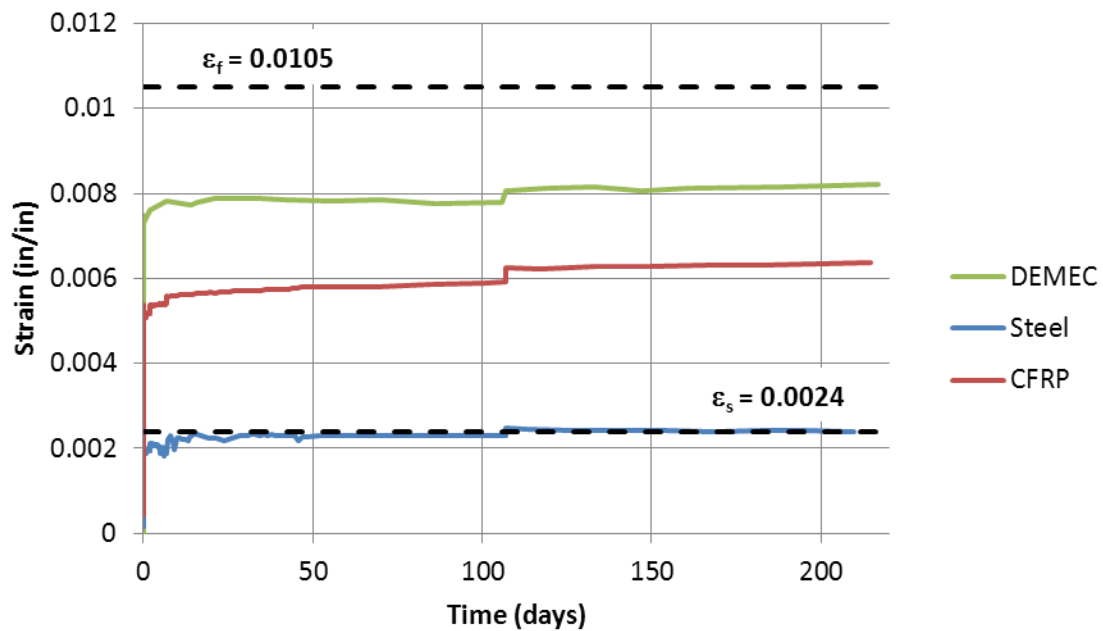


Figure 5-6 Strains, test 24-3-Sust-3

5.2.4 24-3-Sust-4 (Cracked specimen, unbonded CFRP)

Test 24-3-Sust-4 consisted of a specimen that was strengthened using CFRP laminates following the initial cracking of the test specimen. CFRP was applied to the test specimen using an unbonded application. Photos of the loaded test specimen can be seen in Figure 5-7. Once again, concrete cracks observed during testing are outlined in red.

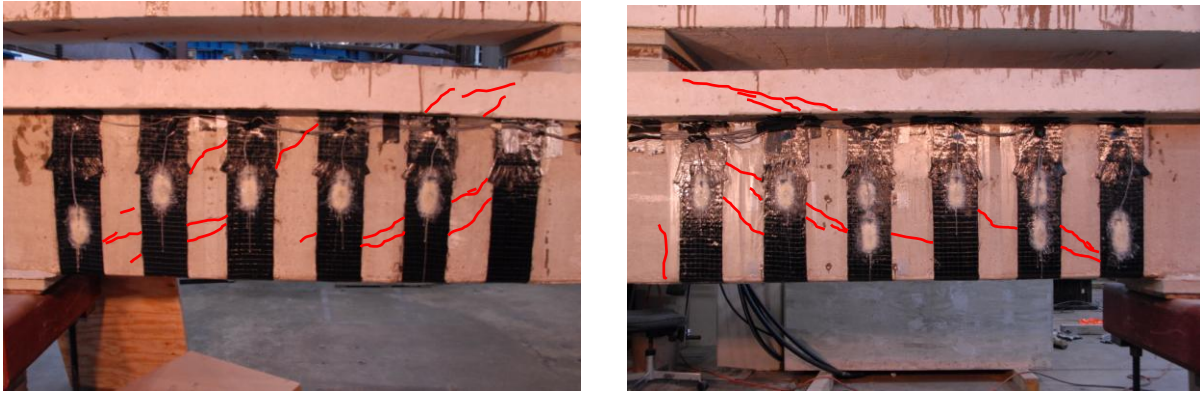


Figure 5-7 Front and back of test 24-3-Sust-4

Similar to test 24-3-Sust-3, the majority of shear cracks formed in test 24-3-Sust-4 during the initial cracking of the test specimen prior to the application of CFRP materials. Initial cracks widened after application of the sustained load, with only minor cracks forming after initial loading. Concrete crack widths increased from 0.075-in. at the start of loading to 0.125-in. after 217 days of loading. Strains in the transverse steel reinforcement, CFRP laminates, and concrete surface were monitored during testing. Once again, a small increase in strain was observed at the 107-day point when the load was adjusted. No steel strain gauges were located in regions near the critical crack and as a result strain data is unable to be properly compared to other tests. The strains in the available gauges remained relatively constant throughout testing with a maximum recorded strain of 0.00146.

Similar to the other tests, CFRP strains increased moderately during test 24-3-Sust-4 with a maximum reported strain of 0.00461. CFRP strains remained relatively constant throughout testing and the maximum reported CFRP strain was recorded near the end of the 217 day testing period. The average strain in all CFRP strips crossing shear cracks was 0.00228. Surface strains were monitored using the DEMEC measuring system described in 3.4.3.2. The critical crack did not intersect with the grid of DEMEC points placed on the surface of the test specimen. Therefore, DEMEC measurements taken for test 24-3-Sust-4 cannot be compared properly with the other three tests. The monitored surface strains remained relatively constant throughout testing. Concrete

crack width comparisons between test 24-3-Sust-4 and the other three tests will result in a more accurate assessment of specimen behavior. A plot of the strains recorded using steel gauges, CFRP gauges, and DEMEC device are presented in Figure 5-8. DEMEC readings measure the average strain over an 8-in. gauge length, whereas the steel and CFRP gauges measure strain at a specific point on the steel and CFRP.

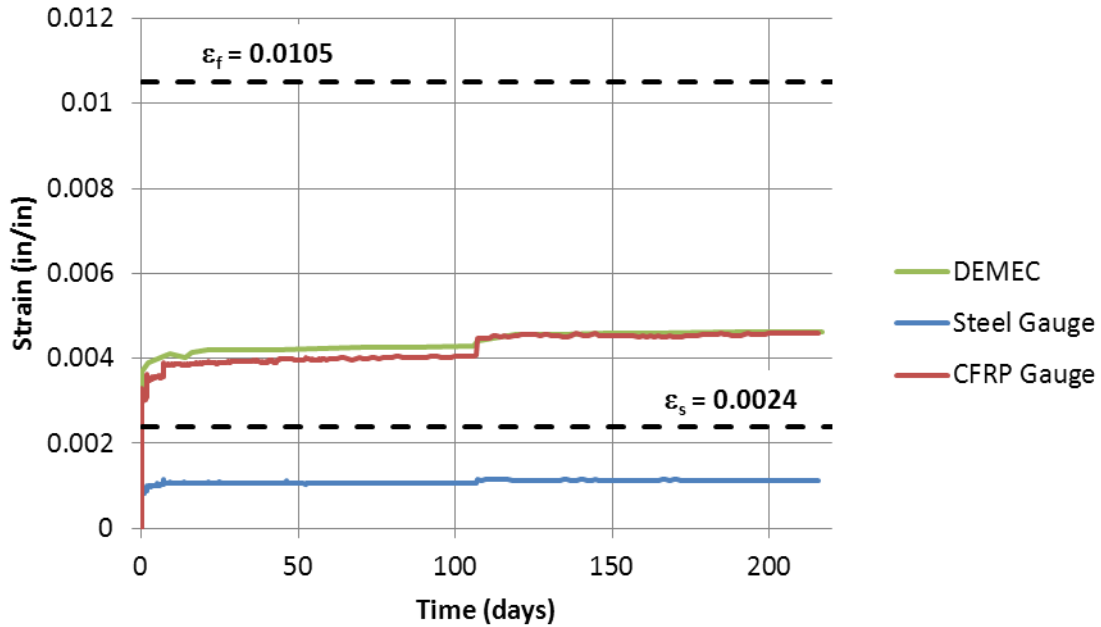


Figure 5-8 Strains, test 24-3-Sust-4

5.2.5 Displacements

End displacements were monitored on each end of the test specimens using DEMEC points similar to those used to obtain surface strain values. A photo of the DEMEC points placed on the surface of the end region of the test set-up is presented in Figure 5-9. The average displacements throughout testing are presented in Figure 5-10. Displacements increased dramatically during the first several days of loading and then continued to increase slowly for the duration of the test. A large jump in displacements were recorded when the load was adjusted at 107 days.



Figure 5-9 End displacement DEMEC points

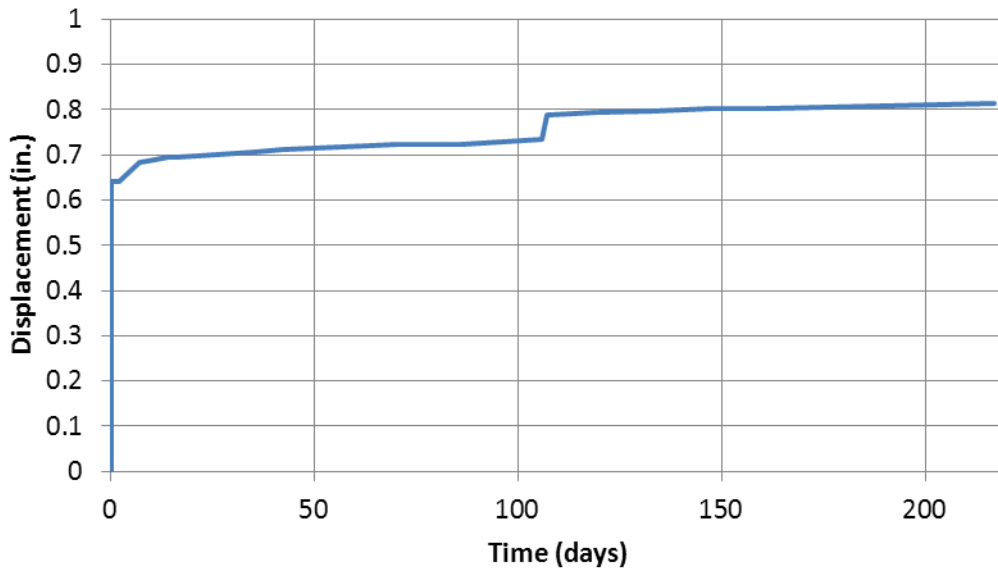


Figure 5-10 Average total displacement

5.3 DISCUSSION OF RESULTS

Specimens strengthened using CFRP laminates and CFRP anchors performed well under sustained loads. No deterioration was observed in either the CFRP laminates

or anchors. Small increases in strain were observed in the CFRP laminates, with the majority of increases occurring within the first two weeks of loading. A summary of the sustained load results are presented in Table 5-2.

Table 5-2 Summary of sustained load results

| Test Number | Crack Widths | | Strains | | | Application Procedure | |
|-------------|---------------------|-------------------|---------------------|-----------------|------------------|-----------------------|-------------------|
| | Initial Crack Width | Final Crack Width | Initial CFRP Strain | Max CFRP Strain | Max Steel Strain | Bonded/Unbonded | Cracked/Uncracked |
| 24-3-Sust-1 | 0.013-in. | 0.020-in. | 0.0035 | 0.0045 | 0.0018 | Bonded | Uncracked |
| 24-3-Sust-2 | 0.040-in. | 0.080-in. | 0.0030 | 0.0048 | Yielded | Unbonded | Uncracked |
| 24-3-Sust-3 | 0.030-in. | 0.060-in. | 0.0053 | 0.0064 | Yielded | Bonded | Cracked |
| 24-3-Sust-4 | 0.075-in. | 0.125-in. | 0.0033 | 0.0046 | Yielded | Unbonded | Cracked |

CFRP strain increases ranged between 0.0011 and 0.0018 for all tests. This is similar to test results conducted by Hoult and Lees (2005) where they found that CFRP strains increased by 0.001 in CFRP laminates over a sustained loading period of 220-days. The strains in the tests presented are higher than those of Hoult and Lees (2005) mainly due to the process of checking the load after 2, 7, and 107-days to verify the applied load. CFRP strains reached values greater than 0.004, the code allowable strain value for specimens strengthened using CFRP laminates in applications where the laminates cannot be wrapped completely around the specimen. Once again, the CFRP anchors allowed the CFRP sheets to reach higher strain values without any observed deterioration.

In test 24-3-Sust-1, the bonded CFRP laminates continued to relieve stress on the internal transverse reinforcement throughout testing and kept the steel from yielding for the duration of the test. Steel strains reached yielding during the initial loading of test 24-3-Sust-2, but remained near 0.0019 for the majority of testing. Bonded and unbonded CFRP laminates helped to reduce the strain demand on the internal transverse reinforcement compared with the specimen strengthened after initial cracking. This confirms work by Uji (1992) that showed that the presence of CFRP laminates helps to reduce the strains in steel stirrups. Steel strains in test 24-3-Sust-3 were at yielding for

the majority of testing. While steel strains were not available for the critical section in test 24-3-Sust-4, crack widths in excess of 1/8-in. give evidence that the steel stirrups in this test were above yielding throughout testing.

Similar to the fatigue tests described in the chapter 4, crack widths on the end strengthened with unbonded CFRP were much larger than the end strengthened using bonded CFRP. Once again, one large shear crack opened and continued to widen during the tests strengthened using unbonded CFRP. Multiple smaller cracks formed in the specimens strengthened using bonded CFRP with deformations being spread out over the depth of the section. Shear cracks were larger in the specimen strengthened after initial cracking compared with the specimen strengthened before cracking. The additional stiffness gained due to the application of CFRP laminates is not as great in specimens strengthened after the initial cracking of the specimen.

The average displacements of the two specimens increased gradually throughout testing with the bulk of the increases coming within the first few weeks of testing. This agrees with results found by Hoult and Lees (2005) where they observed that the majority of increases in the deflections of beams strengthened using CFRP laminates occurred during the first 25 days of loading. They also observed similar increases in CFRP strains during loading signifying possible deflection increases as a result of a shear contribution in addition to flexural effects. In general, CFRP laminates applied using CFRP anchors demonstrated excellent sustained behavior with little loss of strength observed during testing.

CHAPTER 6

Summary and Conclusions

6.1 SUMMARY

Four test specimens were constructed to study the performance of reinforced concrete beams strengthened using Carbon Fiber Reinforced Polymer (CFRP) laminates and CFRP anchors under fatigue and sustained loading. Test specimens consisted of 24-in. deep T-beams with a 14-in. wide web width. The flange of the T-beams was 21-in. wide and 5-in. deep. All specimens were constructed and tested at Phil M. Ferguson Structural Engineering Laboratory at the University of Texas at Austin.

Two specimens were loaded for a period of 217-days to study the sustained load performance of the strengthened specimens and two specimens were subjected to fatigue loads in excess of 3.5-million cycles. The beams subjected to cyclic loads were monotonically loaded to failure following the completion of fatigue loading. Loads were applied at the midpoint of each specimen resulting in a shear span-to-depth ratio of three on each end of the specimen. One end of each specimen was strengthened using unbonded CFRP laminates and the opposite end was strengthened using bonded CFRP laminates. For each set of tests, one specimen was cracked prior to the application of CFRP laminates while the other specimen was uncracked.

Overall, CFRP materials exhibited minimal deterioration due to high cycle fatigue (greater than 3.5-million cycles) or sustained loads. CFRP strains increased between 20 and 60% in both fatigue and sustained load tests. The fatigue loaded specimens subjected to monotonic loading failed at levels that were 5 to 15% lower than results of specimens that were not subjected to fatigue loading. However, most specimens still failed at loads 20 to 30% higher than similar unstrengthened specimens.

6.2 CONCLUSIONS

The following conclusions were developed from the tests conducted on reinforced concrete members strengthened for shear with anchored CFRP laminates under fatigue and sustained loading:

- (1) Anchored CFRP laminates demonstrated minimal degradation due to fatigue and sustained loading.
- (2) Bonded CFRP laminates reduced strains in internal steel reinforcement and decreased shear crack widths. The steel strain reduction and decrease in concrete crack widths was not as great in specimens strengthened with CFRP laminates after initial cracking.
- (3) Careful attention must be given to the fatigue life of the internal steel reinforcement in specimens strengthened using CFRP laminates. It is possible for a specimen to fail due to the fatigue of the internal steel reinforcement when the CFRP laminates have not yet reached their capacity.
- (4) CFRP anchors enabled the CFRP strips to develop their full tensile capacity in excess of the manufacturer reported maximum tensile strain value of 0.0105.
- (5) CFRP strengthened specimens subjected to severe fatigue loading (cycled loads in excess of 3.5-million cycles) produced failure loads 5 to 15% lower than non-fatigued, strengthened specimens.
- (6) CFRP anchors enabled CFRP laminates to maintain strains greater than recommended in existing design guidelines for laminates not wrapped completely around a specimen (greater than 0.004). CFRP anchors also enable CFRP laminates to maintain similar high strain values in specimens subjected to fatigue loading.

6.3 FURTHER CONSIDERATIONS

Additional information is still needed with regards to certain parameters involving reinforced concrete specimen strengthened with CFRP laminates under fatigue and sustained loads:

- (1) Fatigue tests were conducted using a relatively small amplitude range to compare results with reinforced concrete bridges that display lower live load to dead load ratios. The range of loading was kept between 15 to 25% of the applied load. Further studies are needed on the effect of extreme load ranges on CFRP strengthened specimens (Load ranges in excess of 50% of the applied load).
- (2) Sustained load tests are being continued and further information is needed on the effects of sustained loads on the failure capacity of the specimen when monotonically loaded to failure following long periods of sustained loads.
- (3) Under loading to failure following fatigue testing most tests reached strain values in excess of the manufacturer reported tensile strain value of 0.0105, but failure was triggered by rupture of a CFRP anchor. Further research is needed into the effects of fatigue loading on the performance of CFRP anchors.

References

ACI 318-08. (2008). *Building Code Requirements for Structural Concrete*. Farmington Hills, Michigan, USA: American Concrete Institute.

ACI 440.2R-08. (2008). *Guide for the Design and Construction of Externally Bonded FRP Systems for Strengthening Concrete Structures*. Farmington Hills, Michigan, USA: American Concrete Institute.

Aidoo, J., Harries, K.A., & Petrou, M.F. (2004). Fatigue of Carbon Fiber Reinforcement Polymer-Strengthened Reinforced Concrete Bridge Girders. *Journal of Composites for Construction* , 8 (6), 501-509.

Bousselham, A., & Chaallal, O. (2006). Behavior of Reinforced Concrete T-Beams Strengthened in Shear with Carbon Fiber Reinforced Polymer - An Experimental Study. *ACI Structural Journal* , 103 (3), 339-347.

Bousselham, A., & Chaallal, O. (2004). Shear Strengthening of Reinforced Concrete Beams with Fiber Reinforced Polymer: Assessment of Influencing Parameters and Required Research. *ACI Structural Journal* , 101 (2), 219-227.

Brena, S.F., Benouaich, M.A., Kreger, M.E., & Wood, S.L. (2005). Fatigue Tests of Reinforced Concrete Beams Strengthened Using Carbon Fiber-Reinforced Polymer Composites. *ACI Structural Journal* , 102 (2), 305-313.

Choi, K., Meshgin, P., & Taha, M.M.R. (2007). Shear Creep of Epoxy at the Concrete-FRP Interfaces. *Composites Part B: Engineering*, 38 (5-6), 772-780.

Deniaud, C., & Cheng, J.R. (2003). Reinforced Concrete T-Beams Strengthened in Shear with Fiber Reinforced Polymer Sheets. *Journal of Composites for Construction* , 302-310.

Deniaud, C., & Cheng, J.R. (2001). Shear Behavior of Reinforced Concrete T-Beams with Externally Bonded Fiber-Reinforced Polymer Sheets. *ACI Structural Journal* , 98 (3), 386-394.

Ferrier, E., Bigaud, D., Clement, J.C., & Hamelin, P. (2011). Fatigue-Loading Effect on RC Beams Strengthened with Externally Bonded FRP. *Construction and Building Materials* , 25 (2), 539-546.

Forrest, R.W.B., Higgins, C., & Senturk, A.E. (2010). Experimental and Analytical Evaluation of Reinforced Concrete Girders under Low-Cycle Shear Fatigue. *ACI Structural Journal* , 107 (20), 199-207.

Gussenhoven, R., & Brena, S.F. (2005). Fatigue Behavior of Reinforced Concrete Beams Strengthened with Different FRP Laminate Configurations. *SP 230 7th International Symposium on Fiber-Reinforced Polymer (FRP) Reinforcement for Concrete Structures* (pp. 613-630). American Concrete Institute.

Harries, K.A., Reeve, B., & Zorn, A. (2007). Experimental Evaluation of Factors Affecting Monotonic and Fatigue Behavior of Fiber-Reinforced Polymer-to-Concrete Bond in Reinforced Concrete Beams. *ACI Structural Journal*, 104 (6), 667-674.

Hoult, N., & Lees, J. (2005). Long-Term Performance of a CFRP Strap Shear Retrofitting System. *SP 230 7th International Symposium on Fiber-Reinforced Polymer (FRP) Reinforcement for Concrete Structures* (685-704). American Concrete Institute.

NCHRP Report 655. (2010). *Recommended Guide Specification for the Design of Externally Bonded FRP Systems for Repair and Strengthening of Concrete Bridge Elements*. Washington, District of Columbia, USA: Transportation Research Board.

Nishizaki, I., Labossiere, P., & Sarsaniuc, B. (2007). Durability of CFRP Sheet Reinforcement through Exposure Tests. *SP 230 7th International Symposium on Fiber-Reinforced Polymer (FRP) Reinforcement for Concrete Structures* (1419-1428). American Concrete Institute.

Papakonstantinou, C.G., Petrou, M.F., & Harries, K.A. (2001). Fatigue of Reinforced Concrete Beams Strengthened with GFRP Sheets. *Journal of Composites for Construction*, 5 (4), 246-253.

Pham, L.T. (2009). *Development of a Quality Control Test for Carbon Fiber Reinforced Polymer Anchors*. Master of Science Thesis, The University of Texas at

Austin, Department of Civil, Environmental and Architectural Engineering, Austin, Texas.

Quinn, K.T. (2009). *Shear Strengthening of Reinforced Concrete Beams with Carbon Fiber Reinforced Polymer (CFRP) and Improved Anchor Details*. Master of Science Thesis, The University of Texas at Austin, Department of Civil, Environmental and Architectural Engineering, Austin, Texas.

Uji, K. (1992). Improving Shear Capacity of Existing RC Concrete Members by Applying Carbon Fiber Sheets. *Transactions of the Japan Concrete Institute* , 14, 253-256.

Yang, D., Hong, S., & Park, S. (2007). Experimental Observation on Bond-Slip Behavior between Concrete and CFRP Plate. *International Journal of Concrete Structures and Materials*, 1 (1), 37-43.

VITA

Mr. Christopher Neil Satrom was born in Tulsa, OK on February 18, 1986 to Mr. James Donald Satrom and Mrs. Wanda Harvey Satrom. He attended Bishop Kelley High School in Tulsa, OK. Upon successful completion of his work in 2004, Neil enrolled at Kansas State University and received a Bachelor of Science in Architectural Engineering in May 2009. In August 2009, Neil enrolled in a graduate program in Structural Engineering at the University of Texas at Austin. He graduated with a Master of Science in Engineering in August 2011 and will pursue a career in structural engineering at the professional level.

Permanent Address: 618 North Carolina Ave #3
Washington, D.C. 20003

This thesis was typed by the author.